Université de Sherbrooke

In-depth characterization of the NS3:NS5 interaction within the West Nile virus replicase complex during positive strand RNA synthesis

By
Carolin Brand
Biochemistry Program

Thesis presented at the Faculty of Medicine and Health Sciences
for the fulfillment of the Master degree diploma Master of Science (M. Sc.)
in Biochemistry

Sherbrooke, Québec, Canada
April 2017

Members of the evaluation committee:
Prof. Martin Bisaillon, Département de biochimie, Université de Sherbrooke
Prof. Brian Geiss, Department of Microbiology, Immunology and Pathology, Colorado State University
Prof. Xavier Roucou, Département de biochimie, Université de Sherbrooke
Prof. Lee-Hwa Tai, Département de pédiatrie, Université de Sherbrooke

RÉSUMÉ

Caractérisation détaillée de l'interaction entre NS3 et NS5 dans le complexe de réplication du virus du Nil occidental pendant la synthèse d'ARN de polarité positive

Par
Carolin Brand
Programme de biochimie

Mémoire présenté à la Faculté de Médecine et des Sciences de la Santé en vue de l'obtention du diplôme de maitre ès sciences (M. Sc.) en biochimie, Faculté de médecine et des sciences de la santé, Université de Sherbrooke, Sherbrooke, Québec, Canada, J1H 5N4

Les Flavivirus transmis par les moustiques comme le virus du Nil occidental, le virus de la dengue, le virus de la fièvre jaune, le virus de l'encéphalite japonaise et le virus Zika constituent des préoccupations croissantes de santé publique. Ils se sont répandus dans le monde au cours des dernières décennies, et les épidémies sont devenues plus fréquentes et plus sévères. Chaque année, des millions de personnes sont infectées et environ 50 000 patients décèdent d'infections à Flavivirus. Malgré les nombreux efforts de recherche, il n'y a actuellement aucun médicament antiviral spécifique disponible, et des nouvelles stratégies antivirales sont indispensables. Comprendre comment les Flavivirus fonctionnent au niveau moléculaire aidera à découvrir des nouvelles cibles pour l'intervention thérapeutique.

Les Flavivirus ont un génome d'ARN simple brin de polarité positive qui code pour trois protéines structurales et huit protéines non structurales. Seules deux des huit protéines non structurales ont des activités enzymatiques. NS3 possède un domaine protéase et un domaine hélicase, et NS5 a un domaine méthyl- et guanylyltransférase et un domaine ARN polymérase ARN-dépendante. Ensemble, ils répliquent le génome viral. Ici, nous caractérisons l'interaction entre NS3 et NS5 dans le complexe de réplication du virus du Nil occidental pendant la synthèse d'ARN de polarité positive.

Un modèle d'interaction comprenant NS3, NS5 et l'ARN viral a été développé basé sur des structures cristallines connues ainsi que des activités enzymatiques des deux protéines individuelles, et ce modèle a été soumis à des simulations de dynamique moléculaire. Les interactions potentielles entre les protéines NS3 et NS5 ont été identifiées. Les résidus impliqués dans ces interactions ont été mutés dans un réplicon du virus du Nil occidental et les effets de ces mutations sur la réplication virale ont été évalués. Une région particulière à la surface de la protéine NS3 a été identifiée comme étant cruciale pour la réplication virale, très probablement parce qu'elle interagit avec NS5. Cette région pourrait être une cible attrayante pour la recherche de composés qui pourraient interférer avec l'interaction entre NS3 et NS5 et donc posséder un potentiel antiviral intéressant.

Mots clés : Flavivirus, virus du Nil occidental, complexe de réplication, interaction entre NS3 et NS5

SUMMARY

In-depth characterization of the NS3:NS5 interaction within the West Nile virus replicase complex during positive strand RNA synthesis

By
Carolin Brand
Biochemistry Program

Thesis presented at the Faculty of Medicine and Health Sciences for the fulfillment of the Master degree diploma Master of Science (M. Sc.) in biochemistry, Faculty of medicine and health sciences, Université de Sherbrooke, Sherbrooke, Québec, Canada, J1H 5N4

Mosquito-borne Flaviviruses like West Nile virus, Dengue virus, Yellow Fever virus, Japanese encephalitis virus, and Zika virus are increasing public health concerns. They have spread globally during the past decades, and outbreaks have recently become more frequent and more severe. Every year, millions of people are infected, and approximately 50,000 patients die from Flavivirus infections. Despite extensive research efforts, there are currently no specific antiviral drugs available, and new antiviral strategies are greatly needed. Understanding how Flaviviruses work on a molecular level will help in uncovering new points for therapeutic intervention.

Flaviviruses have a single-stranded RNA genome of positive polarity that encodes three structural and eight non-structural proteins. Only two of the eight non-structural proteins have enzymatic activities. NS3 has an N-terminal protease domain and a C-terminal helicase domain, and NS5 has an N-terminal capping enzyme domain and a C-terminal RNA-dependent RNA polymerase domain. Together, they replicate the viral genome. Here we characterize the NS3:NS5 interaction within the West Nile virus RNA replicase complex during positive strand synthesis.

An interaction model including NS3, NS5 and viral RNA was developed based on the known crystal structures as well as enzymatic activities of the two individual proteins, and this model was subjected to molecular dynamics simulations. Potential interactions between the NS3 and NS5 proteins were identified. Residues involved in these interactions were mutated in a West Nile virus replicon, and the effects of these mutations on viral replication were evaluated. One particular region on the surface of the NS3 protein was identified to be crucial for viral replication, most likely because it mediates the interaction with NS5. This region might be an attractive target for the search of compounds that could interfere with the NS3:NS5 interaction and therefore possess an interesting antiviral potential.

Keywords: Flavivirus, West Nile virus, replicase complex, NS3:NS5 interaction

TABLE OF CONTENTS

LIST OF FIGURES

LIST OF TABLES

LIST OF ABBREVIATIONS

°	Degree
(+)ssRNA	Single-stranded ribonucleic acid of positive polarity
µg	Microgram
µl	Microlitre
2K	Non-structural protein 2K
6His	Hexa-histidine
Å	Ångström, 1Å = 0.1 nanometer
ADP	Adenosine 5'-diphosphate
AMP-PNP	Adenosine 5'-(β,γ-imido)triphosphate
ATP	Adenosine 5'-triphosphate
BHK17	Baby hamster kidney cells
C	Capsid protein
CM5	Biacore sensor chip with a matrix of carboxymethylated dextran covalently attached to a gold surface
CMV	Cytomegalovirus
CO_2	Carbon dioxide
dATP	2'-deoxyadenosine 5'-triphosphate
dCTP	2'-deoxycytidine 5'-triphosphate
DEET	N,N-diethyl-meta-toluamide
DENV	Dengue virus
dGTP	2'-deoxyguanosine 5'-triphosphate
DMEM	Dulbecco's Modified Eagle's Medium
DNA	Deoxyribonucleic acid
DpnI	Methylation dependent restriction enzyme, originally found in the bacterium *Diplococcus pneumoniae*
dsRNA	Double-stranded ribonucleic acid
dTTP	Thymidine 5'-triphosphate

E	Envelope protein
E. coli	*Escherichia coli*
ER	Endoplasmic reticulum
FBS	Fetal bovine serum
FLuc	Firefly luciferase
FPLC	Fast protein liquid chromatography
GF	Gel filtration
GMP	Guanosine 5’-monophosphate
GpppA	Guanosine 5'-triphosphate 5'-adenosine (cap analog)
GpppG	Guanosine 5'-triphosphate 5'-guanosine (cap analog)
GpppRNA	Ribonucleic acid with a guanosine linked to the first nucleotide via a 5’-5’ triphosphate bridge
GTase	Guanylyltransferase
GTP	Guanosine 5’-triphosphate
GTPγS	Guanosine 5’-[γ-thio]triphosphate
h	Hour
HA	Human influenza hemagglutinin
IFN	Interferon
IPTG	Isopropyl β-D-1-thiogalactopyranoside
JEV	Japanese encephalitis virus
kb	Kilobase
kDa	Kilodalton
L	Litre
LB	Luria-Bertani medium
M	Membrane protein
m7GDP	7-methylguanosine 5'-diphosphate
m7GpppA	7-methylguanosine 5'-triphosphate 5'-adenosine (cap analog)
m7GpppG	7-methylguanosine 5'-triphosphate 5'-guanosine (cap analog)
m7GpppGm	7-methylguanosine 5'-triphosphate 5'-(2'-*O*-methyl)-guanosine (cap analog)

m7GpppNmRNA	Ribonucleic acid with a complete cap structure (the guanosine is methylated at the N7 position and the first nucleotide is methylated at the ribose 2'-*O* position)
MD	Molecular dynamics
min	Minute
ml	Millilitre
mM	Millimolar
mRNA	Messenger ribonucleic acid
MTase	Methyltransferase
NaCl	Sodium chloride
ng	Nanogram
NIH	U.S. National Institutes of Health
ns	Nanosecond
NS1	Non-structural protein 1
NS2A	Non-structural protein 2A
NS2B	Non-structural protein 2B
NS3	Non-structural protein 3
NS4A	Non-structural protein 4A
NS4B	Non-structural protein 4B
NS5	Non-structural protein 5
NTP	Nucleoside triphosphate
NTPase	Nucleoside triphosphatase
OD_{600}	Optical density at 600 nanometers
Opti-MEM	Improved Minimal Essential Medium
ORF	Open reading frame
PAGE	Polyacrylamide gel electrophoresis
PCR	Polymerase chain reaction
Pfu	Deoxyribonucleic acid polymerase with 3' to 5' exonuclease proofreading activity, originally found in the hyperthermophilic archaeon *Pyrococcus furiosus*

pH	Numeric scale used to specify the acidity or basicity of an aqueous solution
PPI	Protein-protein interaction
PPi	Pyrophosphate
ppRNA	5'-diphosphorylated ribonucleic acid
prM	Premembrane protein
RdRp	Ribonucleic acid-dependent ribonucleic acid polymerase
RNA	Ribonucleic acid
rpm	Rotations per minute
RTPase	Ribonucleic acid triphosphatase
SAH	S-adenosyl-L-homocysteine
SAM	S-adenosyl-L-methionine
SDS	Sodium dodecyl sulfate
sec	Second
sfRNA	Subgenomic Flavivirus ribonucleic acid
SPR	Surface plasmon resonance
ssRNA	Single-stranded ribonucleic acid
TAM	Tyro3, Axl, Mer
TIM	T-cell immunoglobulin and mucin domain
Tris-HCl	2-amino-2-(hydroxymethyl)-1,3-propanediol
UTR	Untranslated region
WHO	World Health Organization
WNV	West Nile virus
YFV	Yellow Fever virus
ZIKV	Zika virus

INTRODUCTION

Flaviviruses

The family *Flaviviridae* contains four genera, namely *Flavivirus*, *Hepacivirus*, *Pegivirus* and *Pestivirus* with 53, 1, 2 and 4 species, respectively (Figure 1) (International Committee on Taxonomy of Viruses, 2015). However, not all *Flaviviridae* viruses have been assigned to one of these genera, and they remain unclassified (Papageorgiou et al., 2016). Some viruses of the *Flavivirus* genus are specific to arthropods whereas others are transmissible to vertebrates, and the latter group can be further divided into non-vector (no known vector), tick-borne and mosquito-borne clusters (Kuno et al., 1998; Vasilakis and Weaver, 2016). The last subgroup is the largest, and it contains important human pathogens such as Dengue virus, West Nile virus, and Yellow fever virus (Kuno et al., 1998; Papageorgiou et al., 2016; Vasilakis and Weaver, 2016).

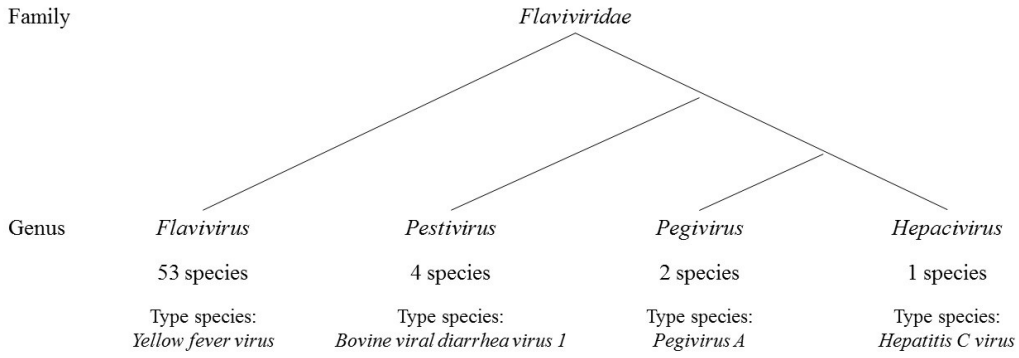

Figure 1. Genera within the *Flaviviridae* family.

The evolutionary relationships between the four genera within the *Flaviviridae* family are schematically shown. For each genus, the number of species as well as the type species are indicated. Figure adapted from (Kuno et al., 1998).

Mosquito-borne Flaviviruses

The mosquito-borne *Flavivirus* cluster contains nine clades numbered VI to XIV (clades I-III being in the non-vector cluster and clades IV and V being in the tick-borne cluster) (Kuno et al., 1998). The evolutionary relationships between these clades are outlined in Figure 2. Viruses of public health importance within the mosquito-borne *Flavivirus* cluster

are Yellow Fever virus (YFV), Dengue virus (DENV), Zika virus (ZIKV), Japanese encephalitis virus (JEV) and West Nile virus (WNV). Their relationships compared to each other are also shown in Figure 2.

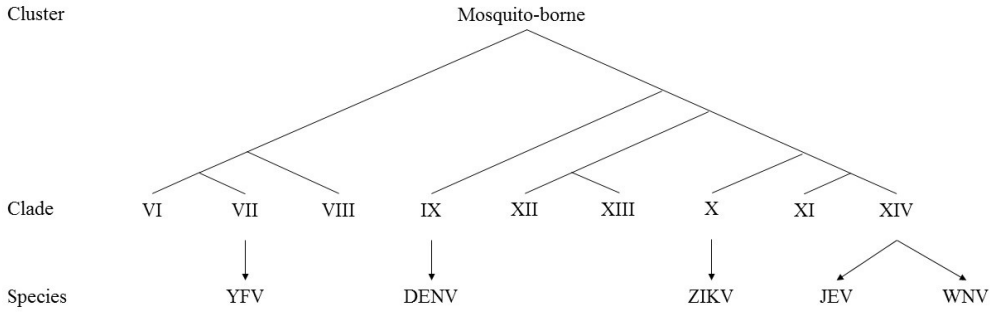

Figure 2. Clades within the mosquito-borne Flavivirus cluster.

The evolutionary relationships between the nine clades within the mosquito-borne Flavivirus cluster are schematically shown. Figure adapted from (Kuno et al., 1998).

Over the last decades, the global incidence of mosquito-borne Flaviviruses has grown dramatically. For instance, before 1999, WNV was absent in the Americas. However, since its introduction in New York 18 years ago, it has rapidly spread over the continent, and today it is found in more than 20 countries in the Western hemisphere (Chancey et al., 2015; Ciota and Kramer, 2013; Elizondo-Quiroga and Elizondo-Quiroga, 2013). The recent emergence of ZIKV is another example of increasing Flavivirus prevalence. Until ten years ago, only a few isolated cases were reported. The first large Zika outbreak occurred in 2007 on Yap Island, followed by outbreaks in French Polynesia, Easter Island, Cook Islands and New Caledonia in 2013-2014 (WHO, 2017). The most recent epidemic originated in Brazil in 2015 and has since then spread to more than 50 countries and territories in Central and South America, Africa and the Western Pacific region (WHO, 2017, 2016a).

Given that Flaviviruses are widely spread, the majority of the world's population is exposed to at least one of these viruses. In addition, millions of infections occur every year, causing thousands of deaths. Current statistics for DENV (WHO, 2016b), YFV (WHO, 2016c, 2014), WNV (Elizondo-Quiroga and Elizondo-Quiroga, 2013) and JEV (WHO, 2015) are shown in Table 1.

Virus	Countries affected	Population at risk	Clinical cases per year	Deaths per year
DENV	128	3.9 billion	96 million	12,500
YFV	47	>900 million	150,000	30,000
WNV	21	>500 million	n/a	n/a
JEV	24	>3 billion	68,000	15,000

Table 1. Current statistics for common mosquito-borne Flaviviruses.

The number of countries affected, people at risk of infection, clinical cases per year and deaths per year due to DENV, YFV, WNV and JEV are shown. Statistics for DENV, YFV and JEV include all countries worldwide whereas statistics for WNV include only countries in the Americas. Data shown in this table were obtained from (Elizondo-Quiroga and Elizondo-Quiroga, 2013; WHO, 2016b, 2016c, 2015, 2014).

Transmission

The above-mentioned Flaviviruses are transferred to new hosts via female mosquitoes' saliva during blood feeding (Chancey et al., 2015; Colpitts et al., 2012; Weaver and Barrett, 2004). *Culex* mosquitoes are the primary vectors of WNV (Chancey et al., 2015; Ciota and Kramer, 2013; Colpitts et al., 2012; Weaver and Barrett, 2004; WHO, 2011) and JEV (Weaver and Barrett, 2004; WHO, 2015) whereas *Aedes* mosquitoes are the principal vectors of DENV (Vasilakis et al., 2011; Vasilakis and Weaver, 2016; Weaver and Barrett, 2004; WHO, 2016b), YFV (Vasilakis and Weaver, 2016; Weaver and Barrett, 2004; WHO, 2016c) and ZIKV (Vasilakis and Weaver, 2016; WHO, 2016d). Transmission cycles and hosts vary between Flaviviruses transmitted by different genera of mosquitoes. On the one hand, DENV, YFV and ZIKV are maintained in two ecologically and evolutionary independent transmission cycles, namely a sylvatic cycle involving arboreal *Aedes* mosquitoes and non-human primates, and an urban cycle involving peridomestic/domestic *Aedes* mosquitoes and humans (Vasilakis et al., 2011; Vasilakis and Weaver, 2016; Weaver and Barrett, 2004). These two cycles are connected by some *Aedes* species that feed on both non-human primates and humans, also called bridge vectors (Vasilakis and Weaver, 2016). On the other hand, the main transmission cycles of JEV and WNV are constituted of *Culex* mosquitoes as vectors and birds as hosts (Chancey et al., 2015; Ciota and Kramer, 2013; Colpitts et al., 2012; Weaver and Barrett, 2004). Humans and other mammals can be infected, but they are dead-end hosts given that their levels of viremia are too low to infect

mosquitoes (Chancey et al., 2015; Ciota and Kramer, 2013; Colpitts et al., 2012; Weaver and Barrett, 2004).

The increasing global distribution of Flaviviruses is due to multiple factors. Regions that are suitable for the survival of the mosquito vectors are expanding to previously unaffected zones due to climate change and rising temperatures (Ciota and Kramer, 2013; Vasilakis et al., 2011; WHO, 2014). In addition, migratory birds have transported WNV and JEV over long distances (Ciota and Kramer, 2013; Weaver and Barrett, 2004). Finally, DENV and YFV were probably introduced into the Americas during slave trade when people from Central and West Africa, i.e. regions where many Flaviviruses originated, were taken to the New World (Vasilakis et al., 2011).

Symptoms

The majority of Flavivirus infections are asymptomatic (WHO, 2016c, 2015, 2011), and in cases that manifest clinically, symptoms vary widely. Most patients experience a flu-like illness including fever, headache, muscle and joint pain, nausea, vomiting, and rash (WHO, 2016b, 2016c, 2016d, 2015, 2011). Severe symptoms such as high fever, seizures, encephalitis, paralysis, jaundice (YFV), haemorrhage (DENV and YFV), coma, and ultimately death occur only in a small number of cases (WHO, 2016b, 2016c, 2015, 2011). Moreover, ZIKV has been linked to microcephaly and Guillain-Barré syndrome (WHO, 2016d).

Treatment and prevention

No specific antiviral drugs are available to cure Flavivirus infections, and treatment consists of supportive care (WHO, 2016b, 2016c, 2015, 2011). Methods of prevention include vector control and vaccination. Safe and effective JEV and YFV vaccines have been available for several decades (Erlanger et al., 2009; Sanofi Pasteur, 2016; WHO, 2016c, 2015). In late 2015, the first DENV vaccine was approved in certain endemic countries, and other dengue vaccine candidates are in clinical trials (WHO, 2016b, 2016e). WNV vaccines are available for use in horses, but vaccine candidates for humans are still in

various stages of (pre)clinical trials (Amanna and Slifka, 2014; WHO, 2011). Due to insufficient vaccination coverage for some viruses or the absence of licensed vaccines for other viruses, vector control and protection from mosquito bites are crucial for the prevention of Flavivirus infections. Eradication of adult mosquitoes using insecticides has been successful in the past, but is now considered environmentally unacceptable (Vasilakis and Weaver, 2016). Current strategies for reducing mosquito populations include the elimination of mosquito breeding sites and larval habitats (Vasilakis and Weaver, 2016; WHO, 2016b, 2016c, 2016d), the use of lethal traps, the release of mosquitoes carrying *Wolbachia* bacteria that suppress viral transmission, and the release of genetically modified mosquitoes carrying a dominant gene that causes the death of all offspring (Vasilakis and Weaver, 2016). Contact between humans and vectors can be reduced by using window screens, sleeping under mosquito nets, wearing light colored clothing that covers most of the body, and applying insect repellant containing DEET (WHO, 2016b, 2016d, 2011). In order to develop effective antiviral drugs to treat infection and reduce the number of fatalities, the molecular mechanisms of Flaviviruses need to be well understood and characterized.

Flavivirus genome and proteins

The Flavivirus genome is a single-stranded RNA (ssRNA) (Stollar et al., 1966; Wengler et al., 1978) of positive polarity (Stollar et al., 1967; Wengler et al., 1978) and approximately 11kb in length (Castle et al., 1986; Rice et al., 1985; Sumiyoshi et al., 1987). In addition to a single open reading frame (ORF), it contains 5' and 3' untranslated regions (UTRs) (Rice et al., 1985; Sumiyoshi et al., 1987). It harbors a 5' type I cap structure (Wengler et al., 1978), and it is not polyadenylated at the 3' terminus (Wengler et al., 1978; Wengler and Wengler, 1981).

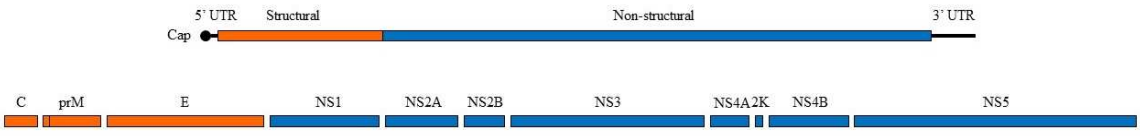

Figure 3. Flavivirus genome and viral proteins.

Schematic linear representation of the Flavivirus genome with its 5' cap structure, 5' and 3' UTRs, and ORF encoding three structural (orange) and eight non-structural (blue) proteins. Figure adapted from (Sampath and Padmanabhan, 2009).

The viral genome also serves as viral mRNA for the translation of the ORF into a large polyprotein (Boulton and Westaway, 1977; Naeve and Trent, 1978) that is co- and post-translationally processed into three structural (C, prM or M, E) (Rice et al., 1985; Shapiro et al., 1971; Stollar, 1969; Trent and Qureshi, 1971) and eight non-structural (NS1, NS2A, NS2B, NS3, NS4A, 2K, NS4B, NS5) proteins (Rice et al., 1985; Sumiyoshi et al., 1987). An outline of the Flavivirus genome and proteins is shown in Figure 3.

Structural proteins

The structural proteins are components of virus particles. They are involved in virus entry into the host cell as well as assembly and release of new virions. The envelope (E) and membrane (M) glycoproteins are inserted into the lipid envelope of mature viruses, and the capsid (C) protein forms the capsid that encloses the viral RNA genome (Kaufmann and Rossmann, 2011; Lindenbach et al., 2007; Mukhopadhyay et al., 2005).

Non-structural proteins

Only two of the eight non-structural proteins are known to possess enzymatic activities, namely NS3 and NS5. Both proteins contain two domains and multiple functions. NS3 is a serine protease (Chambers et al., 1990b; Preugschat et al., 1990; Wengler et al., 1991), RNA helicase (Li et al., 1999; Utama et al., 2000), nucleoside triphosphatase (NTPase) (Takegami et al., 1995; Warrener et al., 1993; Wengler and Wengler, 1991), and RNA triphosphatase (RTPase) (Bartelma and Padmanabhan, 2002; Wengler and Wengler, 1993). NS5 is a methyltransferase (MTase) (Egloff et al., 2002; Ray et al., 2006), guanylyltransferase (GTase) (Issur et al., 2009), and RNA-dependent RNA polymerase (RdRp) (Guyatt et al., 2001; Tan et al., 1996). Together, they form the RNA replicase complex. Besides their enzymatic activities during viral replication, NS3 and NS5 also accomplish other non-enzymatic functions. NS3 is involved in virus assembly (Kümmerer and Rice, 2002; Patkar and Kuhn, 2008), and NS5 participates in the evasion of the immune response by blocking interferon (IFN) signaling (Ashour et al., 2009; Laurent-Rolle et al., 2010).

The other non-structural proteins assume various roles to support viral replication and to evade or modulate the host cell's immune response. NS1 has various functions depending on its oligomerization state and cellular localization. The intracellular NS1 dimer is involved in viral genome replication, most likely by stabilizing the association between the replication complex and membranes (Mackenzie et al., 1996; Muller and Young, 2013; Muylaert et al., 1996). The secreted NS1 hexamer interacts with a wide range of host cell components, engages with both the innate and adaptive immunity and elicits both a protective and pathogenic immune response (Muller and Young, 2013). NS2A (Xie et al., 2013), NS2B (Li et al., 2015), NS4A (Miller et al., 2007; Nemésio et al., 2012), 2K (Miller et al., 2007) and NS4B (Miller et al., 2006; Nemésio et al., 2012) are small proteins containing multiple transmembrane domains. They have been shown to be part of the viral replication complex that is located within replication compartments derived from the endoplasmic reticulum (ER) membrane (Mackenzie et al., 1998; Welsch et al., 2009). NS2A participates in the production of infectious virus particles (Kümmerer and Rice, 2002; Liu et al., 2003; Xie et al., 2013), in the induction of membrane rearrangements (Leung et al., 2008), and in the evasion of the cellular antiviral response by inhibiting the IFN signaling pathway (Liu et al., 2004; Muñoz-Jordán et al., 2003; Tu et al., 2012). NS2B serves as an essential cofactor for the NS3 protease (Chambers et al., 1991; Falgout et al., 1991). NS4A induces ER membrane rearrangements during the formation of the viral replication compartment (Miller et al., 2007; Roosendaal et al., 2006), acts as a cofactor for the NS3 helicase activity (Shiryaev et al., 2009), and participates in immune evasion through the inhibition of IFN signaling (Muñoz-Jordán et al., 2003). 2K is often considered part of the NS4A protein, although it has been shown to serve as signal peptide required for the translocation and the correct insertion of NS4B into the ER membrane (Lin et al., 1993; Muñoz-Jordán et al., 2005). Moreover, it has been proposed to be involved in viral replication through membrane rearrangements or evasion of the immune response (Zou et al., 2009). NS4B serves as a cofactor for the NS3 helicase activity (Umareddy et al., 2006), and it is the main viral protein that inhibits the IFN α/β signaling pathway (Muñoz-Jordán et al., 2003). It has also been proposed to be a mediator of cell death (Evans and Seeger, 2007).

Flavivirus life cycle

Flaviviruses enter host cells through receptor-mediated endocytosis which is triggered by the binding of the envelope (E) protein to receptors and attachment factors on the surface of the host cell (Kaufmann and Rossmann, 2011; Perera-Lecoin et al., 2013). Receptor recognition and attachment has been proposed to involve multiple molecules in combination or consecutively, although the identity of these molecules remains elusive. Glycosaminoglycans have been suggested to act as attachment factors that concentrate virus particles on the cell surface before receptor-mediated internalisation. Calcium-dependent lectin receptors, $\alpha_v\beta_3$ integrin as well as phosphatidylserine, TIM (T-cell immunoglobulin and mucin domain) and TAM (Tyro3, Axl, Mer) receptors have been described as candidate receptors for different Flaviviruses in different cell types, but their precise role in virus endocytosis remains to be determined (Kaufmann and Rossmann, 2011; Perera-Lecoin et al., 2013). Following endocytosis, the acidic environment in the late endosome causes the E protein to undergo a conformational change and to trimerize, resulting in the fusion of the viral and endocytic membranes and the release of the nucleocapsid core into the cytoplasm (Kaufmann and Rossmann, 2011; Stiasny et al., 2011). After dissociation of the viral RNA from the capsid (C) protein, translation of the viral genome into the viral polyprotein takes place on the rough ER (Stohlman et al., 1975). Signal sequences within prM, E and NS1 cause the translocation of these parts of the polyprotein into the ER lumen (Perera and Kuhn, 2008). The transmembrane domains of NS2A, NS2B, NS4A, 2K and NS4B are inserted into the ER membrane whereas C, NS3 and NS5 stay in the cytoplasm (Lindenbach et al., 2007; Perera and Kuhn, 2008). Cleavage of the polyprotein into separate viral proteins is achieved by the viral NS2B-NS3 protease in the cytoplasm and by host signalases inside the ER lumen (Perera and Kuhn, 2008). Polyprotein translocation and processing occurs co- and post-translationally (Lindenbach et al., 2007). Once synthesized, the viral proteins assume their respective functions to initiate replication of the viral genome. The formation of vesicles, also called replication compartments since they are the site of viral genome replication, is induced (Uchil and Satchidanandam, 2003; Welsch et al., 2009). These vesicles are derived from the ER membrane (Gillespie et al., 2010; Miller et al., 2007, 2006; Paul and Bartenschlager, 2013; Welsch et al., 2009) and they are connected to the cytoplasm through a small pore

(Gillespie et al., 2010; Paul and Bartenschlager, 2013; Welsch et al., 2009). They protect viral proteins and RNA from proteases and nucleases (Paul and Bartenschlager, 2013; Uchil and Satchidanandam, 2003) as well as antiviral activity of IFN-stimulated proteins (Hoenen et al., 2007), and they ensure high efficacy of replication by concentrating all necessary components to these structures (Paul and Bartenschlager, 2013). The single-stranded, positive sense genomic RNA is first transcribed into negative sense RNA, resulting in a double stranded RNA (dsRNA) which is also referred to as replicative form RNA. Negative strand synthesis relies primarily on the NS5 RdRp, and NS3 does not seem to be strictly necessary. The dsRNA then serves as the template for the synthesis of a large number of capped (+)ssRNA viral genomes. Positive strand synthesis is a much more complex process which requires dsRNA unwinding and is coupled to positive strand capping, and thus involves the replication complex composed of the NS3 helicase domain and both domains of the NS5 protein (Saeedi and Geiss, 2013). The newly generated viral genomic RNA molecules are released from the replication compartments and used for multiple purposes (Miorin et al., 2013; Saeedi and Geiss, 2013). Some of the nascent genomic RNAs localize to the rough ER for further translation and synthesis of viral proteins. Others seem to be directed toward P-bodies for partial degradation and thus creation of subgenomic flavivirus RNA (sfRNA), a noncoding RNA derived from the 3' UTR of the viral genomic RNA that promotes virus replication, cytopathicity and pathogenicity (Funk et al., 2010; Pijlman et al., 2008). Finally, some of the new viral RNA genomes interact with capsid proteins to form nucleocapsids in the cytoplasm. These bud into the ER lumen through the ER membrane containing prM and E glycoproteins, thus forming immature virus particles (Lindenbach et al., 2007). Budding occurs in close proximity to the neck of replication compartments, limiting the exposure of viral RNA to host cell nucleases and sensors of the innate immune response and suggesting that replication and assembly are coordinated (Welsch et al., 2009). While transiting the trans-Golgi network, the E protein undergoes conformational changes and the prM protein is cleaved into the mature M protein (Perera and Kuhn, 2008). Mature, infectious virus particles are finally released by exocytosis (Lindenbach et al., 2007; Suthar et al., 2013). Subviral particles are also assembled in the ER and released the same way as infectious virions (Mukhopadhyay et al., 2005). However, they only contain a lipid envelope and the

two glycoproteins E and M, but no nucleocapsid, and are therefore non-infectious (Mukhopadhyay et al., 2005; Schalich et al., 1996). These particles, which are also known as defective interfering particles, possess hemagglutination activity and could act as decoys to help confuse the immune system (Heinz and Allison, 2000). The Flavivirus life cycle is graphically summarized in Figure 4.

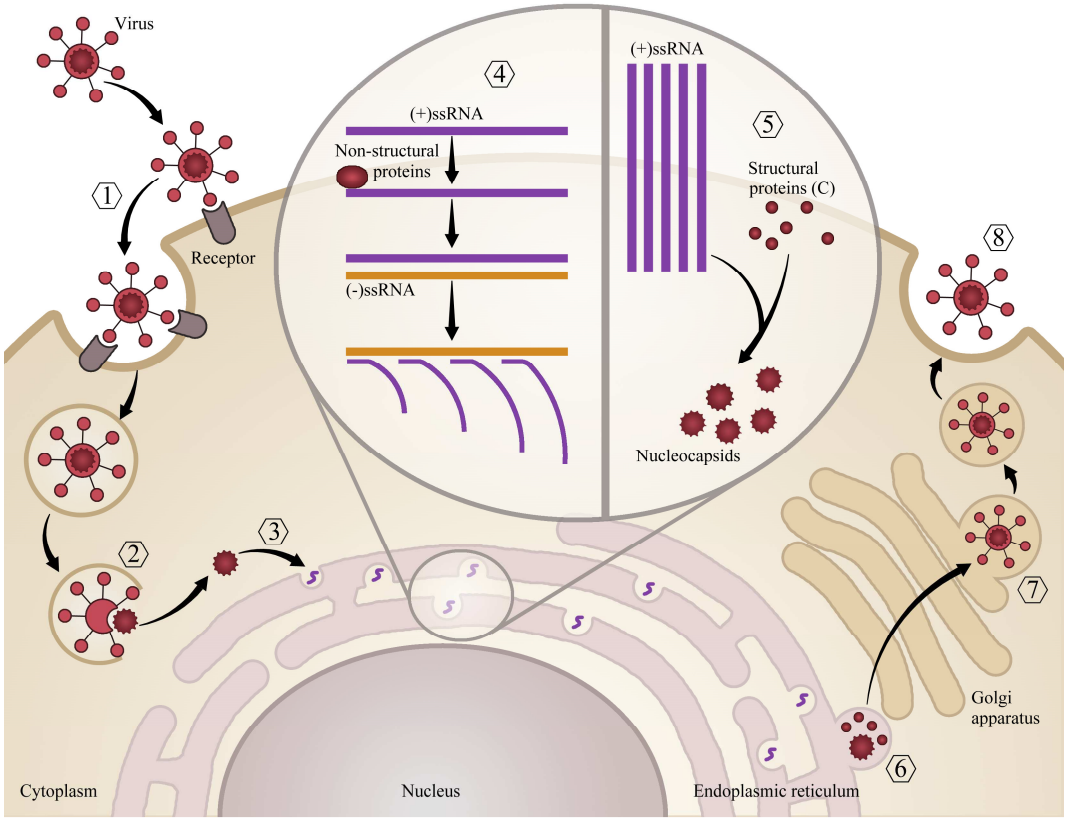

Figure 4. Flavivirus life cycle.

Schematic representation of the viral life cycle. The virus enters the host cell through receptor-mediated endocytosis (1) which is followed by release of the viral genome into the cytoplasm (2). This RNA is translated into viral proteins at the rough ER (3). The non-structural proteins form the replication complex that produces a large number of new viral genomes (4). These genomes are associated with capsid proteins to form nucleocapsids (5) that bud into the ER containing the other structural proteins (6). The nascent virions undergo maturation in the trans-Golgi network (7) and are released from the host cell through exocytosis (8). Figure adapted from (Suthar et al., 2013).

Viral RNA replication is a major process during the viral life cycle. Negative strand synthesis by the NS5 RdRp has been extensively studied and is well understood. However,

there is little information about the mechanisms of positive strand synthesis involving the replicase complex constituted of NS3 and NS5 (Saeedi and Geiss, 2013).

Flavivirus replicase complex

The replicase complex responsible for positive strand RNA synthesis during Flavivirus infection comprises mainly the two viral enzymes NS3 and NS5 (Klema et al., 2015).

Non-structural protein 3

Non-structural protein 3 (NS3) is the second largest and the second most conserved Flavivirus protein. In fact, NS3 proteins from WNV, DENV, JEV, ZIKV and YFV share approximately 65% sequence identity on the amino acid level (Appendix 1). The NS3 protein contains two domains that are coupled via a short flexible linker, namely an N-terminal protease domain and a C-terminal helicase domain (Figure 5) (Luo et al., 2008a). Whereas some studies suggest that the activities of the two domains are independent from one another (Assenberg et al., 2009; Gebhard et al., 2012), most studies indicate a functional coupling between the two domains (Luo et al., 2010, 2008a; Mastrangelo et al., 2007; Xu et al., 2006, 2005).

NS3 structures

Both individual domains as well as full-length NS3 proteins from multiple Flaviviruses have been crystallized and their three-dimensional structures have been resolved (Appendix 2). Different conformations of the full-length proteins with different relative orientations of the two domains have been reported (Luo et al., 2010, 2008a). These findings indicate that there is flexibility between the two domains, and that different conformational states could exist *in vivo*. In fact, RNA binding has been suggested to trigger conformational change in NS3 (Benzaghou et al., 2006; Luo et al., 2008b).

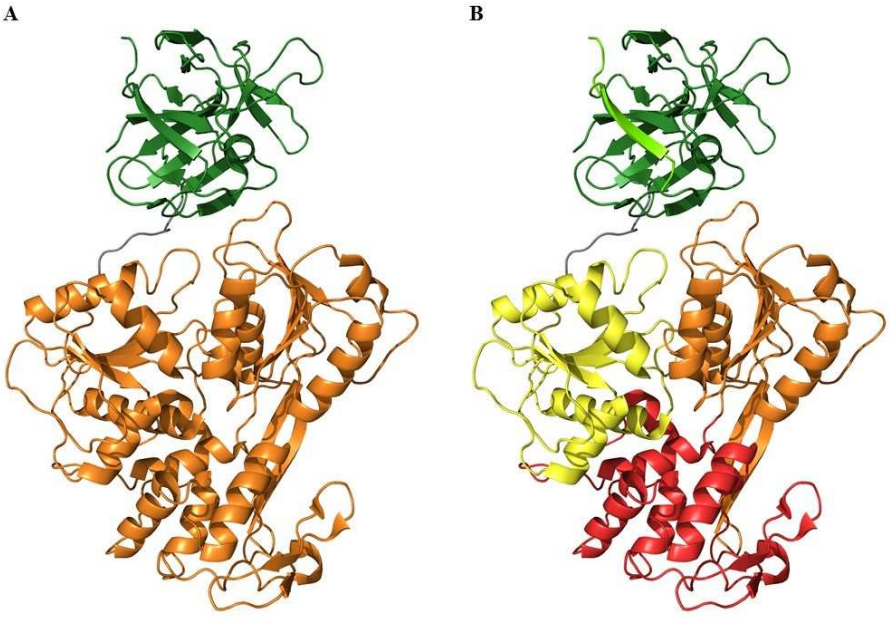

Figure 5. Crystal structure of the NS3 protein.

Full-length NS3 from DENV, pdb 2vbc (Luo et al., 2008a). [A] The protease (NS3 1-168 and NS2B 49-63) is colored in green, the inter-domain linker (169-179) in gray, and the helicase domain (180-618) in orange. [B] The protease domain (1-168) is colored in green, the NS2B cofactor (49-63) in pale green, the inter-domain linker (169-179) in gray, the helicase subdomain 1 (180-326) in yellow, the helicase subdomain 2 (327-481) in orange, and the helicase subdomain 3 (482-618) in red. Boundaries of the linker region and the helicase subdomains are based on reports by (Luo et al., 2010) and (Luo et al., 2008b), respectively.

NS3 protease domain

The protease domain is located in the N-terminal third of NS3 (Chambers et al., 1990b; Preugschat et al., 1990; Wengler et al., 1991). It contains four regions of homology with serine proteases, three of which comprise residues of the catalytic triad H51-D75-S135 (DENV numbering) (Bazan and Fletterick, 1989; Gorbalenya et al., 1989). This triad is strictly conserved among Flaviviruses and it is located in a cleft between two β-barrels (Erbel et al., 2006). The fourth region of homology with serine proteases is part of the substrate binding pocket which includes residues D129, F130, Y150, N152 and G153 (DENV numbering) (Bazan and Fletterick, 1989; Valle and Falgout, 1998). The aspartic acid residue at the bottom of the binding pocket has been suggested to be responsible for the specificity for cleavage sites that generally contain two basic residues followed by a

residue with a small side chain like G(A)RR↓S (Chambers et al., 1990a, 1990b), although the exact sequence varies between cleavage sites and viruses (Yotmanee et al., 2015). Sequences at which NS3 cleaves the viral polyprotein are located at the NS2A/NS2B, NS2B/NS3, NS3/NS4A, NS4A/2K and NS4B/NS5 junctions (Chambers et al., 1991; Lin et al., 1993). In addition, cleavage of the C-terminal membrane-spanning segment of the C protein, which occurs after several basic residues, is mediated by NS3 (Lobigs, 1993).

The cytoplasmic portion of the NS2B protein is essential for the formation of an active NS2B-NS3 protease (Chambers et al., 1993). Residues 53-58 (WNV numbering) form a β-strand which stabilizes the NS3 protease structure by folding into its N-terminal β-barrel (Erbel et al., 2006). Residues 64-96 of NS2B (WNV numbering) wrap around NS3, and upon substrate binding, residues 78-87 undergo a conformational change to form a stabilizing β-hairpin that becomes part of the protease active site (Aleshin et al., 2007; Erbel et al., 2006).

NS3 helicase domain

In addition to helicase activity, the C-terminal helicase domain of NS3 also harbors nucleoside triphosphatase (NTPase) and RNA triphosphatase (RTPase) activities (Li et al., 1999; Wengler and Wengler, 1993, 1991). NTPase and RTPase reactions occur in the same active site (Bartelma and Padmanabhan, 2002; Benarroch et al., 2004b; Sampath et al., 2006) whereas dsRNA unwinding, although driven by ATP hydrolysis, takes place at a distinct site known as helical gate (Mastrangelo et al., 2012). The RTPase reaction removes the γ-phosphate from the newly synthesized viral RNA to form a diphosphorylated RNA and thus constitutes the first step in the synthesis of the 5' cap structure (Wengler and Wengler, 1993). The RNA helicase activity unwinds the dsRNA replication intermediate to make the negative strand available as template for further genome replication and to release the positive strand for translation of viral proteins or packaging into virions, and it disrupts secondary structures in the viral RNA which are found especially in the 5' and 3' UTRs (Li et al., 2014; Luo et al., 2015). The unwinding of these structures is important for assembly of the replicase complex at the 3' end and an efficient RTPase reaction at the 5' end (Wang et al., 2009). As mentioned above, the helicase activity is driven by the energy released

from the hydrolysis of the γ-phosphate of nucleoside triphosphates, especially ATP and GTP, but how these two activities are coupled remains elusive (Li et al., 1999; Luo et al., 2015).

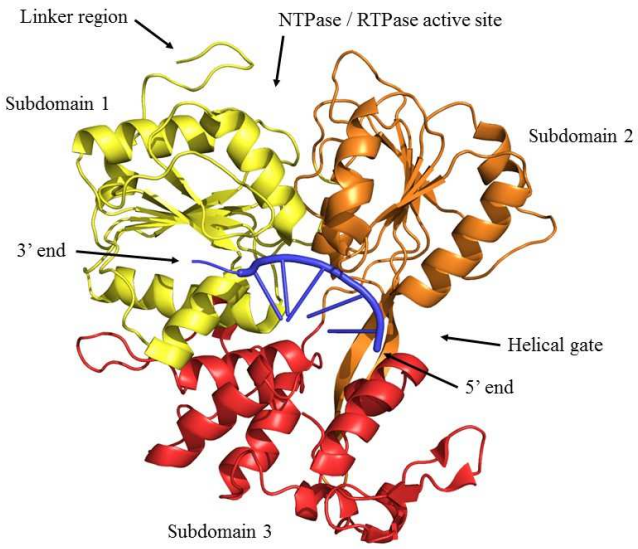

Figure 6. NS3 helicase domain bound to ssRNA.

NS3 helicase domain from DENV in complex with ssRNA, pdb 2jlu (Luo et al., 2008b). Subdomains 1 (168-326), 2 (327-481) and 3 (482-618) are colored in yellow, orange and red, respectively. The NTPase/RTPase active site, the helical gate as well as the 5' and 3' ends of the ssRNA are indicated.

The NS3 helicase domain is further divided into three subdomains (Figure 6). Seven conserved helicase motifs characteristic of superfamily 2 helicases, including Walker A and Walker B motifs, are contained in subdomains 1 and 2 (Mastrangelo et al., 2007; Wu et al., 2005; Xu et al., 2005). The ssRNA binding tunnel is located between subdomains 1 and 2 on one side and subdomain 3 on the other side (Luo et al., 2008b), and the helical gate formed by α-helix 2 of subdomain II, α-helix 6 of subdomain III and a β-hairpin protruding from subdomain II toward subdomain III constitutes the entry site to this groove (Mastrangelo et al., 2012). In fact, the β-hairpin acts as a helix opener by disrupting base stacking between the two strands of dsRNA so that the 3' end of the negative strand enters the RNA binding tunnel whereas the 5' end of the positive strand is forced to move along the protein's surface (Luo et al., 2015, 2008b). The RNA unwinding site is at a distance of about 30Å from the catalytic site where ATP is hydrolyzed (Mastrangelo et al., 2012), and

the exact mechanism by which these two events are coupled remains elusive (Li et al., 2014; Luo et al., 2015). The NTPase / RTPase active site is a basic pocket near the interface between the helicase and protease domains (Luo et al., 2008a). Substrate binding and coordination of a magnesium ion are mediated by residues from the Walker A and Walker B motifs, respectively (Assenberg et al., 2009; Benarroch et al., 2004b; Mastrangelo et al., 2007). Moreover, residues R457, R458, R460 and R463 (DENV numbering) which are located close to the active site have been shown to be crucial for both activities (Sampath et al., 2006). The exit channel for the phosphate product of the NTPase and RTPase reactions has been proposed to be formed by residues P195, A316, T317, P326, A455 and Q456 (DENV numbering) (Luo et al., 2008b).

Enzymatic activities of the NS3 helicase domain are influenced by the presence of other macromolecules. Binding of ssRNA to residues R184, K185, R186 and K187 (DENV numbering) has been shown to stimulate NTPase activity (Li et al., 1999; Warrener et al., 1993; Yon et al., 2005). Moreover, both NTPase and RTPase activities have been shown to be enhanced by the presence of NS5 (Cui et al., 1998; Yon et al., 2005). Finally, NS4A and NS4B are cofactors for the NS3 helicase activity: NS4A binds to the helicase domain and reduces the amount of ATP required for the unwinding of dsRNA (Shiryaev et al., 2009), whereas NS4B interacts with subdomains 2 and 3 (Zou et al., 2015a) and facilitates dissociation of NS3 from ssRNA (Umareddy et al., 2006).

Non-structural protein 5

Non-structural protein 5 (NS5) is the largest Flavivirus protein with approximately 103kDa. It is also the most conserved Flavivirus protein with a sequence identity of approximately 68% between WNV, DENV, JEV, ZIKV and YFV (Appendix 3). Like the other viral enzyme NS3, NS5 contains two domains that are connected via a short linker, namely an N-terminal capping enzyme domain and a C-terminal RNA-dependent RNA polymerase domain (Figure 7) (Lu and Gong, 2013).

NS5 structures

The three-dimensional structures of both domains and the full-length proteins from different Flaviviruses have been determined (Appendix 4). Conformations varying from a rather compact structure to a more extended structure have been reported, suggesting flexibility in the relative orientation of the two domains and the possibility of different conformational states for NS5 (Bussetta and Choi, 2012; Lu and Gong, 2013; Zhao et al., 2015b). Since the inter-domain linker is well-ordered in some crystal structures but without secondary structure in others, it seems to play a central role in the adoption of different conformations (Lu and Gong, 2013; Zhao et al., 2015b). Furthermore, residues G263-T264-R265 which are in close proximity to the linker region have been suggested to be a pivot point between the two domains and may contribute to conformational changes within the protein (Lu and Gong, 2013).

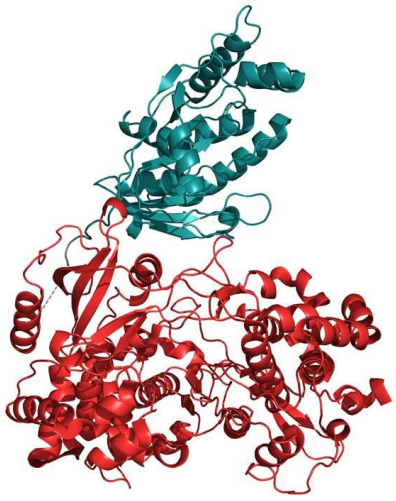

Figure 7. Crystal structure of the NS5 protein.

Full-length NS5 from JEV, pdb 4k6m (Lu and Gong, 2013). The MTase (1-266) domain is colored in blue, the inter-domain linker (267-275) in gray, and the RdRp (276-905) in red. Note that three residues from the linker region were unresolved in the structure and are represented by a dashed line.

NS5 capping enzyme domain

The NS5 N-terminal capping enzyme domain is involved in synthesizing the cap structure at the 5' end of the viral genome. It first executes its GTase activity by transferring a GMP to the 5' diphosphate end of nascent viral RNA (Issur et al., 2009). It then carries out its

MTase activity using S-adenosyl-L-methionine (SAM) as a methyl donor, and methyl groups are transferred to the N7 position of the guanine as well as the 2'-*O* position of the first nucleotide's ribose (Egloff et al., 2002; Ray et al., 2006). Since the NS5 capping enzyme domain mediates two different kinds of enzymatic reactions using different substrates, it has two distinct substrate binding pockets which are separated by a positively charged surface groove of 12-15Å (Figure 8). This region is believed to bind viral RNA during the GTase and MTase reactions (Egloff et al., 2007, 2002; Geiss et al., 2009; Zhou et al., 2007). The entry site of the 5' diphosphorylated RNA (ppRNA) into the capping enzyme has been suggested to be the groove between helices A2 and A3, given that residues F25, K30, R57, K181 and R212 (DENV numbering), which are clustered around the base of helix A2, have been shown to bind ppRNA (Henderson et al., 2011). Interestingly, some of the residues involved in ppRNA binding are also involved in GTP binding. In fact, the GTP binding pocket includes K14, L17, N18, L20, F25, K29 and S150 (DENV numbering), and this pocket is believed to be the active site for the GTase activity (Egloff et al., 2007, 2002). The fact that the phosphates of GTP and the phosphates of ppRNA compete for the same binding site on the capping enzyme suggests that they are bound at different times during the guanylyltransferase reaction. GTP is bound first to form a GMP-enzyme intermediate, and then ppRNA is bound for the transfer of GMP to the RNA, resulting in a GpppRNA product (Henderson et al., 2011; Issur et al., 2009). This basic cap structure then undergoes two methyltransferase reactions to form completely capped m7GpppNmRNA. Both MTase reactions occur at the catalytic tetrad K61-D146-K181-E217 (DENV numbering) (Ray et al., 2006) near the SAM binding pocket which includes residues S56, G86, W87, T104, L105, D131, V132, I147 and Y219 (DENV numbering) (Egloff et al., 2002), and N7-methylation precedes 2'-*O*-methylation (Ray et al., 2006; Zhou et al., 2007). The RNA substrate needs to be repositioned between the two MTase reactions, and the RNA cap structure has been suggested to be bound to the GTP binding pocket during 2'-*O*-methylation (Zhou et al., 2007).

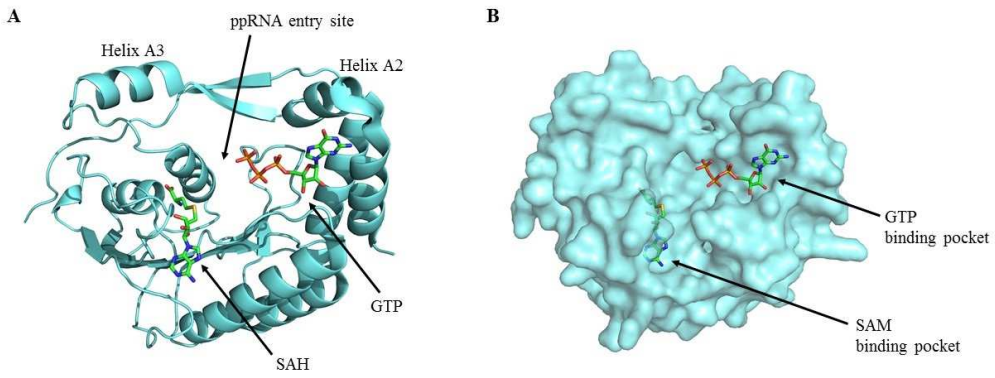

Figure 8. NS5 capping enzyme domain bound to GTP and SAH.

NS5 capping enzyme domain from YFV in complex with GTP and SAH, pdb 3evd (Geiss et al., 2009). [A] Cartoon representation. [B] Surface representation. The ppRNA entry site between helices A2 and A3 as well as the GTP and SAM binding pockets are shown.

NS5 RNA-dependent RNA polymerase domain

Replication of the viral RNA genome takes place in the NS5 C-terminal RNA-dependent RNA polymerase (RdRp) domain (Selisko et al., 2006; Tan et al., 1996). This domain has an approximately spherical shape and adopts the canonical right-hand conformation with fingers, palm and thumb subdomains (Figure 9). The palm subdomain contains five of the seven catalytic motifs (A through E) that are conserved among all viral RdRps whereas the two other motifs (F and G) are located in the fingers subdomain (Malet et al., 2007; Yap et al., 2007). The catalytic active site is situated within the palm subdomain near the interface with the fingers and thumb subdomains. In fact, it is encircled by the fingertips that mediate the interaction between the fingers and thumb subdomains (Malet et al., 2007; Yap et al., 2007). This structure also constitutes the RNA binding tunnel through which the template RNA gains access to the active site (Yap et al., 2007). A second tunnel between the fingers and palm domain, which goes across the entire protein and is approximately perpendicular to the first one, also connects to the active site (Malet et al., 2007). The back of this channel serves as entry site for NTPs, and the dsRNA product would exit the RdRp domain through the front of this channel (Choi and Rossmann, 2009; Malet et al., 2007). However, in all observed structures, the RdRp domain is in a closed conformation in which the C-terminal motif of the thumb subdomain blocks this exit site, and a conformational change to an open

state during elongation would be required to accommodate nascent dsRNA in this channel (Choi and Rossmann, 2009; Malet et al., 2007).

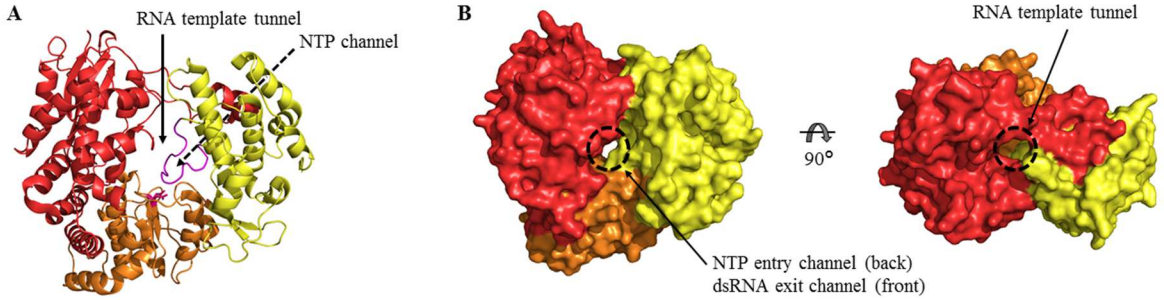

Figure 9. NS5 RdRp domain.

NS5 RdRp domain from WNV, pdb 2hfz (Malet et al., 2007). [A] Cartoon representation. [B] Surface representation. The fingers subdomain (274-498, 542-609) is colored in red, the palm subdomain (499-541, 610-717) in orange, the thumb subdomain (718-905) in yellow, and the priming loop (796-809) in purple. The aspartic acids (536 and 669) that coordinate the catalytic magnesium ions are shown as magenta colored sticks. The RNA template channel is between the fingers and thumb subdomain. NTPs enter the active site through a second channel from the back of the RdRp domain.

The NS5 RdRp performs *de novo* RNA synthesis (Ackermann and Padmanabhan, 2001), and several structural elements have been found to play an important role in initiation. The priming loop (residues 782-809, DENV numbering) protrudes from the thumb subdomain toward the active site in the palm domain and thus partially occludes the template RNA tunnel, allowing only ssRNA to access the active site (Choi and Rossmann, 2009; Yap et al., 2007). Moreover, it contains two conserved residues, W795 and H798 (DENV numbering) that provide an initiation platform by forming stacking interactions with nucleotides during *de novo* initiation (Selisko et al., 2012; Yap et al., 2007). The initiating ATP molecule is stacked against H798 (Selisko et al., 2012) whereas W795 stabilizes a GTP molecule at the *de novo* GTP-binding site (or i-1 position) which is 6-7Å from the catalytic motif (Choi and Rossmann, 2009; Noble and Shi, 2012). This special GTP is crucial for initiation, since *de novo* RNA synthesis has been shown to require a high concentration of GTP regardless of the nucleotide sequence at the 3' terminus of the template RNA (Nomaguchi et al., 2003). The GTP molecule has been proposed to stabilize the initiating ATP at the i position and to contribute to the proper positioning of its 3' hydroxyl group for the nucleophilic attack that results in the formation of a phosphodiester

bond with the second nucleotide at the i+1 position (Choi and Rossmann, 2009). During this reaction, the phosphates of the incoming nucleotide are held in place by two Mg^{2+} ions that are coordinated by D533 and D664 (DENV numbering) (Choi and Rossmann, 2009; Malet et al., 2007; Yap et al., 2007). Once the initiating dinucleotide is synthesized, GTP is released and the RdRp switches to an open conformation to allow elongation of the nascent dsRNA (Choi and Rossmann, 2009). The mechanism of translocation of the RdRp along the template RNA still remains elusive, although motif G of the fingertip region has been proposed to play a role in this process (Choi and Rossmann, 2009; Wu et al., 2015).

Interactions among non-structural proteins

Given that the replicase complex is formed by non-structural proteins 3 and 5 and that its function is supported by some of the other viral proteins, there are multiple interactions among the non-structural proteins. The central hydrophilic region of NS2B, which is located in the cytoplasm, interacts with the NS3 protease domain to fulfill its role as essential cofactor (Aleshin et al., 2007; Erbel et al., 2006). NS4A and NS4B are cofactors for the helicase activity of NS3 and therefore interact with the NS3 helicase domain (Shiryaev et al., 2009; Umareddy et al., 2006; Zou et al., 2015a). Since NS2B, NS4A and NS4B possess transmembrane regions in addition to regions that interact with NS3, they anchor the replicase complex to the ER membrane (Li et al., 2015; Miller et al., 2007, 2006). Moreover, NS4B and NS4A interact with each other, and NS4B also interacts with NS1 (Chatel-Chaix et al., 2015). NS5 does not interact with any small transmembrane non-structural protein, and it is recruited to the membrane-associated replication complex only via its interaction with NS3 (Klema et al., 2015).

NS3:NS5 interaction

The interaction between NS3 and NS5 has been shown by multiple techniques (Brooks et al., 2002; Chen et al., 1997; Cui et al., 1998; Johansson et al., 2001; Kapoor et al., 1995; Moreland et al., 2012; Takahashi et al., 2012; Tay et al., 2015; Vasudevan et al., 2001; Yu et al., 2013; Zou et al., 2011). No other viral protein has been found to be required, suggesting that NS3 and NS5 interact directly (Kapoor et al., 1995). The NS3:NS5

interaction is believed to be mediated by the NS5 RdRp domain (Brooks et al., 2002; Johansson et al., 2001; Moreland et al., 2012; Tay et al., 2015; Vasudevan et al., 2001) and the NS3 helicase domain (Johansson et al., 2001; Moreland et al., 2012), although some studies also suggest the contribution of the NS3 protease domain (Takahashi et al., 2012; Zou et al., 2011). A schematic model of this interaction has been proposed, and the interaction between NS3 and NS5 is suggested to be mediated by the NS3 helicase subdomain III and the NS5 RdRp thumb subdomain (Tay et al., 2015). However, data from this study is questionable because the SAXS data presented is severely biased by the artificial covalent fusion of the NS5 320-341 peptide to the C-terminus of the helicase subdomain III via a short linker, and conclusions drawn from the experiments might not be correct. Moreover, the model focusses on proteins only, and it fails to consider RNA as a component of the replicase complex. Further studies including both proteins as well as the replicative form of viral RNA are needed to elucidate the interactions between NS3 and NS5 within the Flavivirus RNA replicase complex during positive strand synthesis.

Rationale and hypothesis

Considering that viral replication requires the enzymatic activities of both NS3 and NS5 proteins, they have been shown to interact, and they most likely coordinate their respective activities during positive strand RNA synthesis, it is reasonable to hypothesize that the NS3:NS5 interaction within the replicase complex is essential for an efficient viral replication. In that case, this interaction could be an interesting target for the development of antiviral therapeutics. In the first place, however, the NS3:NS5 interaction needs to be well characterized and its precise role in viral replication needs to be elucidated.

Goals

#1: Develop a model of the interactions between NS3, NS5 and viral RNA as they would occur within the WNV replicase complex during positive strand synthesis, and determine the amino acid residues on both proteins that mediate the NS3:NS5 interaction.

#2: Introduce point mutations of the above-determined residues into the NS3 and NS5 coding sequences in expression vectors, express and purify recombinant NS3 and NS5

proteins (wild-type and mutant), and measure their interaction *in vitro* in the presence and absence of RNA. This will help validate the NS3:NS5 interaction model developed *in silico*.

#3: Introduce point mutations of the above-determined residues into a WNV replicon and evaluate the effect of these mutations on viral replication. These replicon assays will help validate the biochemical interaction assays and characterize the NS3:NS5 interaction in a more complex cellular environment.

MATERIALS AND METHODS

NS3:NS5 interaction model

An interaction model between NS3, NS5 and a single-stranded RNA was developed based on data already available in the literature, such as the crystal structures of the individual proteins, locations of active sites and known RNA-binding regions on both proteins. Homology structures of the full-length African Lineage II WNV proteins were generated on the Swissmodel Server (Arnold et al., 2006) using DENV NS3 (pdb 2vbc) and JEV NS5 (pdb 4k6m) as structure templates. The single-stranded RNA molecule was 20 nucleotides in length and had the random sequence GGUCAGUGUAACAACUGACC. The three macromolecules were then imported into Sculptor 2 (Wahle and Wriggers, 2015), a structural modeling program primarily used for fitting protein structures into low-resolution density maps. Manual docking was performed to generate a model representing interactions between NS3, NS5 and ssRNA within the replication complex during positive strand RNA synthesis.

Molecular dynamics simulations

In order to improve the interaction model generated by manual docking, it was subjected to molecular dynamics (MD) simulations using NAMD (Phillips et al., 2005). However, before starting the MD simulation, the interaction model was slightly modified. RNA was removed from the complex, and the full-length NS3 protein was replaced with the NS3 helicase domain bound to ssRNA (pdb 2jlu served as template for the homology structure of WNV NS3). This modified interaction model was developed with PyMOL (Schrödinger, LLC). So far, MD simulations have been carried out with the modified interaction model containing the two proteins only, in the absence of RNA. If an RNA molecule were included in the simulation, it would have to be actively pulled towards the RdRp catalytic site during the simulation to bring the proteins into a stable complex and to simulate protein translocation along the RNA, thus making the simulation much more complex. Moreover, by performing the simulation without RNA at first and with RNA later on, it will be

possible to compare the evolution of the complex and to determine if the RNA is important for retaining the overall structure of the replicase complex.

The dynamical evolution of the NS3:NS5 complex was monitored by exporting structures of the interaction model after various time points in the simulation and visual analysis of interaction distances between amino acid side chains between the NS3 and NS5 proteins was accomplished.

Recombinant proteins

Molecular cloning

The coding sequences of NS3 and NS5 were amplified from an African Lineage II West Nile replicon (Pierson et al., 2006) and cloned into bacterial expression vectors pET21b and pET28a, respectively. NS3 was fused in-frame with residues 49-66 of NS2B at its N-terminus as well as an HA-tag and a 6His-tag at its C-terminus whereas NS5 was fused in-frame with a 6His-tag at its N-terminus. In these contexts, expression of tagged proteins is driven by a T7 RNA polymerase promoter.

Protein expression

The plasmids pET21b-NS2B$_{49\text{-}66}$-NS3 and pET28a-NS5 were transformed into *E. coli* BL21(DE3) and *E. coli* Rosetta2(DE3)pLysS cells, respectively. 1L cultures of BL21(DE3)/pET21b-NS2B$_{49\text{-}66}$-NS3 and Rosetta2(DE3)pLysS/pET28a-NS5 were grown at 37°C in LB medium containing the appropriate selective antibiotic (100µg/ml ampicillin or 30µg/ml kanamycin, respectively) until the OD_{600} reached 0.5. The cultures were then incubated on ice for 30min. IPTG (BioShop, IPT001) and ethanol were added to final concentrations of 0.4mM and 2%, respectively, and the cultures were incubated at 18°C for 20h. Cells were harvested by centrifugation at 5000rpm for 10min in a Sorvall SLA-1500 rotor.

Protein purification

All procedures were performed at 4°C. Pelleted bacteria were resuspended in 30ml resuspension buffer (50mM Tris-HCl pH 7.5, 400mM NaCl, 10% sucrose, 25mM imidazole), and cells were lysed by adding lysozyme and Triton X-100 to final concentrations of 50µg/ml and 0.1%, respectively. The lysates were sonicated (2min, 5sec pulse on, 5sec pulse off) and insoluble material was removed by centrifugation at 10,000rpm for 45min in a Sorvall SS-34 rotor.

The soluble extract was applied to a 5ml HisTrap HP column (GE Healthcare, 17-5248-01) previously equilibrated with 25ml buffer A (50mM Tris-HCl pH 7.5, 400mM NaCl, 10% sucrose, 0.1% Triton X-100, 25mM imidazole) and connected to an ÄKTA Pure FPLC system (GE). The column was washed with 50ml buffer A, and proteins were eluted with a 25ml linear gradient from 0% buffer B (50mM Tris-HCl pH 7.5, 400mM NaCl, 10% sucrose, 0.1% Triton X-100, 25mM imidazole) to 100% buffer B. Purified protein was collected in 1.5ml fractions and stored at -80°C.

Fractions containing protein, as determined by SDS-PAGE and Coomassie blue staining, were further purified on a 120ml HiLoad 16/60 Superdex 200pg column (GE, 17-1069-01) connected to an ÄKTA Pure FPLC system (GE). A maximum of 5ml sample was applied to the column and eluted with 130ml GF buffer (50mM Tris-HCl, 400mM NaCl, 10% sucrose). 1.5ml fractions were collected, and protein purity was confirmed by SDS-PAGE (10% acrylamide) followed by Coomassie blue staining. Protein identity was confirmed by SDS-PAGE followed by western blotting with a primary Penta-His mouse antibody (Qiagen, 34660) or HA mouse antibody (Santa Cruz, sc-7392), both at a final concentration of 0.2µg/ml, and with a secondary anti-mouse HRP antibody (NEB, 7076). Purified protein was stored at -80°C.

WNV replicon

A WNV replicon (Pierson et al., 2006) was used to study viral replication levels (Figure 10). Upon transfection of this vector into cells, there is transcription of the replicon by RNA polymerase II, followed by translation into proteins (viral non-structural proteins and

FLuc). Once the viral proteins are synthesized, they assemble to form the viral genome replication complex that produces a large number of copies of the viral RNA that will be translated into proteins by the host cell. In order to determine luciferase activity that comes from viral replication only, an inactive replicon (mutation D668V in the RNA-dependent RNA polymerase active site of the NS5 protein (Gullberg et al., 2015)) is used to measure background luciferase activity coming from transcription of the replicon from the plasmid by RNA polymerase II and translation of these transcripts.

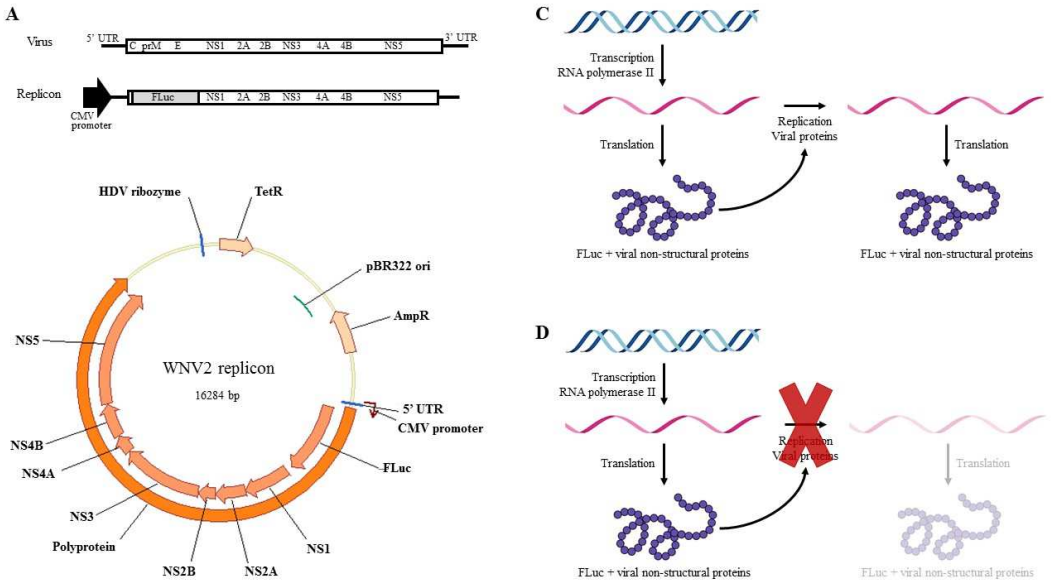

Figure 10. WNV replicon.

[A] The differences between the virus and the replicon are illustrated. First, the viral genome is a (+)ssRNA whereas the replicon is on a DNA plasmid downstream of a CMV promoter. Second, the structural proteins are replaced by a firefly luciferase (FLuc) reporter gene in the replicon. [B] Map of the replicon plasmid. [C and D] Schematic representation of processes taking place when the replicon is transfected into mammalian cells. In the case of the wild-type replicon (C), there is transcription of the replicon sequence on the plasmid by host cell RNA polymerase II, followed by translation of the transcripts. Once the viral non-structural proteins are synthesized, they form the replication complex that produces copies of the viral RNA that are then also translated into proteins. In the case of the replicon which contains the D668V mutation in the NS5 RdRp active site (D), the replication complex is inactive. The only source of luciferase and viral proteins in D668V mutants is translation of transcripts that were generated by host cell RNA polymerase II.

Site-directed mutagenesis

Site-directed mutagenesis of the WNV replicon was performed using the QuikChange method developed by Agilent. Two custom-made complementary DNA oligonucleotides, approximately 35 nucleotides in length, harboring the desired mutation in the center, were purchased from Integrated DNA Technologies. A polymerase chain reaction (PCR) was performed using 25ng of the wild-type WNV replicon as a template, 0.5µM of each oligonucleotide with the desired mutation, 0.5mM dATP (Sigma-Aldrich, D4788), 0.5mM dCTP (Sigma-Aldrich, D4913), 0.5mM dGTP (Sigma-Aldrich, D5038), 0.5mM dTTP (Sigma-Aldrich, T9656), 5% DMSO, 1.5X PfuUltra Reaction Buffer AD and 2.5U PfuUltra High-fidelity DNA Polymerase AD (Agilent, 600385) in a total volume of 25µl. After an initial denaturation at 92°C for 2min, 20 three-step cycles (denaturation at 92°C for 50sec, annealing at 60°C for 50sec and elongation at 68°C for 34min) as well as a final elongation at 68°C for 10min were carried out. The sample was then subjected to a restriction digest with 1µl DpnI (NEB, R0176S) to degrade template DNA. 5µl of the digested PCR product was then transformed into *Escherichia coli* XL1 blue cells. Transformants were grown on LB plates containing 100µg/ml ampicillin at 37°C over night.

A few isolated colonies were picked and grown in 5ml LB medium containing 100µg/ml ampicillin at 37°C over night. Plasmid DNA was extracted using a commercially available miniprep kit according to the manufacturer's instructions (Sigma-Aldrich, PLN350). Purified plasmid DNA was sequenced to confirm the introduction of the desired mutation into the replicon. In order to obtain sufficient amounts of the replicon for downstream applications, plasmid DNA was extracted from a 100ml overnight culture using a midiprep (Sigma-Aldrich, NA0200) or maxiprep (OMEGA bio-tek, D6922) kit.

Luciferase assay

BHK17 cells were grown at 37°C and 5% CO_2 in DMEM (Wisent, 319-015-CL) supplemented with 10% FBS (Wisent, 080-150) and 1mM sodium pyruvate (Wisent, 600-110-EL). 24h prior to transfection, cells were seeded into 12-well plates at a concentration of 50,000 cells per well. They were then transfected with 250ng of the replicon using 0.5µl

Lipofectamine 2000 transfection reagent (Invitrogen, 11668019) in opti-MEM (Gibco, 31958070). The luciferase activity was determined 48h post-transfection by mixing 10µl of cell lysate (total amount of lysate for each well: 200µl) with 50µl of luciferase assay substrate (Promega, E4550) and measuring emitted light with a GloMax 20/20 Luminometer (Promega). Data was collected from at least three independent experiments, each containing triplicates. Luciferase activity from the wild-type replicon was fixed at 100%, and luciferase activity from each mutant was expressed relative to the wild-type. A one-sample t-test with a hypothetical value of 100 was performed for each mutant. Mutants with a p-value below 0.05, 0.005, 0.001 and 0.0001 were labelled with 1 star, 2 stars, 3 stars and 4 stars, respectively.

RESULTS

NS3:NS5 interaction model

Initial model of the Flavivirus replicase complex

In order to study the NS3:NS5 interaction as it occurs within the viral replication complex, an interaction model including NS3, NS5 and RNA was developed based on data already available in the literature, as described above. The model of the replication complex was made with proteins from Lineage II WNV because a WNV replicon was available for subsequent testing of the model in the lab (Pierson et al., 2006). Known crystal structures of the individual full-length proteins as well as location of active sites and RNA binding regions were taken into account for the assembly of the three macromolecules into a complex. In the resulting model (Figure 11), the NS3:NS5 interaction is mediated by the NS3 helicase domain (subdomains 1 and 3) and the NS5 RdRp domain (fingers and thumb subdomains). Furthermore, the incoming dsRNA replication intermediate is separated into two individual strands by the NS3 helicase, the positive strand being guided into the NS5 capping enzyme to undergo GTase and MTase reactions for the formation of a complete cap structure, and the negative strand being guided through the NS3 helicase domain and into the NS5 polymerase domain to serve as template for the synthesis of a new positive strand of viral RNA. This way, most of the different enzymatic activities are well coordinated for efficient viral replication. Only the NS3 NTPase/RTPase active site is out of position for the positive strand to undergo the RTPase reaction before being fed into the NS5 capping enzyme domain. However, since this is a preliminary model, the proteins may rotate in relation to each other as the model is further developed, and the final position of the NTPase/RTPase active site may change.

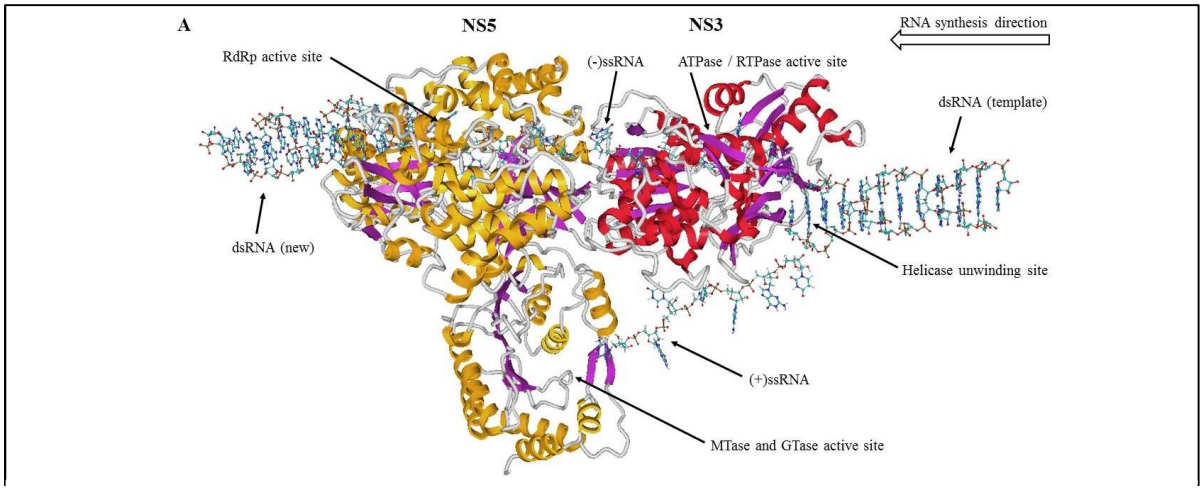

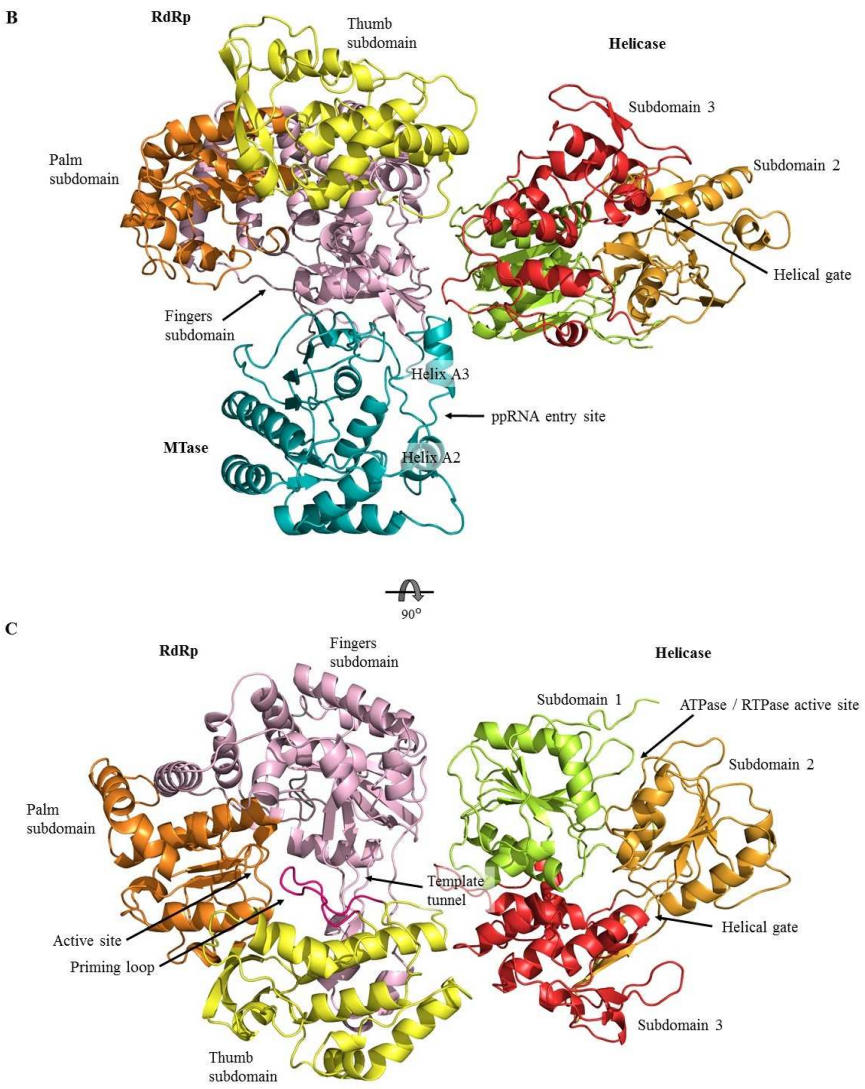

Figure 11. Initial NS3:NS5 interaction model.

A model for the interaction between NS3, NS5 and RNA within the viral RNA replication complex during positive strand synthesis is shown. NS3 and NS5 interact via their helicase and RdRp domain, respectively. [A] NS3 is colored in red, NS5 is colored in orange and RNA is colored in blue. [B and C] Only the two proteins are shown, and their subdomains are differently colored. The NS3:NS5 complex is shown from a side view (B) and from a top view (C). In the top view, it is apparent that the RNA binding tunnel of NS3 is in line with the template tunnel of NS5.

Hydrogen bonds between the two proteins as well as all residues involved in these interactions were identified using PyMOL (Figure 12). Three hydrogen bonds were identified: NS3 V276 – NS5 K314, NS3 N278 – NS5 K314 and NS3 K532 – NS5 G750. More precisely, the oxygen atom of the NS3 V276 backbone interacts with a hydrogen

atom of the amino group on the NS5 K314 side chain, the oxygen atom of the amide group on the NS3 N278 side chain interacts with another hydrogen atom of the amino group on the NS5 K314 side chain, and a hydrogen atom of the amino group on the NS3 K532 side chain interacts with the oxygen atom of the NS5 G750 backbone. In addition, several other residues were found to point toward the area between the two proteins, suggesting that they might also participate in the interaction: NS3 R218, NS3 R250, NS3 H274, NS3 R275, NS3 E529, NS5 S292, NS5 E312 and NS5 E416.

A

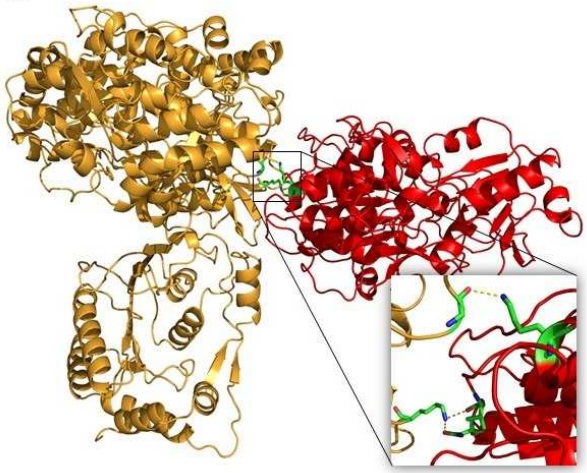

B

NS3	NS5
V276	K314
N278	K314
K532	G750

C

NS3	NS5
R218	S292
R250	E312
H274	E416
R275	
E529	

Figure 12. Interactions between NS3 and NS5 in the initial interaction model.

[A] Three hydrogen bonds between the two proteins were found. [B] Residues involved in these interactions. [C] Other residues at the interface between the two proteins that might participate in interactions.

Molecular dynamics simulations

Equilibrated model

In the interest of improving the NS3:NS5 interaction model, it was submitted to a molecular dynamics simulation. The first simulation was very short and it served to equilibrate the complex. During this short simulation, the two proteins were found to rotate in relation to each other. The interaction surface was increased and eight hydrogen bonds between NS3 and NS5 were identified: NS3 R185 – NS5 E416, NS3 K187 – NS5 E416, NS3 R216 – NS5 E426, NS3 E306 – NS5 K314, NS3 N503 – NS5 G317, NS3 E523 – NS5

R45, NS3 R5225 – NS5 E46 and NS3 R527 – NS5 E46. Of the residues involved in these interactions, only one was involved in interactions in the initial model (Figure 13).

A

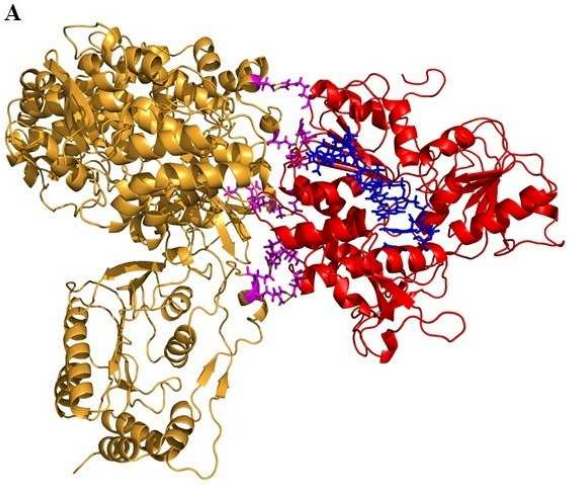

B

NS3	NS5
R185	E416
K187	E416
R216	E426
E306	K314
N503	G317
E523	R45
R525	E46
R527	E46

Figure 13. Equilibrated NS3:NS5 interaction model.

[A] Eight hydrogen bonds between the two proteins were found. [B] Residues involved in these interactions.

Progression of NS3:NS5 interactions through a 220ns molecular dynamics simulation

The equilibrated model was subjected to further molecular dynamics simulations. So far, the simulation has been carried out for approximately 220ns, and the evolution of the complex has been monitored at various time points (Figure 14). Its global structure remained almost unchanged compared to the equilibration simulation. The two proteins rotated approximately 20° in relation to each other during the first 100ns and then remained mostly static, and only small movements were observed. The interactions between NS3 and NS5 were sampled at 15ns, 25ns, 100ns, 140ns, 160ns and 220ns during the simulation (Figure 15). The number of hydrogen bonds between the two proteins varied between five and ten, and residues involved in these interactions also varied during the simulation. Even though the interacting pairs fluctuated, many residues involved in interactions at one instant were still involved in interactions in later time points, only with a different interacting partner (e.g. NS5 K314). Some interactions appeared, stayed stable for some time and then disappeared (e.g. NS3 K186 – NS5 E289). Other interactions were maintained during almost the entire simulation (e.g. NS3 R216 – NS5 D430).

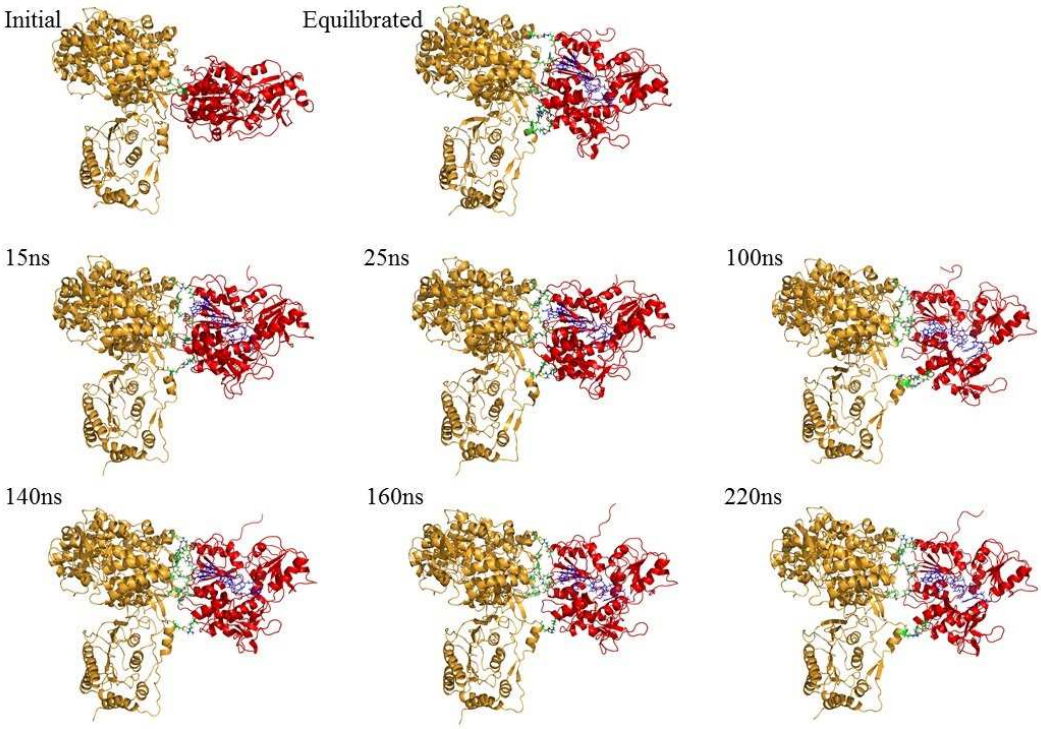

Figure 14. Evolution of the interaction model during MD simulation.

The global structure of the NS3:NS5 complex at different time points during the molecular dynamics simulation is displayed.

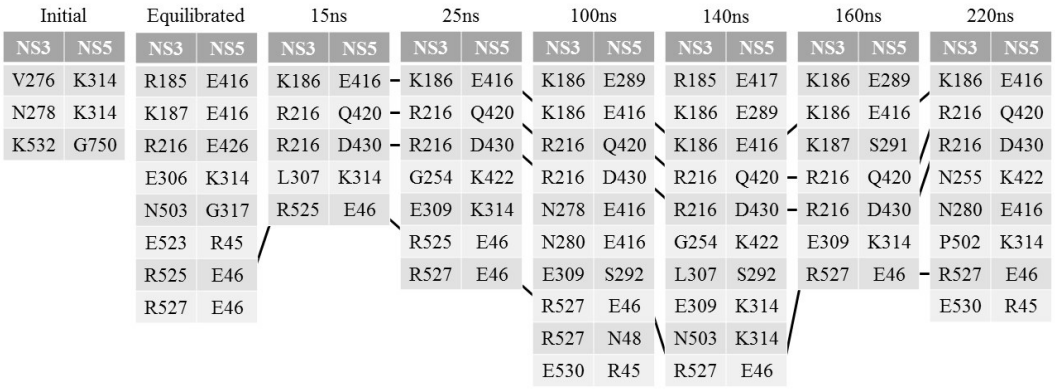

Figure 15. Interactions between NS3 and NS5 at various time points in the MD simulation.

Interacting residues within the NS3:NS5 complex at different time points during the molecular dynamics simulation are listed. Interactions that are maintained between different times are connected with lines.

In general, the longer an interaction is stable during a molecular dynamics simulation, the higher the chances that this interaction actually takes place *in vivo*. Therefore, the NS3:NS5

interaction model seems to be a quite good model of the real interaction between NS3 and NS5. It is expected that the residues that mediate the interaction vary slightly over time considering that all interactions are dynamic.

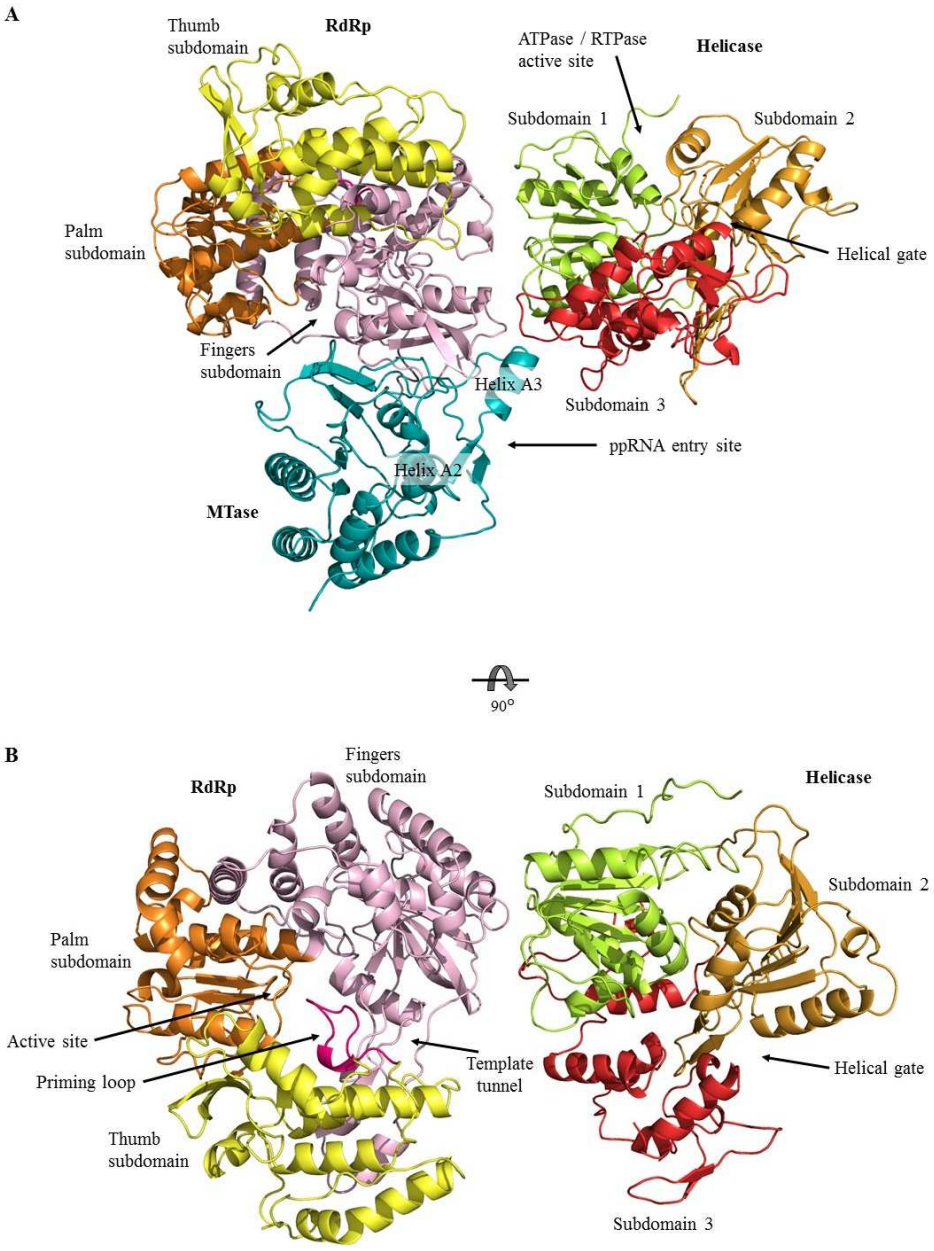

Figure 16. Interaction model after 220ns MD simulation.

[A] Side view. [B] Top view. During the MD simulation, the NS3 and NS5 rotated in relation to each other (note that the MD simulation did not include RNA which would restrict the degrees of freedom of the complex). The helical gate, the NS3 RNA binding tunnel and the NS5 RNA template channel are still aligned. However, the NS3 RTPase active site is no longer near the NS5 capping enzyme domain.

The overall evolution of the NS3:NS5 complex is quite interesting. As shown in Figure 16, the RNA-binding tunnel of the NS3 helicase domain and the RNA template channel of the NS5 RdRp domain are still aligned, allowing the negative strand RNA to be fed into the polymerase after dsRNA unwinding at the helical gate. However, the two proteins rotated in relation to each other, and the ATPase/RTPase active site moved even further away from the capping enzyme domain. Therefore, the positive strand RNA would be able to undergo the first step of the capping reaction at the RTPase site, but it would not be near the capping enzyme domain for the two other reactions. Nevertheless, the model presented here may be valid. The NS5 protein has been shown to be flexible, and various conformations and relative orientations of the two domains have been reported (Bussetta and Choi, 2012; Lu and Gong, 2013; Zhao et al., 2015b). It is possible that the crystal structure of NS5 used for the development of the NS3:NS5 interaction model is not in the right conformation for positive strand synthesis, and that the MTase domain is actually positioned in a way that would allow the coupling of the RTPase, GTase and MTase reactions. Alternatively, the replicase complex may have a stoichiometry other than 1:1, and the positive strand RNA may be fed into the capping enzyme domain of a different NS5 protein within the complex.

Production of recombinant proteins for protein interaction analysis

In order to test the NS3:NS5 model developed *in silico*, an *in vitro* interaction assay which uses purified proteins is currently being developed. Both NS3 and NS5 have been cloned into expression vectors for the production of recombinant proteins in *E. coli*. Point mutations of the amino acid residues that mediate the NS3:NS5 interaction per the interaction model presented here were introduced into the NS3 and NS5 coding sequences. Once expressed and purified, these proteins (wild-type and mutants) can be used to measure the interaction between NS3 and NS5 in the presence and absence of RNA *in vitro*. Moreover, the effects of the mutations on the enzymatic activities of NS3 and NS5 can be assessed to further characterize the role of the mutated residues.

Protein expression

Expression of recombinant NS2B$_{49\text{-}66}$-NS3-HA-6His and NS5-6His was tested in three different strains of *Escherichia coli* (Figure 17). Expression of NS2B$_{49\text{-}66}$-NS3 was found to be optimal in BL21(DE3) cells whereas expression of NS5 was maximal in Rosetta2(DE3)pLysS cells.

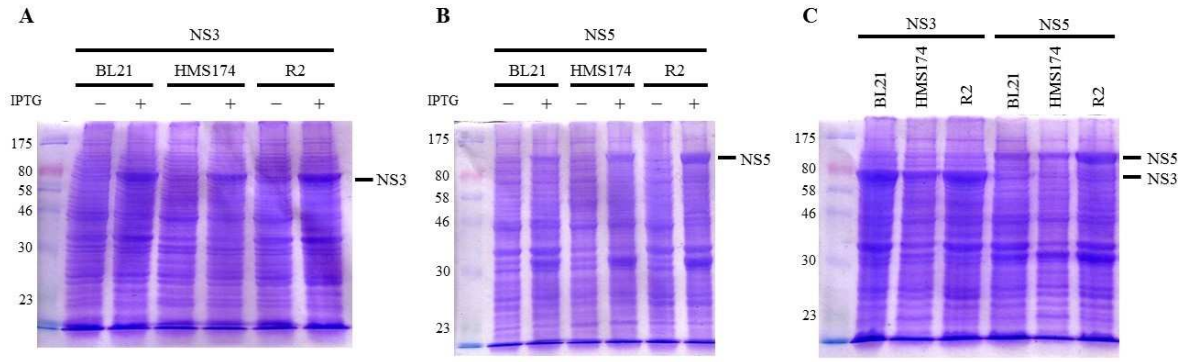

Figure 17. Expression of recombinant proteins in different *E. coli* strains.

Expression of both NS2B$_{49\text{-}66}$-NS3 and NS5 was tested in BL21(DE3) cells, HMS174(DE3) cells and Rosetta2(DE3)pLysS cells. [A] Bacterial lysates before and after the induction of NS2B$_{49\text{-}66}$-NS3 expression. [B] Bacterial lysates before and after the induction of NS5 expression. [C] Bacterial lysates after the induction of NS2B$_{49\text{-}66}$-NS3 and NS5 expression.

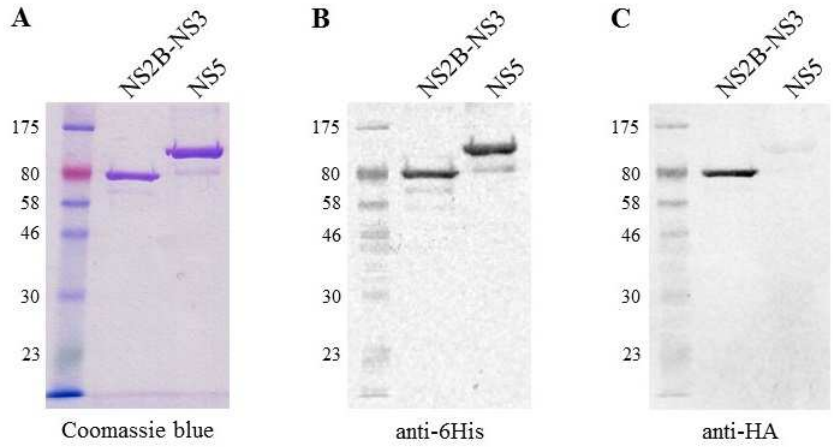

Figure 18. Purification of recombinant proteins.

Purified proteins were analyzed by SDS-PAGE. [A] Protein purity was confirmed by Coomassie blue staining. [B] Both NS2B$_{49\text{-}66}$-NS3-HA-6His and NS5-6His were revealed on an anti-6His western blot. [C] Only NS2B$_{49\text{-}66}$-NS3-HA-6His was revealed on an anti-HA western blot.

Protein purification

Given that both NS2B$_{49\text{-}66}$-NS3 and NS5 are fused in-frame with a 6His tag, both proteins were purified by affinity chromatography on a HisTrap HP column. Full-length proteins were co-purified with the individual domain that contained the 6His-tag (data not shown). Therefore, eluates were further purified by size exclusion. Full-length proteins were successfully separated from the individual domains (Figure 18).

To date, out of 54 mutants to be made, 47 have been confirmed by sequencing, 43 have been expressed, 24 have been purified by affinity chromatography and 16 have been purified by gel filtration chromatography (Appendix 5). As the project moves forward, they will be tested in biochemical assays. These experiments will help characterize the NS3:NS5 interaction in the presence and absence of RNA *in vitro* and prove or disprove the interaction model presented here (see discussion).

Assessment of potential interacting residues on viral replication efficiency

A WNV replicon (Pierson et al., 2006) was used for further testing of the interaction model and characterization of the NS3:NS5 interaction in a more complex cellular environment. Point mutations of residues involved in the NS3:NS5 interaction were introduced into the WNV replicon, and the effect of these mutations on viral replication was determined.

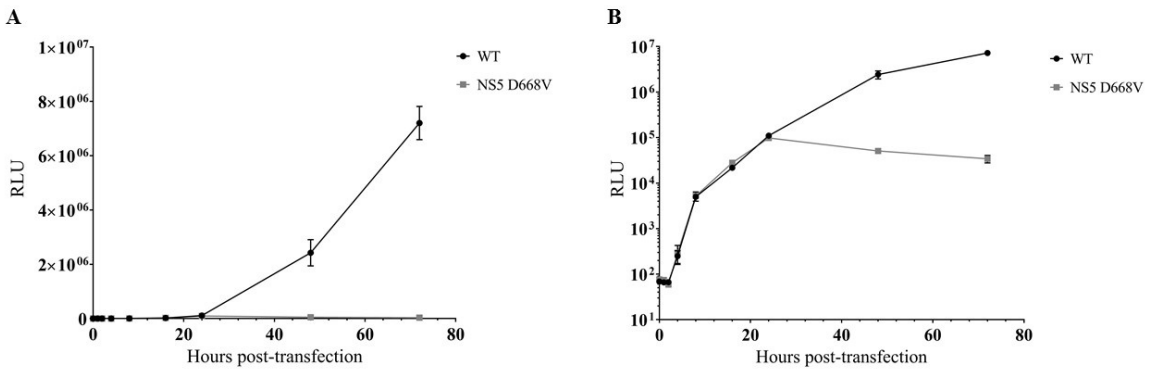

Figure 19. WNV replicon time course.

The wild-type WNV replicon as well as the inactive NS5 D668V mutant were transfected into cells, and luciferase activity was measured at 1h, 2h, 4h, 8h, 16h, 24h, 48h and 72h post-transfection. Results are shown on a linear scale [A] and on a logarithmic scale [B].

A time course experiment with the WNV replicon was conducted to determine how long it takes for the replicon plasmid to be transcribed and translated into viral proteins that form an active replication complex (Figure 19). As soon as 4h post-transfection, luciferase activity began to increase, indicating that the replicon plasmid had entered cells and was being transcribed, and the resulting transcripts were translated into proteins. Up to 24h post-transfection, the luciferase activity from the wild-type replicon as well as from the inactive NS5 D668V mutant were the same, suggesting that there was only transcription of the replicon from the plasmid by RNA polymerase II and translation of these transcripts but no activity of the viral replication complex. At 48h and 72h post-transfection, there was a 47.8-fold and a 210.7-fold difference in the luciferase activity of cells transfected with the wild-type replicon and the NS5 D668V mutant, respectively. These results indicate that most of the luciferase activity measured after 48h is attributable to viral replication. Therefore, all subsequent luciferase assays were performed at 48h post-transfection.

Mutants from the initial model

Residues potentially involved in the NS3:NS5 interaction according to the initial interaction model (Figure 12) were mutated on the WNV replicon, and the effect of these mutations on viral replication was determined (Figure 20, Appendix 6). More precisely, the residues involved in hydrogen bonds between NS3 and NS5 were substituted by alanine (Figure 19a) as well as by similar residues (Figure 20b). Potential compensatory mutations were also made (Figure 20c). Finally, several other residues at the interface between the two proteins were substituted by alanine (Figure 20d).

Mutants could be divided into three groups: some had little to no effect on viral replication, some had a moderate effect and some severely affected replication. Substitution of NS3 V276 with alanine and leucine reduced replication to 5.7% and 62.9%, respectively. Interestingly, modifications on the side chain of NS3 V276 affects the level of viral replication, although the interaction with NS5 would be mediated by its backbone according to our model. Substitution of NS3 N278 with alanine, aspartate and glutamine yielded replication levels of 41.3%, 4.4% and 52.0%, respectively. These results indicate that the amide group on the side chain is important, possibly for the interaction with NS5 as

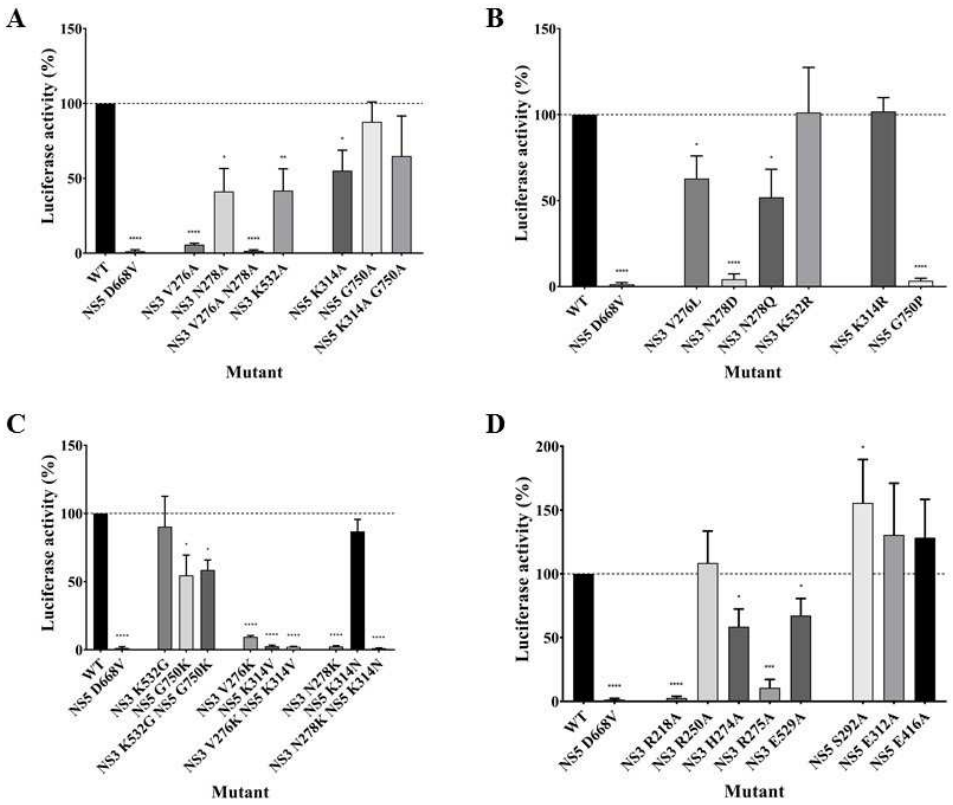

Figure 20. Viral replication levels of mutants based on the initial interaction model.

[A] Alanine substitutions of the residues involved in interactions. [B] Conservative mutations of the residues involved in interactions. [C] Compensatory mutations. [D] Alanine substitutions of other residues possibly involved in interactions.

suggested by the interaction model. In addition, the length of the side chain seems to play an important role, since it is the only difference between asparagine and glutamine, but substitution of the asparagine by glutamine reduces replication to 52.0%. The double mutant NS3 V276A-N278A severely affects viral replication with a residual level of 1.5%. Most of the effect can be attributed to the substitution of V276, although the substitution of N278 seems to contribute given that replication of the V276A mutant alone was slightly higher with 5.7%. Substitution of NS3 K532 to alanine and arginine produced replication levels of 41.9% and 101.3%, respectively, suggesting that a basic group at this position is of importance. Very similar results were observed for the mutation of NS5 K314 to alanine and arginine, yielding replication levels of 55.2% and 102.0%, respectively. Substitution of NS5 G750 with alanine and proline resulted in 87.7% and 3.5% replication, respectively. These results indicate that this glycine does not interact with the NS3 protein. The drastic

reduction of replication in the G750P mutant is most likely due to a change in the local structure that displaces other residues involved in the NS3:NS5 interaction. The double mutant NS5 K314A-G750A reduced replication to 64.9% which is close to the residual replication of the K314A mutation alone, confirming that G750 does not participate in the interaction with NS3. In order to further investigate if the identified residues really interact with each other, compensatory mutants were made. If two residues interact, then mutating one of them would disrupt the interaction, but mutating both of them would re-establish the interaction and thus viral replication. None of the three double mutants yielded a higher replication level than the corresponding individual mutants, suggesting that those particular residues do not interact directly. Finally, among the other residues at the interface between the two proteins, NS3 R218 and NS3 R250 were found to be critical since their substitution by alanine caused replication to drop to 2.7% and 10.7%, respectively. Substitution of NS3 H274, NS3 E529 and NS5 S292 had a moderate effect on viral replication, and mutation of NS3 R250, NS5 E312 and NS5 E416 did not significantly affect replication. Overall, some residues involved in interactions according to the model were shown to be crucial for efficient viral replication whereas others seemed to be of little importance. These results were expected, since all mutants were based on a preliminary interaction model developed by manual docking, and it was unlikely that all residues that are critical for the NS3:NS5 interaction would have been identified right away. Nevertheless, this model was a very good starting point for the detailed characterization of the interaction between NS3 and NS5.

Mutants from models during the molecular dynamics simulations

Mutants from the equilibrated model

All the residues involved in hydrogen bonds per the equilibrated model were mutated in the WNV replicon, and viral replication was measured for each mutant (Figure 21, Appendix 6).

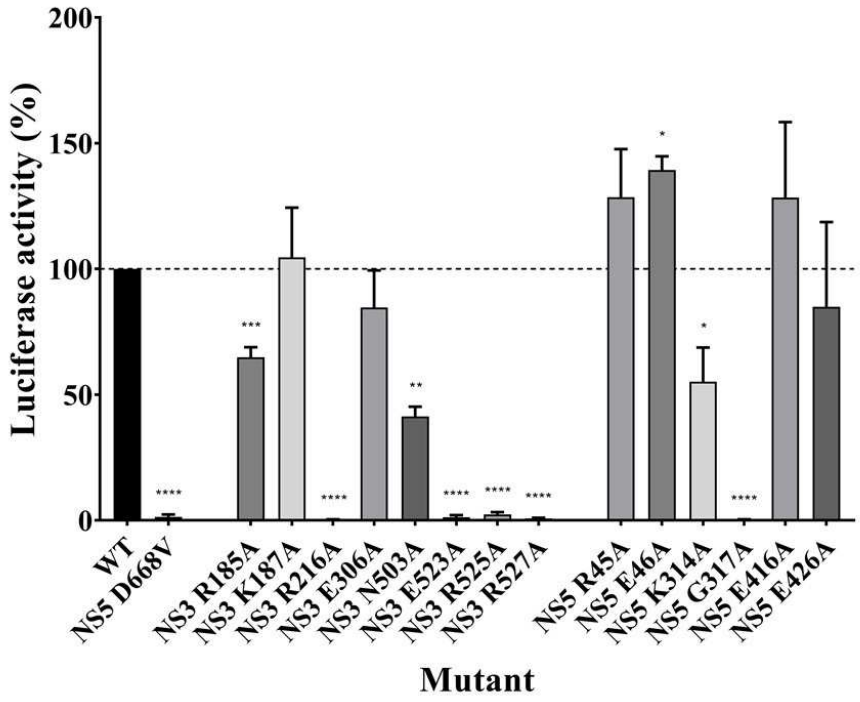

Figure 21. Viral replication levels of mutants based on the equilibrated interaction model.

Residues involved in hydrogen bonds according to the equilibrated interaction model were substituted by alanine in the WNV replicon and the effects of those mutations on viral replication were measured.

Alanine substitutions of residues R216, E523, R525 and R527 on NS3 were found to drastically reduce viral replication to 0.2%, 1.2%, 2.3% and 0.8%, respectively. In addition, substitution of NS3 R185 and NS3 N503 moderately reduced replication to 64.8% and 41.3%, respectively. Mutations of NS3 K187 and NS3 E306 had no significant effect on replication. Only one alanine substitution on NS5 had a severe effect on replication: the G317A mutant yielded 0.3% replication. Substitution of NS5 K314 reduced replication to 55.2%, substitution of NS5 R45, E416 and E426 did not significantly affect replication, and substitution of NS5 E46 by alanine even increased replication to 139.3%. The identification of four additional residues on NS3 that abolish viral replication suggests that this region on NS3 is indeed crucial for replication, presumably because of its interaction with NS5. However, given that only one mutation on NS5 greatly reduced replication, the model needs to be further improved to identify the region on NS5 that interacts with NS3.

Mutants from models at different times during the 220ns molecular dynamics simulation

All residues involved in hydrogen bonds at some time during the molecular dynamics simulation were mutated in the replicon and viral replication was measured for each mutant (Figure 22, Appendix 6). As before, the mutants can be divided into three groups. Some have little to no effect on viral replication, some have a moderate effect and some severely impair replication. Interestingly, there are more NS3 mutants than NS5 mutants that are deleterious for replication. Furthermore, among the mutants that allow replication, mutations on NS3 generally have a greater negative effect on replication than mutations on NS5 (Figure 23, Appendix 6). These finding suggest that the surface region on NS3 in which the mutated residues are clustered is important for viral replication, presumably because it mediates the interaction with NS5. However, the corresponding region on NS5 has not been entirely determined, and further MD simulations are necessary.

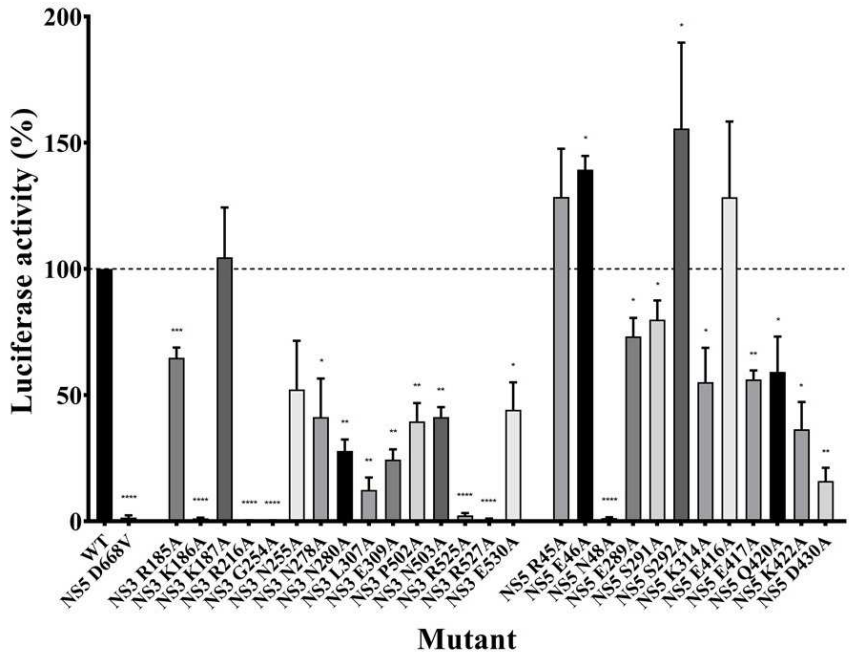

Figure 22. Viral replication levels of mutants based on models at various time points in the MD simulation.

Residues involved in hydrogen bonds at 15ns, 25ns, 100ns, 140ns, 160ns and/or 220ns into the MD simulation were substituted by alanine in the WNV replicon and the effects of those mutations on viral replication were measured.

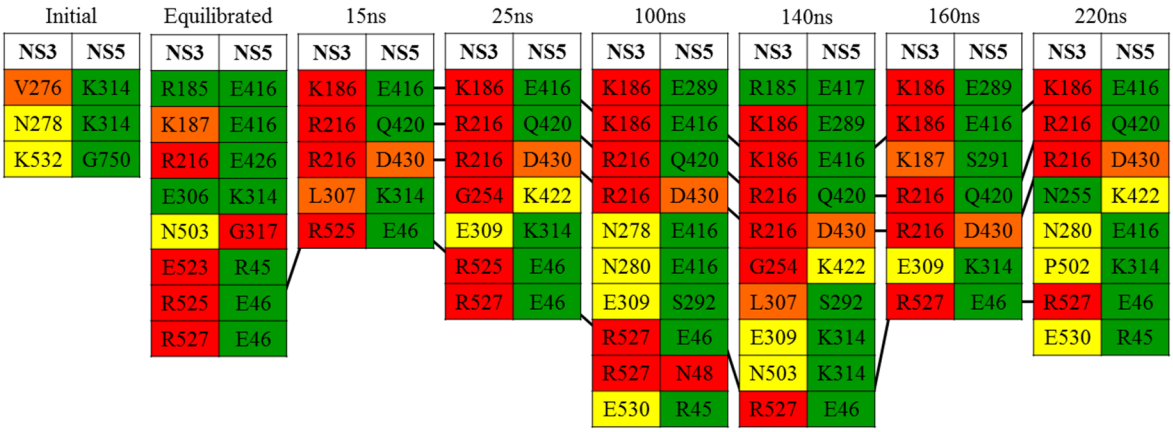

Figure 23. Interacting residues at different time points during the MD simulation and the importance of those residues for viral replication.

Interacting residues within the NS3:NS5 complex at different time points during the molecular dynamics simulation are shown. Residues are colored according to viral replication levels when they substituted by alanine. Residues that show <5% replication are red, 5-20% are orange, 20-50% are yellow and >50% are green.

DISCUSSION

A preliminary interaction model of the WNV replicase complex which includes NS3, NS5 and viral RNA has been developed. Data already available in the literature, such as crystal structures of the individual proteins, locations of catalytic active sites and known RNA-binding regions were taken into account, and the three macromolecules were assembled in a way that would allow coupling of the respective enzymatic activities of NS3 and NS5 and thus favour efficient viral replication. The resulting NS3:NS5 complex without RNA was submitted to a molecular dynamics simulation of approximately 220ns, and its evolution was monitored at various time points during the simulation. For all versions of the NS3:NS5 interaction model (initial model and models during the MD simulation), the amino acid residues that mediate the interaction between NS3 and NS5 were determined. These residues were substituted by alanine in a WNV replicon, and the effects of these mutations on viral replication were evaluated. In general, mutants could be divided into three groups: some had little effect on replication, some had a moderate effect, and some severely impaired replication. More precisely, alanine substitution of K186, R216, R218, G254, E523, R525 and R527 on NS3 as well as N48 and G317 on NS5 reduced viral replication to less than 5% of the wild-type replicon.

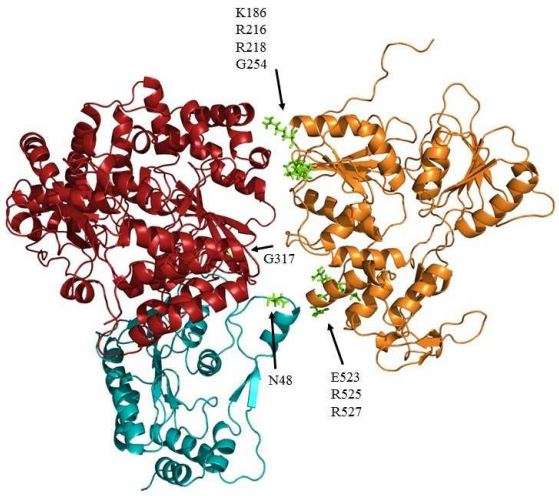

Figure 24. Mutations that severely affect viral replication.

Residues whose substitution by alanine reduces viral replication to less than 5% of the wild-type replicon were mapped onto the NS3:NS5 interaction model after 220ns of MD simulation and displayed as green sticks.

Residues K186, R216, R218 and G254 are located on the NS3 helicase subdomain 1 whereas E523, R525 and R527 are located on subdomain 3. Regarding the two residues on NS5, N48 is part of the capping enzyme domain and G317 is located on the RdRp fingers subdomain (Figure 24). These findings are slightly different from results obtained by other groups who have suggested that the NS3:NS5 interaction is mediated by the NS3 helicase domain and the NS5 RdRp domain, with residues 566-585 of the helicase subdomain III and residues 320-341 of the RdRp thumb subdomain being essential for the interaction (Tay et al., 2015; Zou et al., 2011). However, when these two regions are placed in close proximity and the RNA-binding grooves of the NS3 helicase domain and the NS5 RdRp domain are aligned, the resulting NS3:NS5 complex does not appear functional (Figure 25).

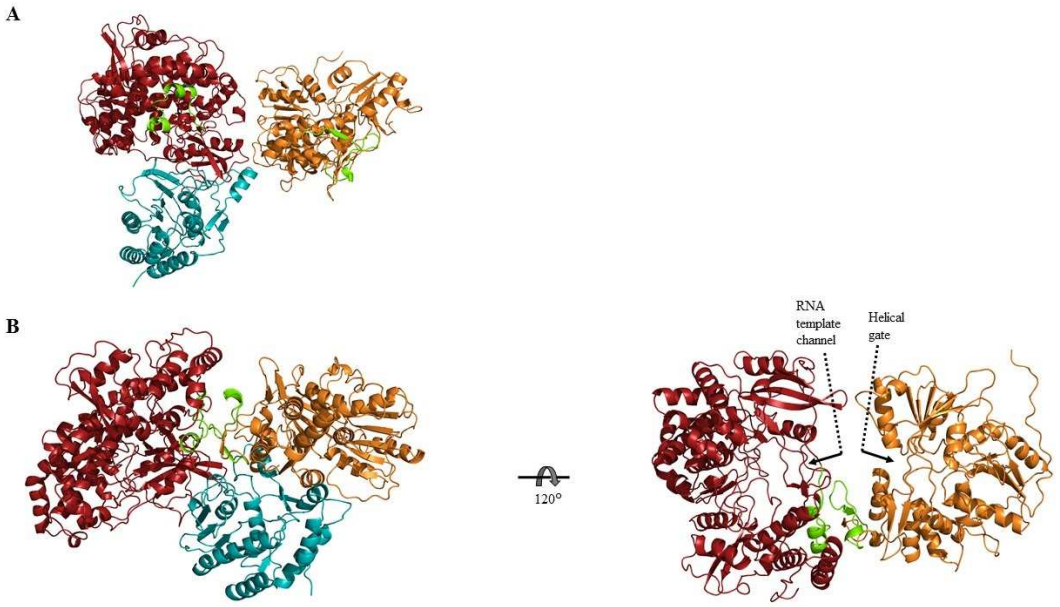

Figure 25. Comparison of our NS3:NS5 interaction model with findings of other groups.

[A] Residues NS3 566-585 and NS5 320-341 were mapped onto the NS3:NS5 interaction model after 220ns of MD simulation and colored in green. The NS3 helicase domain is colored in orange, the NS5 capping enzyme domain in teal, and the NS5 RdRp domain in red. [B] NS3 and NS5 were rotated in relation to each other to allow interaction of the above-mentioned regions, and the RNA-binding tunnels of the NS3 helicase domain and the NS5 RdRp domain were aligned.

The helical gate, where the dsRNA is split into two individual strands, is located close to the interface between NS3 and NS5, and there does not seem to be enough space to accommodate a dsRNA at this site. Moreover, the RNA-binding tunnels of the two proteins

are aligned, but the RNA would flow through the NS3 helicase and the NS5 RdRp in opposite directions, which seems very unlikely. Therefore, residues 566-585 of NS3 and residues 320-341 of NS5 may mediate the interaction between the two proteins *in vitro* or it may be an experimental artifact due to the biased SAXS data, but this interaction is very improbable to occur within the replicase complex during positive strand synthesis *in vivo*. Our NS3:NS5 interaction model proposes an alternative means of interaction between these two proteins. In addition, as opposed to interaction models proposed by other groups, it takes into account how the proteins would actually work together at the molecular level during positive strand RNA synthesis, and it considers viral RNA as a replicase complex component.

Here I report the results from two different approaches used to test the preliminary NS3:NS5 interaction model, namely an *in silico* MD simulation and an *in vitro* replication assay (summarized in Figure 23). The MD simulation shows that the NS3:NS5 complex is relatively stable over time with four interactions (NS3 K186 – NS5 E416, NS3 R216 – NS5 Q420, NS3 R216 – NS5 D430, NS3 R527 – NS5 E46) being maintained during almost the entire simulation. This suggests that the seven residues involved in these four interactions are indeed important for the interaction between NS3 and NS5. However, when these residues are substituted in the WNV replicon and viral replication is determined for each mutant, only some mutations significantly reduce viral replication. More precisely, NS3 K186A, NS3 R216A, and NS3 R527A show less than 5% of replication compared to the wild-type, NS5 D430A shows approximately 16% of replication compared to the wild-type whereas NS5 E46A, NS5 E416A and NS5 Q420A show more than 50% of replication compared to the wild-type replicon. These results confirm that NS3 K186, NS3 R216, NS3 R527, and to a lesser extent NS5 D430 are important for viral replication, presumably because they contribute to the NS3:NS5 interaction. However, the results from the replication assay also suggest that NS5 E46, NS5 E416 and NS5 Q420 do not play an important role in viral replication, and might therefore not be crucial for the interaction between NS3 and NS5, which is inconsistent with the results from the MD simulation. This discrepancy highlights the need for further validation of the NS3:NS5 interaction model with at least one other method. Moreover, there is the possibility that the low replication

levels observed in the cell-based assay are due to another reason than the loss of the NS3:NS5 interaction, for example less expression of the viral proteins from the mutant replicons than from the wild-type replicon, or misfolding of the mutant proteins which leads to impaired catalytic activity. Therefore, validation of the preliminary results presented here is necessary to discard these possibilities and clearly link the loss of viral replication to the loss of NS3:NS5 interaction. For example, lysates from cells transfected with the replicons could be analyzed by western blotting to confirm that the protein expression levels from all mutant replicons is the same as from the wild-type replicon. This would require specific antibodies against the viral proteins, which are currently not commercially available, or fusing the viral proteins to tags that can be detected with specific antibodies. However, introducing tags into the replicon is likely to interfere with polyprotein processing and/or protein activity. Alternatively, recombinant NS3 and NS5 could be expressed in *E. coli* and purified to verify proper folding of all mutants using circular dichroism spectroscopy, and to test enzymatic activities using various *in vitro* assays. Theoretically, results from these experiments should be the same for wild-type and mutant proteins. Finally, an *in vitro* interaction assay would allow to directly measure the interaction between recombinant NS3 and NS5 (wild-type or mutant) and thus determine if there is a correlation between the loss of viral replication and the loss of protein-protein interaction. This would prove the importance of the NS3:NS5 interaction for replication and would provide evidence that this protein-protein interaction may be an interesting target for the development of antiviral compounds. Furthermore, it could be interesting to combine multiple mutations that greatly reduce the NS3:NS5 interaction and thus viral replication, for example NS3 K186A, NS3 R216A and NS3 R527A, and investigate if such a mutant virus could be a vaccine candidate. However, this would require an animal model as well as the infectious virus instead of the replicon, and since WNV is a biosafety level 3 pathogen, these experiments might be a bit more difficult to realize.

Future work

As mentioned earlier, further MD simulations are required to determine the surface region on NS5 that interacts with NS3, and RNA should be added to the two proteins for a better model of the replicase complex. Moreover, biochemical interaction data is needed to

confirm that loss in viral replication observed upon mutations in the WNV replicon is indeed due to loss of NS3:NS5 interaction.

In vitro NS3:NS5 interaction assay

Recombinant NS3 and NS5 proteins (wild-type and mutants) have been expressed in *E. coli* and purified by affinity and size exclusion chromatography. They will be used in a Biacore surface plasmon resonance (SPR) assay. These experiments will determine the binding affinity of the two proteins for each other (K_d) as well as the stoichiometry of the NS3:NS5 complex. Results from these assays will help prove or disprove the model presented here regarding the number of NS3 and NS5 proteins in the replicase complex. Moreover, by comparing the interaction between the two wild-type proteins and one mutant protein with the other wild-type protein, the results from these experiments will contribute to the determination of key residues for the NS3:NS5 interaction. In preparation for the SPR assay, the optimal pH for the amine coupling of an HA antibody to a CM5 chip has been determined (Figure 26).

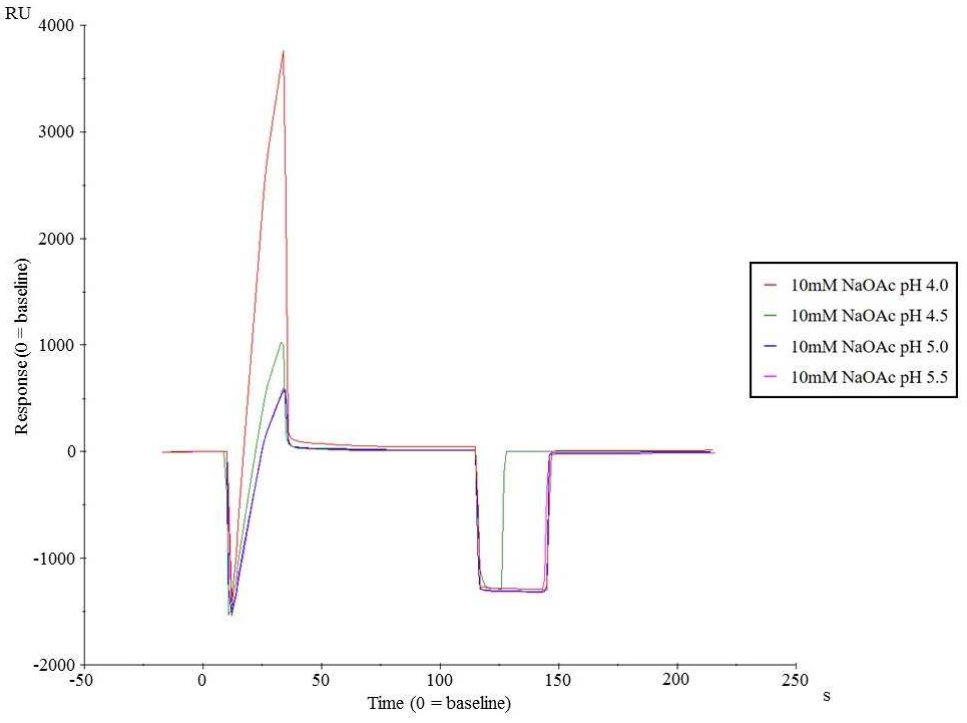

Figure 26. pH scouting for the amine coupling of the HA antibody to the CM5 chip.

The optimal pH for the covalent binding of the HA antibody to the CM5 chip was determined to be 4.0.

Once the HA antibody is covalently bound to the chip, purified HA-tagged NS3 will be injected and retained on the chip due to its affinity for the HA antibody. Then, purified NS5 will be injected and its binding to NS3 will be measured. Finally, both NS3 and NS5 will be washed off of the chip, and it will be ready for the next assay. Using this method, the affinity of all NS3 mutants for wild-type NS5 as well as the affinity of all NS5 mutants for wild-type NS3 will be determined. In addition, the K_d of the NS3:NS5 interaction in the presence and absence of RNA will be measured. If there is a correlation between the NS3:NS5 interaction *in vitro* and viral replication in cells, it will be reasonable to conclude that the NS3:NS5 interaction is essential for an efficient viral replication, and this interaction could be a new target for the development of antiviral drugs.

Flavivirus drug development

Despite several decades of research efforts, no specific antiviral drugs are currently available to treat and cure Flavivirus infections. Therefore, new antiviral strategies, including new drug candidates and/or new targets, are greatly needed. Understanding how Flaviviruses work on a molecular level, for example during positive strand RNA synthesis, will help in uncovering new points for therapeutic intervention.

NS3 and NS5 as drug targets

Given that both NS3 and NS5 have been well characterized, they have been studied as targets for antiviral drug development. Several compounds that inhibit one of the enzymatic activities of NS3 *in vitro* have been identified, yet none has been approved for clinical trials due to the lack of specific binding pockets for helicase inhibitors which likely leads to significant toxicity (Luo et al., 2015), or because of low specificity, permeability and stability in the case of protease inhibitors (Brecher et al., 2013; Lim et al., 2013b). As for NS5, few MTase inhibitors have been identified, most of which are not cell permeable and thus have not been further developed (Lim et al., 2015). Regarding the NS5 RdRp, many inhibitory compounds have been found, most of which did not reach the preclinical stage (Lim et al., 2015). Of the compounds that have been retained as drug candidates, one was associated with toxicity in preclinical trials (Yin et al., 2009), and one showed no efficacy

in a phase II clinical trial (Nguyen et al., 2013). One NS5 inhibitor is currently in a phase II/III clinical trial in Thailand (Lim et al., 2015; NIH, 2017).

So far, most studies aiming to identify antiviral drug candidates have focussed on searching inhibitors that target an active site of one of the domains of NS3 or NS5. However, compounds found using this approach may work well *in vitro*, but there is a considerable risk of non-specificity which is associated with toxic effects. In fact, the catalytic sites of viral enzymes resemble the catalytic sites of host cell enzymes that execute the same or a similar function, and it is challenging to develop inhibitors that target the viral enzyme without affecting the host cell enzyme (Lim et al., 2013b). One way to avoid these toxicity issues is to choose a target that is very specific to the virus, like the interaction between two viral proteins.

Protein-protein interactions as drug targets

Any interaction between viral proteins that is crucial for viral replication could be a potential drug target. So far, the NS2B:NS3 (Brecher et al., 2013; Chappell et al., 2008), NS3:NS4B (Zou et al., 2015a), NS4A:NS4B (Zou et al., 2015b) and NS3:NS5 (Takahashi et al., 2012; Zou et al., 2011) interactions have been proposed to be interesting targets for antiviral therapeutics. Since interactions between viral proteins most likely do not resemble any interaction between cellular proteins, they are potentially very specific targets, and inhibitors might be less likely to cause toxicity. In addition, given that the inhibitory compound does not need to mimic an endogenous molecule, there are many possible chemotypes that can bind efficiently (Mullard, 2012). In order to target a protein-protein interaction (PPI), this interaction needs to be structurally well characterized and key residues or binding regions on the proteins should be identified (Arkin and Wells, 2004). The detailed characterisation of the NS3:NS5 interaction presented here provides the basis for the search of compounds that might interfere with this protein-protein interaction and that might be interesting candidates for the development of specific drugs against Flaviviruses.

At this stage, two surface regions of NS3, involving residues K186/R216/R218/G254 and E523/R525/R527, as well as two residues on NS5, N48 and G317, have been shown to be critical for viral replication and could therefore be attractive targets for the development of inhibitory compounds of the NS3:NS5 interaction. Given that a single point mutation of any of these residues reduces viral replication to less than 5% of the wild-type, targeting only one of these four regions with an inhibitor will most likely be sufficient to disrupt the interaction between NS3 and NS5. In fact, it has been shown that only a small proportion of residues at protein-protein interfaces, which are clustered in so-called "hot spots", are critical for the interaction and confer most of the binding energy, and that PPI inhibitors bind these hot spots and not the entire protein-protein interface (Arkin et al., 2014). Regarding the nature of inhibitors, both small molecules and peptides have been shown to successfully interfere with PPIs (Arkin et al., 2014; Arkin and Wells, 2004). Therefore, once the NS3:NS5 interaction model is final, it can be used for *in silico* drug screening using Autodock or Autodock Vina and different drug libraries, and PPI hot spots on both NS3 and NS5 can be targeted. Compounds that have a good binding affinity can then be purchased and tested for their antiviral potential. At first, they could be used in an *in vitro* interaction assay to determine if they are able to interfere with the NS3:NS5 interaction. Next, cells transfected with the wild-type replicon could be treated with the potential inhibitors to assess their ability to restrict viral replication. Finally, it would be interesting to test their antiviral potential as well as their toxicity in the context of an actual infection, in cells and/or in an animal model.

Importance of the project & my contributions

I contributed to the project presented here in multiple ways. I visually analyzed the different stages of the NS3:NS5 interaction model developed *in silico* to determine the amino acid residues on both proteins that mediate the NS3:NS5 interaction. I also participated in the design of the wet lab experiments, and I carried out the *in vitro* and cell culture work. Finally, I generated the figures presented here and I wrote this thesis.

This project has moved the field forward by proposing the first model of the Flavivirus replicase complex that includes viral RNA as a major component of the complex and that

addresses how the NS3 and NS5 proteins would work together at the molecular level. Methods to test this model even in the absence of a co-crystal structure have been shown. Understanding how NS3 and NS5 interact within the replicase complex will help define the mechanism of positive strand synthesis and potentially uncover new points for therapeutic intervention.

ACKNOWLEDGEMENTS

First of all, I would like to thank my mentors Prof. Martin Bisaillon and Prof. Brian Geiss for giving me the opportunity to do exciting research under their supervision. I have appreciated their support and guidance during my master's project. In addition, Prof. Brian Geiss developed the initial NS3:NS5 interaction model that was the basis for my research.

I would like to acknowledge Kevin Votaw and Prof. Martin McCullagh at Colorado State University who did the molecular dynamics simulations on the initial interaction model.

I am grateful for the help with the molecular cloning of NS3 and NS5 into expression vectors, as well as discussions on various aspects of the project with Marie-Joëlle Doré, Maude Tremblay-Létourneau and Andréa Allaire.

I would like to thank all four members of the evaluation committee for accepting to read my master's thesis and providing comments on my work.

I would also like to thank the Faculté de Médecine et des Sciences de la Santé de l'Université de Sherbrooke for the generous scholarship.

Finally, I would like to express my gratitude to my parents Peter and Elisabeth as well as my boyfriend Philippe for their unconditional support and encouragements. I would also like to thank Philippe for helping me with creating or adapting figures and schematics.

LIST OF REFERENCES

Ackermann, M., Padmanabhan, R., 2001. De Novo Synthesis of RNA by the Dengue Virus RNA-dependent RNA polymerase Exhibits Temperature Dependence at the Initiation but Not Elongation Phase. J. Biol. Chem. 276, 39926–39937.

Aleshin, A.E., Shiryaev, S.A., Strongin, A.Y., Liddington, R.C., 2007. Structural evidence for regulation and specificity of flaviviral proteases and evolution of the Flaviviridae fold. Protein Sci. 16, 795–806.

Amanna, I.J., Slifka, M.K., 2014. Current trends in West Nile virus vaccine development. Expert Rev. Vaccines 13, 589–608.

Arkin, M.R., Tang, Y., Wells, J.A., 2014. Small-Molecule Inhibitors of Protein-Protein Interactions: Progressing toward the Reality. Chem. Biol. 21, 1102–1114.

Arkin, M.R., Wells, J.A., 2004. Small-Molecule Inhibitors of Protein-Protein Interactions: Progressing Towards The Dream. Nat. Rev. Drug Discov. 3, 301–317.

Arnold, K., Bordoli, L., Kopp, J., Schwede, T., 2006. The SWISS-MODEL workspace: a web-based environment for protein structure homology modelling. Bioinformatics 22, 195–201.

Ashour, J., Laurent-Rolle, M., Shi, P.-Y., García-Sastre, A., 2009. NS5 of Dengue Virus Mediates STAT2 Binding and Degradation. J. Virol. 83, 5408–5418.

Assenberg, R., Mastrangelo, E., Walter, T.S., Verma, A., Milani, M., Owens, R.J., Stuart, D.I., Grimes, J.M., Mancini, E.J., 2009. Crystal Structure of a Novel Conformational State of the Flavivirus NS3 protein: Implications for Polyprotein Processing and Viral Replication. J. Virol. 83, 12895–12906.

Bartelma, G., Padmanabhan, R., 2002. Expression, Purification, and Characterization of the RNA 5'-triphosphatase activity of Dengue Virus Type 2 Nonstructural Protein 3. Virology 299, 122–132.

Bazan, J.F., Fletterick, R.J., 1989. Detection of a Trypsin-like Serine Protease Domain in Flaviviruses and Pestiviruses. Virology 171, 637–639.

Benarroch, D., Egloff, M.-P., Mulard, L., Guerreiro, C., Romette, J.-L., Canard, B., 2004a. A Structural Basis for the Inhibition of the NS5 Dengue Virus mRNA 2'-O-Methyltransferase Domain by Ribavirin 5'-Triphosphate. J. Biol. Chem. 279, 35638–35643.

Benarroch, D., Selisko, B., Locatelli, G.A., Maga, G., Romette, J.-L., Canard, B., 2004b. The RNA helicase, nucleotide 5'-triphosphatase, and RNA 5'-triphosphatase activities of Dengue virus protein NS3 are Mg2+-dependent and require a functional Walker B motif in the helicase catalytic core. Virology 328, 208–218.

Benmansour, F., Trist, I., Coutard, B., Decroly, E., Querat, G., Brancale, A., Barral, K., 2017. Discovery of novel dengue virus NS5 methyltransferase non-nucleoside inhibitors by fragment-based drug design. Eur. J. Med. Chem. 125, 865–880.

Benzaghou, I., Bougie, I., Picard-Jean, F., Bisaillon, M., 2006. Energetics of RNA binding

by the West Nile virus RNA triphosphatase. FEBS Lett. 580, 867–877.

Boulton, R.W., Westaway, E.G., 1977. Togavirus RNA: Reversible Effect of Urea on Genomes and Absence of Subgenomic Viral RNA in Kunjin Virus-Infected Cells. Arch. Virol. 55, 201–208.

Brecher, M., Chen, H., Li, Z., Banavali, N.K., Jones, S.A., Zhang, J., Kramer, L.D., Li, H., 2015. Identification and Characterization of Novel Broad-Spectrum Inhibitors of the Flavivirus Methyltransferase. ACS Infect. Dis. 1, 340–349.

Brecher, M., Zhang, J., Li, H., 2013. The Flavivirus Protease As a Target for Drug Discovery. Virol. Sin. 28, 326–336.

Brecher, M.B., Li, Z., Zhang, J., Chen, H., Lin, Q., Liu, B., Li, H., 2015. Refolding of a fully functional flavivirus methyltransferase revealed that S-adenosyl methionine but not S-adenosyl homocysteine is copurified with flavivirus methyltransferase. Protein Sci. 24, 117–128.

Brooks, A.J., Johansson, M., John, A. V., Xu, Y., Jans, D.A., Vasudevan, S.G., 2002. The Interdomain Region of Dengue NS5 Protein That Binds to the Viral Helicase NS3 Contains Independently Functional Importin β1 and Importin α/β-Recognized Nuclear Localization Signals. J. Biol. Chem. 277, 36399–36407.

Bussetta, C., Choi, K.H., 2012. Dengue Virus Nonstructural Protein 5 Adopts Multiple Conformations in Solution. Biochemistry 51, 5921–5931.

Cao, X., Li, Y., Jin, X., Li, Y., Guo, F., Jin, T., 2016. Molecular mechanism of divalent-metal-induced activation of NS3 helicase and insights into Zika virus inhibitor design. Nucleic Acids Res. 44, 10505–10514.

Castle, E., Leidner, U., Nowak, T., Wengler, G., Wengler, G., 1986. Primary Structure of the West Nile Flavivirus Genome Region Coding for All Nonstructural Proteins. Virology 149, 10–26.

Centre for Integrative Bioinformatics Vrije Universiteit Amsterdam, 2017. PRALINE multiple sequence alignment [WWW Document]. URL http://www.ibi.vu.nl/programs/pralinewww/

Chambers, T.J., Grakoui, A., Rice, C.M., 1991. Processing of the Yellow Fever Virus Nonstructural Polyprotein: a Catalytically Active NS3 Proteinase Domain and NS2B Are Required for Cleavages at Dibasic Sites. J. Virol. 65, 6042–6050.

Chambers, T.J., Hahn, C.S., Galler, R., Rice, C.M., 1990a. Flavivirurs Genome Organization, Expression and Replication. Annu. Rev. Microbiol. 44, 649–688.

Chambers, T.J., Nestorowicz, A., Amberg, S.M., Rice, C.M., 1993. Mutagenesis of the Yellow Fever Virus NS2B Protein: Effects on Proteolytic Processing, NS2B-NS3 Complex Formation, and Viral Replication. J. Virol. 67, 6797–6807.

Chambers, T.J., Weir, R.C., Grakoui, A., McCourt, D.W., Bazan, J.F., Fletterick, R.J., Rice, C.M., 1990b. Evidence that the N-terminal domain of nonstructural protein NS3 from yellow fever virus is a serine protease responsible for site-specific cleavages in the viral polyprotein. Proc. Natl. Acad. Sci. U. S. A. 87, 8898–8902.

Chancey, C., Grinev, A., Volkova, E., Rios, M., 2015. The Global Ecology and Epidemiology of West Nile Virus. Biomed Res. Int. 2015, 376230.

Chandramouli, S., Joseph, J.S., Daudenarde, S., Gatchalian, J., Cornillez-Ty, C., Kuhn, P., 2010. Serotype-Specific Structural Differences in the Protease-Cofactor Complexes of the Dengue Virus Family. J. Virol. 84, 3059–3067.

Chappell, K.J., Stoermer, M.J., Fairlie, D.P., Young, P.R., 2008. West Nile Virus NS2B/NS3 Protease As An Antiviral Target. Curr. Med. Chem. 15, 2771–2784.

Chatel-Chaix, L., Fischl, W., Scaturro, P., Cortese, M., Kallis, S., Bartenschlager, M., Fischer, B., Bartenschlager, R., 2015. A Combined Genetic-Proteomic Approach Identifies Residues within Dengue Virus NS4B Critical for Interaction with NS3 and Viral Replication. J. Virol. 89, 7170–7186.

Chen, C.J., Kuo, M.D., Chien, L.J., Hsu, S.L., Wang, Y.M., Lin, J.H., 1997. RNA-Protein Interactions: Involvement of NS3, NS5, and 3' Noncoding Regions of Japanese Encephalitis Virus Genomic RNA. J. Virol. 71, 3466–3473.

Choi, K.H., Rossmann, M.G., 2009. RNA-dependent RNA polymerases from Flaviviridae. Curr. Opin. Struct. Biol. 19, 746–751.

Ciota, A.T., Kramer, L.D., 2013. Vector-Virus Interactions and Transmission Dynamics of West Nile Virus. Viruses 5, 3021–3047.

Coloma, J., Jain, R., Rajashankar, K.R., García-Sastre, A., Aggarwal, A.K., 2016. Structures of NS5 Methyltransferase from Zika Virus. Cell Rep. 16, 3097–3102.

Colpitts, T.M., Conway, M.J., Montgomery, R.R., Fikrig, E., 2012. West Nile Virus: Biology, Transmission, and Human Infection. Clin. Microbiol. Rev. 25, 635–648.

Coutard, B., Barral, K., Lichière, J., Selisko, B., Martin, B., Aouadi, W., Ortiz Lombardia, M., Debart, F., Vasseur, J.-J., Guillemot, J.C., Canard, B., Decroly, E., 2017. Zika Virus Methyltransferase: Structure and Functions for Drug Design Perspectives. J. Virol. 91, e02202-16.

Coutard, B., Decroly, E., Li, C., Sharff, A., Lescar, J., Bricogne, G., Barral, K., 2014. Assessment of Dengue virus helicase and methyltransferase as targets for fragment-based drug discovery. Antiviral Res. 106, 61–70.

Cui, T., Sugrue, R.J., Xu, Q., Lee, A.K.W., Chan, Y.-C., Fu, J., 1998. Recombinant Dengue Virus Type 1 NS3 Protein Exhibits Specific Viral RNA Binding and NTPase Activity Regulated by the NS5 Protein. Virology 246, 409–417.

Dong, H., Liu, L., Zou, G., Zhao, Y., Li, Z., Lim, S.P., Shi, P.-Y., Li, H., 2010. Structural and Functional Analyses of a Conserved Hydrophobic Pocket of Flavivirus Methyltransferase. J. Biol. Chem. 285, 32586–32595.

Egloff, M.-P., Benarroch, D., Selisko, B., Romette, J.-L., Canard, B., 2002. An RNA cap (nucleoside-2'-O-)-methyltransferase in the flavivirus RNA polymerase NS5: crystal structure and functional characterization. EMBO J. 21, 2757–2768.

Egloff, M.-P., Decroly, E., Malet, H., Selisko, B., Benarroch, D., Ferron, F., Canard, B., 2007. Structural and Functional Analysis of Methylation and 5′-RNA Sequence Requirements of Short Capped RNAs by the Methyltransferase Domain of Dengue Virus NS5. J. Mol. Biol. 372, 723–736.

Elizondo-Quiroga, D., Elizondo-Quiroga, A., 2013. West Nile Virus and its Theories, a Big Puzzle in Mexico and Latin America. J. Glob. Infect. Dis. 5, 168–175.

Erbel, P., Schiering, N., D'Arcy, A., Renatus, M., Kroemer, M., Lim, S.P., Yin, Z., Keller, T.H., Vasudevan, S.G., Hommel, U., 2006. Structural basis for the activation of flaviviral NS3 proteases from dengue and West Nile virus. Nat. Struct. Mol. Biol. 13, 372–373.

Erlanger, T.E., Weiss, S., Keiser, J., Utzinger, J., Wiedenmayer, K., 2009. Past, Present, and Future of Japanese Encephalitis. Emerg. Infect. Dis. 15, 1–7.

Evans, J.D., Seeger, C., 2007. Differential Effects of Mutations in NS4B on West Nile Virus Replication and Inhibition of Interferon Signaling. J. Virol. 81, 11809–11816.

Falgout, B., Pethel, M., Zhang, Y.-M., Lai, C.-J., 1991. Both Nonstructural Proteins NS2B and NS3 Are Required for the Proteolytic Processing of Dengue Virus Nonstructural Proteins. J. Virol. 65, 2467–2475.

Funk, A., Truong, K., Nagasaki, T., Torres, S., Floden, N., Balmori Melian, E., Edmonds, J., Dong, H., Shi, P.-Y., Khromykh, A.A., 2010. RNA Structures Required for Production of Subgenomic Flavivirus RNA. J. Virol. 84, 11407–11417.

Gebhard, L.G., Kaufman, S.B., Gamarnik, A. V., 2012. Novel ATP-Independent RNA Annealing Activity of the Dengue Virus NS3 Helicase. PLoS One 7, e36244.

Geiss, B.J., Thompson, A.A., Andrews, A.J., Sons, R.L., Gari, H.H., Keenan, S.M., Peersen, O.B., 2009. Analysis of Flavivirus NS5 Methyltransferase Cap Binding. J. Mol. Biol. 385, 1643–1654.

Gillespie, L.K., Hoenen, A., Morgan, G., Mackenzie, J.M., 2010. The Endoplasmic Reticulum Provides the Membrane Platform for Biogenesis of the Flavivirus Replication Complex. J. Virol. 84, 10438–10447.

Gorbalenya, A.E., Donchenko, A.P., Koonin, E. V., Blinov, V.M., 1989. N-terminal domains of putative helicases of flavi- and pestiviruses may be serine proteases. Nucleic Acids Res. 17, 3889–97.

Gullberg, R.C., Steel, J.J., Moon, S.L., Soltani, E., Geiss, B.J., 2015. Oxidative stress influences positive strand RNA virus genome synthesis and capping. Virology 475, 219–229.

Guyatt, K.J., Westaway, E.G., Khromykh, A.A., 2001. Expression and purification of enzymatically active recombinant RNA-dependent RNA polymerase (NS5) of the flavivirus Kunjin. J. Virol. Methods 92, 37–44.

Hammamy, M.Z., Haase, C., Hammami, M., Hilgenfeld, R., Steinmetzer, T., 2013. Development and Characterization of New Peptidomimetic Inhibitors of the West Nile Virus NS2B-NS3 Protease. ChemMedChem 8, 231–241.

Heinz, F.X., Allison, S.L., 2000. Structures and Mechanisms in Flavivirus Fusion. Adv. Virus Res. 55, 231–269.

Henderson, B.R., Saeedi, B.J., Campagnola, G., Geiss, B.J., 2011. Analysis of RNA Binding by the Dengue Virus NS5 RNA Capping Enzyme. PLoS One 6, e25795.

Hoenen, A., Liu, W., Kochs, G., Khromykh, A.A., Mackenzie, J.M., 2007. West Nile virus-induced cytoplasmic membrane structures provide partial protection against the interferon-induced antiviral MxA protein. J. Gen. Virol. 88, 3013–3017.

International Committee on Taxonomy of Viruses, 2015. Virus Taxonomy: 2015 Release [WWW Document]. URL http://www.ictvonline.org/virusTaxonomy.asp

Issur, M., Geiss, B.J., Bougie, I., Picard-Jean, F., Despins, S., Mayette, J., Hobdey, S.E., Bisaillon, M., 2009. The flavivirus NS5 protein is a true RNA guanylyltransferase that catalyzes a two-step reaction to form the RNA cap structure. RNA 15, 2340–2350.

Jain, R., Coloma, J., García-Sastre, A., Aggarwal, A.K., 2016. Structure of the NS3 helicase from Zika virus. Nat. Struct. Mol. Biol. 23, 752–754.

Johansson, M., Brooks, A.J., Jans, D.A., Vasudevan, S.G., 2001. A small region of the dengue virus-encoded RNA-dependent RNA polymerase, NS5, confers interaction with both the nuclear transport receptor importin-β and the viral helicase, NS3. J. Gen. Virol. 82, 735–745.

Kapoor, M., Zhang, L., Ramachandra, M., Kusukawa, J., Ebner, K.E., Padmanabhan, R., 1995. Association between NS3 and NS5 Proteins of Dengue Virus Type 2 in the Putative RNA Replicase Is Linked to Differential Phosphorylation of NS5. J. Biol. Chem. 270, 19100–19106.

Kaufmann, B., Rossmann, M.G., 2011. Molecular mechanisms involved in the early steps of flavivirus cell entry. Microbes Infect. 13, 1–9.

Klema, V.J., Padmanabhan, R., Choi, K.H., 2015. Flaviviral Replication Complex: Coordination between RNA Synthesis and 5'-RNA Capping. Viruses 7, 4640–4656.

Klema, V.J., Ye, M., Hindupur, A., Teramoto, T., Gottipati, K., Padmanabhan, R., Choi, K.H., 2016. Dengue Virus Nonstructural Protein 5 (NS5) Assembles into a Dimer with a Unique Methyltransferase and Polymerase Interface. PLoS Pathog. 12, e1005451.

Kümmerer, B.M., Rice, C.M., 2002. Mutations in the Yellow Fever Virus Nonstructural Protein NS2A Selectively Block Production of Infectious Particles. J. Virol. 76, 4773–4784.

Kuno, G., Chang, G.-J., Tsuchiya, K.R., Karabatsos, N., Cropp, C.B., 1998. Phylogeny of the Genus Flavivirus. J. Virol. 72, 73–83.

Laurent-Rolle, M., Boer, E.F., Lubick, K.J., Wolfinbarger, J.B., Carmody, A.B., Rockx, B., Liu, W., Ashour, J., Shupert, W.L., Holbrook, M.R., Barrett, A.D., Mason, P.W., Bloom, M.E., García-Sastre, A., Khromykh, A.A., Best, S.M., 2010. The NS5 Protein of the Virulent West Nile Virus NY99 Strain Is a Potent Antagonist of Type I Interferon-Mediated JAK-STAT Signaling. J. Virol. 84, 3503–3515.

Lei, J., Hansen, G., Nitsche, C., Klein, C.D., Zhang, L., Hilgenfeld, R., 2016. Crystal structure of Zika virus NS2B-NS3 protease in complex with a boronate inhibitor. Science (80-.). 353, 503–505.

Leung, J.Y., Pijlman, G.P., Kondratieva, N., Hyde, J., Mackenzie, J.M., Khromykh, A.A., 2008. Role of Nonstructural Protein NS2A in Flavivirus Assembly. J. Virol. 82, 4731–4741.

Li, H., Clum, S., You, S., Ebner, K.E., Padmanabhan, R., 1999. The Serine Protease and RNA-Stimulated Nucleoside Triphosphatase and RNA Helicase Functional Domains of Dengue Virus Type 2 NS3 Converge within a Region of 20 Amino Acids. J. Virol. 73, 3108–3116.

Li, K., Phoo, W.W., Luo, D., 2014. Functional interplay among the flavivirus NS3 protease, helicase, and cofactors. Virol. Sin. 29, 74–85.

Li, Y., Li, Q., Wong, Y.L., Liew, L.S.Y., Kang, C., 2015. Membrane topology of NS2B of dengue virus revealed by NMR spectroscopy. Biochim. Biophys. Acta 1848, 2244–2252.

Lim, S.P., Koh, J.H.K., Seh, C.C., Liew, C.W., Davidson, A.D., Chua, L.S., Chandrasekaran, R., Cornvik, T.C., Shi, P.-Y., Lescar, J., 2013a. A Crystal Structure of the Dengue Virus Non-structural Protein 5 (NS5) Polymerase Delineates Interdomain Amino Acid Residues That Enhance Its Thermostability and de Novo Initiation Activities. J. Biol. Chem. 288, 31105–31114.

Lim, S.P., Noble, C.G., Seh, C.C., Soh, T.S., El Sahili, A., Chan, G.K.Y., Lescar, J., Arora, R., Benson, T., Nilar, S., Manjunatha, U., Wan, K.F., Dong, H., Xie, X., Shi, P.-Y., Yokokawa, F., 2016. Potent Allosteric Dengue Virus NS5 Polymerase Inhibitors: Mechanism of Action and Resistance Profiling. PLoS Pathog. 12, e1005737.

Lim, S.P., Noble, C.G., Shi, P.-Y., 2015. The dengue virus NS5 protein as a target for drug discovery. Antiviral Res. 119, 57–67.

Lim, S.P., Sonntag, L.S., Noble, C., Nilar, S.H., Ng, R.H., Zou, G., Monaghan, P., Chung, K.Y., Dong, H., Liu, B., Bodenreider, C., Lee, G., Ding, M., Chan, W.L., Wang, G., Jian, Y.L., Chao, A.T., Lescar, J., Yin, Z., Vedananda, T.R., Keller, T.H., Shi, P.-Y., 2011. Small Molecule Inhibitors That Selectively Block Dengue Virus Methyltransferase. J. Biol. Chem. 286, 6233–6240.

Lim, S.P., Wang, Q.-Y., Noble, C.G., Chen, Y.-L., Dong, H., Zou, B., Yokokawa, F., Nilar, S., Smith, P., Beer, D., Lescar, J., Shi, P.-Y., 2013b. Ten years of dengue drug discovery: Progress and prospects. Antiviral Res. 100, 500–519.

Lin, C., Amberg, S.M., Chambers, T.J., Rice, C.M., 1993. Cleavage at a Novel Site in the NS4A Region by the Yellow Fever Virus NS2B-3 Proteinase Is a Prerequisite for Processing at the Downstream 4A/4B Signalase Site. J. Virol. 67, 2327–35.

Lindenbach, B.D., Thiel, H.-J., Rice, C.M., 2007. Flaviviridae: The Viruses and Their Replication. In: Fields Virology, 5th Edition. pp. 1101–1152.

Liu, W.J., Chen, H.B., Khromykh, A.A., 2003. Molecular and Functional Analyses of Kunjin Virus Infectious cDNA Clones Demonstrate the Essential Roles for NS2A in Virus Assembly and for a Nonconservative residue in NS3 in RNA replication. J. Virol. 77, 7804–7813.

Liu, W.J., Chen, H.B., Wang, X.J., Huang, H., Khromykh, A.A., 2004. Analysis of Adaptive Mutations in Kunjin Virus Replicon RNA Reveals a Novel Role for the Flavivirus Nonstructural Protein NS2A in Inhibition of Beta Interferon Promoter-Driven Transcription. J. Virol. 78, 12225–12235.

Lobigs, M., 1993. Flavivirus premembrane protein cleavage and spike heterodimer secretion require the function of the viral proteinase NS3. Proc. Natl. Acad. Sci. U. S. A. 90, 6218–6222.

Lu, G., Gong, P., 2013. Crystal Structure of the Full-Length Japanese Encephalitis Virus NS5 Reveals a Conserved Methyltransferase-Polymerase Interface. PLoS Pathog. 9,

e1003549.

Luo, D., Vasudevan, S.G., Lescar, J., 2015. The flavivirus NS2B-NS3 protease-helicase as a target for antiviral drug development. Antiviral Res. 118, 148–158.

Luo, D., Wei, N., Doan, D.N., Paradkar, P.N., Chong, Y., Davidson, A.D., Kotaka, M., Lescar, J., Vasudevan, S.G., 2010. Flexibility between the Protease and Helicase Domains of the Dengue Virus NS3 Protein Conferred by the Linker Region and Its Functional Implications. J. Biol. Chem. 285, 18817–18827.

Luo, D., Xu, T., Hunke, C., Grüber, G., Vasudevan, S.G., Lescar, J., 2008a. Crystal Structure of the NS3 Protease-Helicase from Dengue Virus. J. Virol. 82, 173–183.

Luo, D., Xu, T., Watson, R.P., Scherer-Becker, D., Sampath, A., Jahnke, W., Yeong, S.S., Wang, C.H., Lim, S.P., Strongin, A., Vasudevan, S.G., Lescar, J., 2008b. Insights into RNA unwinding and ATP hydrolysis by the flavivirus NS3 protein. EMBO J. 27, 3209–3219.

Mackenzie, J.M., Jones, M.K., Young, P.R., 1996. Immunolocalization of the Dengue Virus Nonstructural Glycoprotein NS1 Suggests a Role in Viral RNA Replication. Virology 220, 232–240.

Mackenzie, J.M., Khromykh, A.A., Jones, M.K., Westaway, E.G., 1998. Subcellular Localization and Some Biochemical Properties of the Flavivirus Kunjin Nonstructural Proteins NS2A and NS4A. Virology 245, 203–215.

Malet, H., Egloff, M.-P., Selisko, B., Butcher, R.E., Wright, P.J., Roberts, M., Gruez, A., Sulzenbacher, G., Vonrhein, C., Bricogne, G., Mackenzie, J.M., Khromykh, A.A., Davidson, A.D., Canard, B., 2007. Crystal Structure of the RNA Polymerase Domain of the West Nile Virus Non-structural Protein 5. J. Biol. Chem. 282, 10678–10689.

Mastrangelo, E., Bolognesi, M., Milani, M., 2012. Flaviviral helicase: Insights into the mechanism of action of a motor protein. Biochem. Biophys. Res. Commun. 417, 84–87.

Mastrangelo, E., Milani, M., Bollati, M., Selisko, B., Peyrane, F., Pandini, V., Sorrentino, G., Canard, B., Konarev, P. V., Svergun, D.I., de Lamballerie, X., Coutard, B., Khromykh, A.A., Bolognesi, M., 2007. Crystal Structure and Activity of Kunjin Virus NS3 Helicase; Protease and Helicase Domain Assembly in the Full Length NS3 Protein. J. Mol. Biol. 372, 444–455.

Miller, S., Kastner, S., Krijnse-Locker, J., Bühler, S., Bartenschlager, R., 2007. The Non-structural Protein 4A of Dengue Virus Is an Integral Membrane Protein Inducing Membrane Alterations in a 2K-regulated Manner. J. Biol. Chem. 282, 8873–8882.

Miller, S., Sparacio, S., Bartenschlager, R., 2006. Subcellular Localization and Membrane Topology of the Dengue Virus Type 2 Non-structural Protein 4B. J. Biol. Chem. 281, 8854–8863.

Miorin, L., Romero-Brey, I., Maiuri, P., Hoppe, S., Krijnse-Locker, J., Bartenschlager, R., Marcello, A., 2013. Three-Dimensional Architecture of Tick-Borne Encephalitis Virus Replication Sites and Trafficking of the Replicated RNA. J. Virol. 87, 6469–6481.

Moreland, N.J., Tay, M.Y.F., Lim, E., Rathore, A.P.S., Lim, A.P.C., Hanson, B.J., Vasudevan, S.G., 2012. Monoclonal antibodies against dengue NS2B and NS3

proteins for the study of protein interactions in the flaviviral replication complex. J. Virol. Methods 179, 97–103.

Mukhopadhyay, S., Kuhn, R.J., Rossmann, M.G., 2005. A structural perspective of the flavivirus life cycle. Nat. Rev. Microbiol. 3, 13–22.

Mullard, A., 2012. Protein-protein interaction inhibitors get into the groove. Nat. Rev. Drug Discov. 11, 173–175.

Muller, D.A., Young, P.R., 2013. The flavivirus NS1 protein: Molecular and structural biology, immunology, role in pathogenesis and application as a diagnostic biomarker. Antiviral Res. 98, 192–208.

Muñoz-Jordán, J.L., Laurent-Rolle, M., Ashour, J., Martínez-Sobrido, L., Ashok, M., Lipkin, W.I., García-Sastre, A., 2005. Inhibition of Alpha/Beta Interferon Signaling by the NS4B Protein of Flaviviruses. J. Virol. 79, 8004–8013.

Muñoz-Jordán, J.L., Sánchez-Burgos, G.G., Laurent-Rolle, M., García-Sastre, A., 2003. Inhibition of interferon signaling by dengue virus. Proc. Natl. Acad. Sci. U. S. A. 100, 14333–14338.

Muylaert, I.R., Chambers, T.J., Galler, R., Rice, C.M., 1996. Mutagenesis of the N-Linked Glycosylation Sites of the Yellow Fever Virus NS1 Protein: Effects on Virus Replication and Mouse Neurovirulence. Virology 222, 159–168.

Naeve, C.W., Trent, D.W., 1978. Identification of Saint Louis Encephalitis Virus mRNA. J. Virol. 25, 535–545.

Nemésio, H., Palomares-Jerez, F., Villalaín, J., 2012. NS4A and NS4B proteins from dengue virus: Membranotropic regions. Biochim. Biophys. Acta 1818, 2818–2830.

Nguyen, N.M., Tran, C.N.B., Phung, L.K., Duong, K.T.H., Huynh, H.L.A., Farrar, J., Nguyen, Q.T.H., Tran, H.T., Nguyen, C.V.V., Merson, L., Hoang, L.T., Hibberd, M.L., Aw, P.P.K., Wilm, A., Nagarajan, N., Nguyen, D.T., Pham, M.P., Nguyen, T.T., Javanbakht, H., Klumpp, K., Hammond, J., Petric, R., Wolbers, M., Nguyen, C.T., Simmons, C.P., 2013. A Randomized, Double-Blind Placebo Controlled Trial of Balapiravir, a Polymerase Inhibitor, in Adult Dengue Patients. J. Infect. Dis. 207, 1442–1450.

NIH, 2017. Efficacy and Safety of Ivermectin Against Dengue Infection [WWW Document]. URL https://clinicaltrials.gov/ct2/show/NCT02045069

Nitsche, C., Zhang, L., Weigel, L.F., Schilz, J., Graf, D., Bartenschlager, R., Hilgenfeld, R., Klein, C.D., 2016. Peptide-Boronic Acid Inhibitors of Flaviviral Proteases: Medicinal Chemistry and Structural Biology. J. Med. Chem. 60, 511–516.

Noble, C.G., Li, S.-H., Dong, H., Chew, S.H., Shi, P.-Y., 2014. Crystal structure of dengue virus methyltransferase without S-adenosyl-L-methionine. Antiviral Res. 111, 78–81.

Noble, C.G., Lim, S.P., Arora, R., Yokokawa, F., Nilar, S., Seh, C.C., Wright, S.K., Benson, T.E., Smith, P.W., Shi, P.-Y., 2016. A Conserved Pocket in the Dengue Virus Polymerase Identified through Fragment-based Screening. J. Biol. Chem. 291, 8541–8548.

Noble, C.G., Lim, S.P., Chen, Y.-L., Liew, C.W., Yap, L., Lescar, J., Shi, P.-Y., 2013. Conformational Flexibility of the Dengue Virus RNA-Dependent RNA Polymerase

Revealed by a Complex with an Inhibitor. J. Virol. 87, 5291–5295.

Noble, C.G., Seh, C.C., Chao, A.T., Shi, P.-Y., 2012. Ligand-Bound Structures of the Dengue Virus Protease Reveal the Active Conformation. J. Virol. 86, 438–446.

Noble, C.G., Shi, P.-Y., 2012. Structural biology of dengue virus enzymes: Towards rational design of therapeutics. Antiviral Res. 96, 115–126.

Nomaguchi, M., Ackermann, M., Yon, C., You, S., Padmanbhan, R., 2003. De Novo Synthesis of Negative-Strand RNA by Dengue Virus RNA-Dependent RNA Polymerase In Vitro: Nucleotide, Primer, and Template Parameters. J. Virol. 77, 8831–8842.

Papageorgiou, L., Loukatou, S., Sofia, K., Maroulis, D., Vlachakis, D., 2016. An updated evolutionary study of Flaviviridae NS3 helicase and NS5 RNA-dependent RNA polymerase reveals novel invariable motifs as potential pharmacological targets. Mol. Biosyst. 12, 2080–2093.

Patkar, C.G., Kuhn, R.J., 2008. Yellow Fever Virus NS3 Plays an Essential Role in Virus Assembly Independent of Its Known Enzymatic Functions. J. Virol. 82, 3342–3352.

Paul, D., Bartenschlager, R., 2013. Architecture and biogenesis of plus-strand RNA virus replication factories. World J. Virol. 2, 32–48.

Perera-Lecoin, M., Meertens, L., Carnec, X., Amara, A., 2013. Flavivirus Entry Receptors: An Update. Viruses 6, 69–88.

Perera, R., Kuhn, R.J., 2008. Structural proteomics of dengue virus. Curr. Opin. Microbiol. 11, 369–377.

Phillips, J.C., Braun, R., Wang, W., Gumbart, J., Tajkhorshid, E., Villa, E., Chipot, C., Skeel, R.D., Kalé, L., Schulten, K., 2005. Scalable Molecular Dynamics with NAMD. J. Comput. Chem. 26, 1781–1802.

Phoo, W.W., Li, Y., Zhang, Z., Lee, M.Y., Loh, Y.R., Tan, Y.B., Ng, E.Y., Lescar, J., Kang, C., Luo, D., 2016. Structure of the NS2B-NS3 protease from Zika virus after self-cleavage. Nat. Commun. 7, 13410.

Pierson, T.C., Sánchez, M.D., Puffer, B.A., Ahmed, A.A., Geiss, B.J., Valentine, L.E., Altamura, L.A., Diamond, M.S., Doms, R.W., 2006. A rapid and quantitative assay for measuring antibody-mediated neutralization of West Nile virus infection. Virology 346, 53–65.

Pijlman, G.P., Funk, A., Kondratieva, N., Leung, J., Torres, S., van der Aa, L., Liu, W.J., Palmenberg, A.C., Shi, P.-Y., Hall, R.A., Khromykh, A.A., 2008. A Highly Structured, Nuclease-Resistant, Noncoding RNA Produced by Flaviviruses Is Required for Pathogenicity. Cell Host Microbe 4, 579–591.

Preugschat, F., Yao, C.-W., Strauss, J.H., 1990. In vitro Processing of Dengue Virus Type 2 Nonstructural Proteins NS2A, NS2B, and NS3. J. Virol. 64, 4364–4374.

Ray, D., Shah, A., Tilgner, M., Guo, Y., Zhao, Y., Dong, H., Deas, T.S., Zhou, Y., Li, H., Shi, P.-Y., 2006. West Nile Virus 5'-Cap Structure Is Formed by Sequential Guanine N-7 and Ribose 2'-O Methylations by Nonstructural Protein 5. J. Virol. 80, 8362–8370.

Rice, C.M., Lenches, E.M., Eddy, S.R., Shin, S.J., Sheets, R.L., Strauss, J.H., 1985. Nucleotide Sequence of Yellow Fever Virus: Implications for Flavivirus Gene Expression and Evolution. Science (80-.). 229, 726–733.

Robin, G., Chappell, K., Stoermer, M.J., Hu, S.-H., Young, P.R., Fairlie, D.P., Martin, J.L., 2009. Structure of West Nile Virus NS3 Protease: Ligand Stabilization of the Catalytic Conformation. J. Mol. Biol. 385, 1568–1577.

Roosendaal, J., Westaway, E.G., Khromykh, A., Mackenzie, J.M., 2006. Regulated Cleavages at the West Nile Virus NS4A-2K-NS4B Junctions Play a Major Role in Rearranging Cytoplasmic Membranes and Golgi Trafficking of the NS4A Protein. J. Virol. 80, 4623–4632.

Saeedi, B.J., Geiss, B.J., 2013. Regulation of flavivirus RNA synthesis and capping. Wiley Interdiscip. Rev. RNA 4, 723–735.

Sampath, A., Padmanabhan, R., 2009. Molecular targets for flavivirus drug discovery. Antiviral Res. 81, 6–15.

Sampath, A., Xu, T., Chao, A., Luo, D., Lescar, J., Vasudevan, S.G., 2006. Structure-Based Mutational Analysis of the NS3 Helicase from Dengue Virus. J. Virol. 80, 6686–6690.

Sanofi Pasteur, 2016. Yellow Fever Vaccine YF-VAX [WWW Document]. URL http://www.fda.gov/downloads/BiologicsBloodVaccines/Vaccines/ApprovedProducts/UCM142831.pdf

Schalich, J., Allison, S.L., Stiasny, K., Mandl, C.W., Kunz, C., Heinz, F.X., 1996. Recombinant Subviral Particles from Tick-Borne Encephalitis Virus Are Fusogenic and Provide a Model System for Studying Flavivirus Envelope Glycoprotein Functions. J. Virol. 70, 4549–4557.

Selisko, B., Dutartre, H., Guillemot, J.-C., Debarnot, C., Benarroch, D., Khromykh, A., Desprès, P., Egloff, M.-P., Canard, B., 2006. Comparative mechanistic studies of de novo RNA synthesis by flavivirus RNA-dependent RNA polymerases. Virology 351, 145–158.

Selisko, B., Potisopon, S., Agred, R., Priet, S., Varlet, I., Thillier, Y., Sallamand, C., Debart, F., Vasseur, J.-J., Canard, B., 2012. Molecular Basis for Nucleotide Conservation at the Ends of the Dengue Virus Genome. PLoS Pathog. 8, e1002912.

Shapiro, D., Brandt, W.E., Cardiff, R.D., Russell, P.K., 1971. The Proteins of Japanese Encephalitis Virus. Virology 44, 108–124.

Shiryaev, S.A., Chernov, A. V., Aleshin, A.E., Shiryaeva, T.N., Strongin, A.Y., 2009. NS4A regulates the ATPase activity of the NS3 helicase: a novel cofactor role of the non-structural protein NS4A from West Nile virus. J. Gen. Virol. 90, 2081–2085.

Stiasny, K., Fritz, R., Pangerl, K., Heinz, F.X., 2011. Molecular mechanisms of flavivirus membrane fusion. Amino Acids 41, 1159–1163.

Stohlman, S.A., Wisseman, C.L.J., Eylar, O.R., Silverman, D.J., 1975. Dengue Virus-Induced Modifications of Host Cell Membranes. J. Virol. 16, 1017–1026.

Stollar, V., 1969. Studies on the Nature of Dengue Viruses. IV. The Structural Proteins of Type 2 Dengue Virus. Virology 39, 426–438.

Stollar, V., Schlesinger, R.W., Stevens, T.M., 1967. Studies on the Nature of Dengue Viruses. III. RNA Synthesis in Cells Infected with Type 2 Dengue Virus. Virology 33, 650–658.

Stollar, V., Stevens, T.M., Schlesinger, R.W., 1966. Studies on the Nature of Dengue Viruses. II. Characterization of Viral RNA and Effects of Inhibitors of RNA Synthesis. Virology 30, 303–312.

Sumiyoshi, H., Mori, C., Fuke, I., Morita, K., Kuhara, S., Kondou, J., Kikuchi, Y., Nagamatu, H., Igarashi, A., 1987. Complete Nucleotide Sequence of the Japanese Encephalitis Virus Genome RNA. Virology 161, 497–510.

Surana, P., Satchidanandam, V., Nair, D.T., 2014. RNA-dependent RNA polymerase of Japanese encephalitis virus binds the initiator nucleotide GTP to form a mechanistically important pre-initiation state. Nucleic Acids Res. 42, 2758–2773.

Suthar, M.S., Diamond, M.S., Gale, M.J., 2013. West Nile virus infection and immunity. Nat. Rev. Microbiol. 11, 115–128.

Takahashi, H., Takahashi, C., Moreland, N.J., Chang, Y.-T., Sawasaki, T., Ryo, A., Vasudevan, S.G., Suzuki, Y., Yamamoto, N., 2012. Establishment of a robust dengue virus NS3-NS5 binding assay for identification of protein-protein interaction inhibitors. Antiviral Res. 96, 305–314.

Takegami, T., Sakamuro, D., Furukawa, T., 1995. Japanese Encephalitis Virus Nonstructural Protein NS3 Has RNA Binding and ATPase Activities. Virus Genes 9, 105–112.

Tan, B.-H., Fu, J., Sugrue, R.J., Yap, E.-H., Chan, Y.-C., Tan, Y.H., 1996. Recombinant Dengue Type 1 Virus NS5 Protein Expressed in Escherichia coli Exhibits RNA-Dependent RNA Polymerase Activity. Virology 216, 317–325.

Tarantino, D., Cannalire, R., Mastrangelo, E., Croci, R., Querat, G., Barreca, M.L., Bolognesi, M., Manfroni, G., Cecchetti, V., Milani, M., 2016. Targeting flavivirus RNA dependent RNA polymerase through a pyridobenzothiazole inhibitor. Antiviral Res. 134, 226–235.

Tay, M.Y.F., Saw, W.G., Zhao, Y., Chan, K.W.K., Singh, D., Chong, Y., Forwood, J.K., Ooi, E.E., Grüber, G., Lescar, J., Luo, D., Vasudevan, S.G., 2015. The C-terminal 50 Amino Acid Residues of Dengue NS3 Protein Are Important for NS3-NS5 Interaction and Viral Replication. J. Biol. Chem. 290, 2379–2394.

Tian, H., Ji, X., Yang, X., Xie, W., Yang, K., Chen, C., Wu, C., Chi, H., Mu, Z., Wang, Z., Yang, H., 2016a. The crystal structure of Zika virus helicase: basis for antiviral drug design. Protein Cell 7, 450–454.

Tian, H., Ji, X., Yang, X., Zhang, Z., Lu, Z., Yang, K., Chen, C., Zhao, Q., Chi, H., Mu, Z., Xie, W., Wang, Z., Lou, H., Yang, H., Rao, Z., 2016b. Structural basis of Zika virus helicase in recognizing its substrates. Protein Cell 7, 562–570.

Trent, D.W., Qureshi, A.A., 1971. Structural and Nonstructural Proteins of Saint Louis Encephalitis Virus. J. Virol. 7, 379–388.

Tu, Y.-C., Yu, C.-Y., Liang, J.-J., Lin, E., Liao, C.-L., Lin, Y.-L., 2012. Blocking Double-Stranded RNA-Activated Protein Kinase PKR by Japanese Encephalitis Virus

Nonstructural Protein 2A. J. Virol. 86, 10347–10358.

Uchil, P.D., Satchidanandam, V., 2003. Architecture of the Flaviviral Replication Complex. Protease, nuclease, and detergents reveal encasement within double-layered membrane compartments. J. Biol. Chem. 278, 24388–24398.

Umareddy, I., Chao, A., Sampath, A., Gu, F., Vasudevan, S.G., 2006. Dengue virus NS4B interacts with NS3 and dissociates it from single-stranded RNA. J. Gen. Virol. 87, 2605–2614.

Utama, A., Shimizu, H., Morikawa, S., Hasebe, F., Morita, K., Igarashi, A., Hatsu, M., Takamizawa, K., Miyamura, T., 2000. Identification and characterization of the RNA helicase activity of Japanese encephalitis virus NS3 protein. FEBS Lett. 465, 74–78.

Valle, R.P.C., Falgout, B., 1998. Mutagenesis of the NS3 Protease of Dengue Virus Type 2. J. Virol. 72, 624–632.

Vasilakis, N., Cardosa, J., Hanley, K.A., Holmes, E.C., Weaver, S.C., 2011. Fever from the forest: prospects for the continued emergence of sylvatic dengue virus and its impact on public health. Nat. Rev. Microbiol. 9, 532–541.

Vasilakis, N., Weaver, S.C., 2016. Flavivirus transmission focusing on Zika. Curr. Opin. Virol. 22, 30–35.

Vasudevan, S.G., Johansson, M., Brooks, A.J., Llewellyn, L.E., Jans, D.A., 2001. Characterisation of inter- and intra-molecular interactions of the dengue virus RNA dependent RNA polymerase as potential drug targets. Farmaco 56, 33–36.

Wahle, M., Wriggers, W., 2015. Multi-scale Visualization of Molecular Architecture Using Real-Time Ambient Occlusion in Sculptor. PLoS Comput. Biol. 11, e1004516.

Wang, C.-C., Huang, Z.-S., Chiang, P.-L., Chen, C.-T., Wu, H.-N., 2009. Analysis of the nucleoside triphosphatase, RNA triphosphatase, and unwinding activities of the helicase domain of dengue virus NS3 protein. FEBS Lett. 583, 691–696.

Warrener, P., Tamura, J.K., Collett, M.S., 1993. RNA-Stimulated NTPase Activity Associated with Yellow Fever Virus NS3 Protein Expressed in Bacteria. J. Virol. 67, 989–996.

Weaver, S.C., Barrett, A.D.T., 2004. Transmission cycles, host range, evolution and emergence of arboviral disease. Nat. Rev. Microbiol. 2, 789–801.

Weinert, T., Olieric, V., Waltersperger, S., Panepucci, E., Chen, L., Zhang, H., Zhou, D., Rose, J., Ebihara, A., Kuramitsu, S., Li, D., Howe, N., Schnapp, G., Pautsch, A., Bargsten, K., Prota, A.E., Surana, P., Kottur, J., Nair, D.T., Basilico, F., Cecatiello, V., Pasqualato, S., Boland, A., Weichenrieder, O., Wang, B.-C., Steinmetz, M.O., Caffrey, M., Wang, M., 2015. Fast native-SAD phasing for routine macromolecular structure determination. Nat. Methods 12, 131–133.

Welsch, S., Miller, S., Romero-Brey, I., Merz, A., Bleck, C.K.E., Walther, P., Fuller, S.D., Antony, C., Krijnse-Locker, J., Bartenschlager, R., 2009. Composition and Three-Dimensional Architecture of the Dengue Virus Replication and Assembly Sites. Cell Host Microbe 5, 365–375.

Wengler, G., Czaya, G., Färber, P.M., Hegemann, J.H., 1991. In vitro synthesis of West Nile virus proteins indicates that the amino-terminal segment of the NS3 protein

contains the active centre of the protease which cleaves the viral polyprotein after multiple basic amino acids. J. Gen. Virol. 72, 851–858.

Wengler, G., Wengler, G., 1981. Terminal Sequences of the Genome and Replicative-Form RNA of the Flavivirus West Nile Virus: Absence of Poly(A) and Possible Role in RNA Replication. Virology 113, 544–555.

Wengler, G., Wengler, G., 1991. The Carboxy-Terminal Part of the NS 3 Protein of the West Nile Flavivirus Can Be Isolated as a Soluble Protein after Proteolytic Cleavage and Represents an RNA-stimulated NTPase. Virology 184, 707–715.

Wengler, G., Wengler, G., 1993. The NS 3 Nonstructural Protein of Flaviviruses Contains an RNA Triphosphatase Activity. Virology.

Wengler, G., Wengler, G., Gross, H.J., 1978. Studies on Virus-Specific Nucleic Acids Synthesized in Vertebrate and Mosquito Cells Infected with Flaviviruses. Virology 89, 423–437.

WHO, 2011. West Nile virus: Fact sheet No 354 (July 2011) [WWW Document]. URL http://www.who.int/mediacentre/factsheets/fs354/en/#

WHO, 2014. Yellow fever: Fact sheet No 100 (March 2014) [WWW Document]. URL http://www.who.int/mediacentre/factsheets/fs100/en/

WHO, 2015. Japanese encephalitis: Fact sheet No 386 (December 2015) [WWW Document]. URL http://www.who.int/mediacentre/factsheets/fs386/en/

WHO, 2016a. Situation report: Zika virus, Microcephaly, Guillain-Barré Syndrome. 24 November 2016 [WWW Document]. URL http://www.who.int/emergencies/zika-virus/situation-report/24-november-2016/en/

WHO, 2016b. Dengue: Fact sheet (July 2016) [WWW Document]. URL http://www.who.int/mediacentre/factsheets/fs117/en

WHO, 2016c. Yellow fever: Fact sheet No 100 (May 2016) [WWW Document]. URL http://www.who.int/entity/mediacentre/factsheets/fs100/en/

WHO, 2016d. Zika virus: Fact sheet (June 2016) [WWW Document]. URL http://www.who.int/entity/mediacentre/factsheets/zika/en/

WHO, 2016e. Dengue vaccine: WHO position paper - July 2016 [WWW Document]. URL http://www.who.int/wer/2016/wer9130.pdf?ua=1

WHO, 2017. The History of Zika Virus [WWW Document]. URL http://www.who.int/emergencies/zika-virus/history/en/

Wu, J., Bera, A.K., Kuhn, R.J., Smith, J.L., 2005. Structure of the Flavivirus Helicase : Implications for Catalytic Activity , Protein Interactions , and Proteolytic Processing. J. Virol. 79, 10268–10277.

Wu, J., Liu, W., Gong, P., 2015. A Structural Overview of RNA-Dependent RNA Polymerases from the Flaviviridae Family. Int. J. Mol. Sci. 16, 12943–12957.

Xie, X., Gayen, S., Kang, C., Yuan, Z., Shi, P.-Y., 2013. Membrane Topology and Function of Dengue virus NS2A protein. J. Virol. 87, 4609–4622.

Xu, T., Sampath, A., Chao, A., Wen, D., Nanao, M., Chene, P., Vasudevan, S.G., Lescar,

J., 2005. Structure of the Dengue Virus Helicase/Nucleoside Triphosphatase Catalytic Domain at a Resolution of 2.4 Å. J. Virol. 79, 10278–10288.

Xu, T., Sampath, A., Chao, A., Wen, D., Nanao, M., Luo, D., Chene, P., Vasudevan, S.G., Lescar, J., 2006. Towards the design of flavivirus helicase/NTPase inhibitors: crystallographic and mutagenesis studies of the dengue virus NS3 helicase catalytic domain. Novartis Found. Symp. 277, 87–97.

Yamashita, T., Unno, H., Mori, Y., Tani, H., Moriishi, K., Takamizawa, A., Agoh, M., Tsukihara, T., Matsuura, Y., 2008. Crystal structure of the catalytic domain of Japanese encephalitis virus NS3 helicase/nucleoside triphosphatase at a resolution of 1.8 Å. Virology 373, 426–436.

Yap, L.J., Luo, D., Chung, K.Y., Lim, S.P., Bodenreider, C., Noble, C., Shi, P.-Y., Lescar, J., 2010. Crystal Structure of the Dengue Virus Methyltransferase Bound to a 5'-Capped Octameric RNA. PLoS One 5, e12836.

Yap, T.L., Xu, T., Chen, Y.-L., Malet, H., Egloff, M.-P., Canard, B., Vasudevan, S.G., Lescar, J., 2007. Crystal Structure of the Dengue Virus RNA-Dependent RNA Polymerase Catalytic Domain at 1.85-Angstrom Resolution. J. Virol. 81, 4753–4765.

Yildiz, M., Ghosh, S., Bell, J.A., Sherman, W., Hardy, J.A., 2013. Allosteric inhibition of the NS2B-NS3 Protease from Dengue Virus. ACS Chem. Biol. 8, 2744–2752.

Yin, Z., Chen, Y.-L., Schul, W., Wang, Q.-Y., Gu, F., Duraiswamy, J., Konreddi, R.R., Niyomrattanakit, P., Lakshminarayana, S.B., Goh, A., Xu, H.Y., Liu, W., Liu, B., Lim, J.Y.H., Ng, C.Y., Qing, M., Lim, C.C., Yip, A., Wang, G., Chan, W.L., Tan, H.P., Lin, K., Zhang, B., Zou, G., Bernard, K.A., Garrett, C., Beltz, K., Dong, M., Weaver, M., He, H., Pichota, A., Dartois, V., Keller, T.H., Shi, P.-Y., 2009. An adenosine nucleoside inhibitor of dengue virus. Proc. Natl. Acad. Sci. U. S. A. 106, 20435–20439.

Yokokawa, F., Nilar, S., Noble, C.G., Lim, S.P., Rao, R., Tania, S., Wang, G., Lee, G., Hunziker, J., Karuna, R., Manjunatha, U., Shi, P.-Y., Smith, P.W., 2016. Discovery of Potent Non-Nucleoside Inhibitors of Dengue Viral RNA-Dependent RNA Polymerase from a Fragment Hit Using Structure-Based Drug Design. J. Med. Chem. 59, 3935–3952.

Yon, C., Teramoto, T., Mueller, N., Phelan, J., Ganesh, V.K., Murthy, K.H.M., Padmanabhan, R., 2005. Modulation of the Nucleoside Triphosphatase/RNA Helicase and 5'-RNA Triphosphatase Activities of Dengue Virus Type 2 Nonstructural Protein 3 (NS3) by Interaction with NS5, the RNA-dependent RNA Polymerase. J. Biol. Chem. 280, 27412–27419.

Yotmanee, P., Rungrotmongkol, T., Wichapong, K., Choi, S.B., Wahab, H.A., Kungwan, N., Hannongbua, S., 2015. Binding specificity of polypeptide substrates in NS2B/NS3pro serine protease of dengue virus type 2: A molecular dynamics Study. J. Mol. Graph. Model. 60, 24–33.

Yu, L., Takeda, K., Markoff, L., 2013. Protein-protein interactions among West Nile non-structural proteins and transmembrane complex formation in mammalian cells. Virology 446, 365–377.

Zhang, C., Feng, T., Cheng, J., Li, Y., Yin, X., Zeng, W., Jin, X., Li, Y., Guo, F., Jin, T.,

2016. Structure of the NS5 methyltransferase from Zika virus and implications in inhibitor design. Biochem. Biophys. Res. Commun.

Zhang, Z., Li, Y., Loh, Y.R., Phoo, W.W., Hung, A.W., Kang, C., Luo, D., 2016. Crystal structure of unlinked NS2B-NS3 protease from Zika virus. Science (80-.). 354, 1597–1600.

Zhao, Y., Soh, T.S., Lim, S.P., Chung, K.Y., Swaminathan, K., Vasudevan, S.G., Shi, P.-Y., Lescar, J., Luo, D., 2015a. Molecular basis for specific viral RNA recognition and 2'-O-ribose methylation by the dengue virus nonstructural protein 5 (NS5). Proc. Natl. Acad. Sci. U. S. A. 112, 14834–14839.

Zhao, Y., Soh, T.S., Zheng, J., Chan, K.W.K., Phoo, W.W., Lee, C.C., Tay, M.Y.F., Swaminathan, K., Cornvik, T.C., Lim, S.P., Shi, P.-Y., Lescar, J., Vasudevan, S.G., Luo, D., 2015b. A Crystal Structure of the Dengue Virus NS5 Protein Reveals a Novel Inter-domain Interface Essential for Protein Flexibility and Virus Replication. PLoS Pathog. 11, e1004682.

Zhou, Y., Ray, D., Zhao, Y., Dong, H., Ren, S., Li, Z., Guo, Y., Bernard, K.A., Shi, P.-Y., Li, H., 2007. Structure and Function of Flavivirus NS5 Methyltransferase. J. Virol. 81, 3891–3903.

Zou, G., Chen, Y.-L., Dong, H., Lim, C.C., Yap, L.J., Yau, Y.H., Geifman Shochat, S., Lescar, J., Shi, P.-Y., 2011. Functional Analysis of Two Cavities in Flavivirus NS5 Polymerase. J. Biol. Chem. 286, 14362–14372.

Zou, G., Puig-Basagoiti, F., Zhang, B., Qing, M., Chen, L., Pankiewicz, K.W., Felczak, K., Yuan, Z., Shi, P.-Y., 2009. A single-amino acid substitution in West Nile virus 2K peptide between NS4A and NS4B confers resistance to lycorine, a flavivirus inhibitor. Virology 384, 242–252.

Zou, J., Lee, L.T., Wang, Q.Y., Xie, X., Lu, S., Yau, Y.H., Yuan, Z., Geifman Shochat, S., Kang, C., Lescar, J., Shi, P.-Y., 2015a. Mapping the Interactions between the NS4B and NS3 Proteins of Dengue Virus. J. Virol. 89, 3471–3483.

Zou, J., Xie, X., Wang, Q.-Y., Dong, H., Lee, M.Y., Kang, C., Yuan, Z., Shi, P.-Y., 2015b. Characterization of Dengue Virus NS4A and NS4B Protein Interaction. J. Virol. 89, 3455–3470.

APPENDIXES

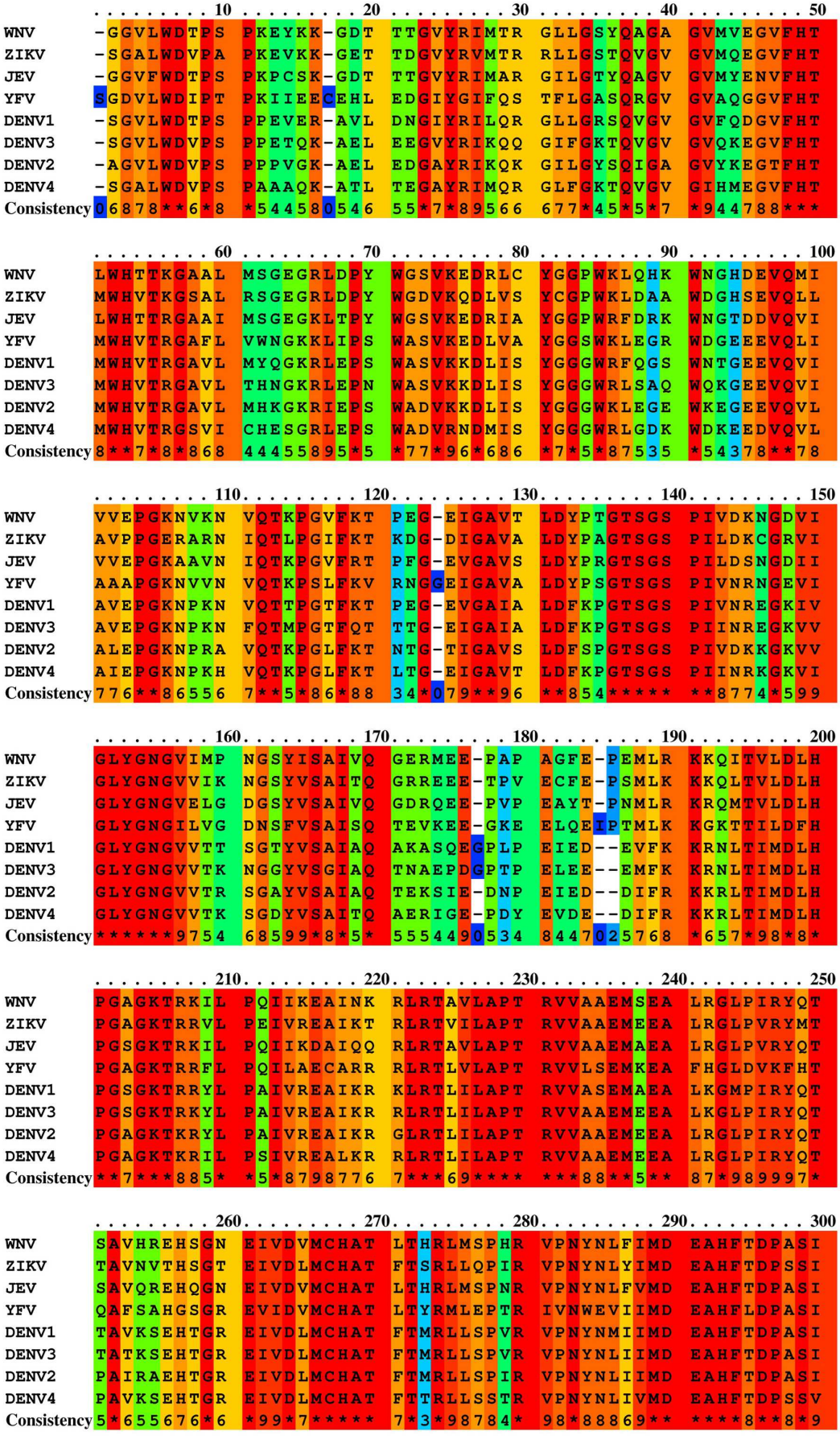
10 20 30 40 50
WNV -GGVLWDTPS PKEYKK-GDT TTGVYRIMTR GLLGSYQAGA GVMVEGVFHT
ZIKV -SGALWDVPA PKEVKK-GET TDGVYRVMTR RLLGSTQVGV GVMQEGVFHT
JEV -GGVFWDTPS PKPCSK-GDT TTGVYRIMAR GILGTYQAGV GVMYENVFHT
YFV SGDVLWDIPT PKIIEECEHL EDGIYGIFQS TFLGASQRGV GVAQGGVFHT
DENV1 -SGVLWDTPS PPEVER-AVL DNGIYRILQR GLLGRSQVGV GVFQDGVFHT
DENV3 -SGVLWDVPS PPETQK-AEL EEGVYRIKQQ GIFGKTQVGV GVQKEGVFHT
DENV2 -AGVLWDVPS PPPVGK-AEL EDGAYRIKQK GILGYSQIGA GVYKEGTFHT
DENV4 -SGALWDVPS PAAAQK-ATL TEGAYRIMQR GLFGKTQVGV GIHMEGVFHT
Consistency 06878**6*8 *54458054 6 55*7*89566 677*45*5*7 *944788***
60 70 80 90 100
WNV LWHTTKGAAL MSGEGRLDPY WGSVKEDRLC YGGPWKLQHK WNGHDEVQMI
ZIKV MWHVTKGSAL RSGEGRLDPY WGDVKQDLVS YCGPWKLDAA WDGHSEVQLL
JEV LWHTTRGAAI MSGEGKLTPY WGSVKEDRIA YGGPWRFDRK WNGTDDVQVI
YFV MWHVTRGAFL VWNGKKLIPS WASVKEDLVA YGGSWKLEGR WDGEEEVQLI
DENV1 MWHVTRGAVL MYQGKRLEPS WASVKKDLIS YGGGWRFQGS WNTGEEVQVI
DENV3 MWHVTRGAVL THNGKRLEPN WASVKKDLIS YGGGWRLSAQ WQKGEEVQVI
DENV2 MWHVTRGAVL MHKGKRIEPS WADVKKDLIS YGGGWKLEGE WKEGEEVQVL
DENV4 MWHVTRGSVI CHESGRLEPS WADVRNDMIS YGGGWRLGDK WDKEEDVQVL
Consistency 8**7*8*868 44455895*5 *77*96*686 *7*5*87535 *54378**78
110 120 130 140 150
WNV VVEPGKNVKN VQTKPGVFKT PEG-EIGAVT LDYPTGTSGS PIVDKNGDVI
ZIKV AVPPGERARN IQTLPGIFKT KDG-DIGAVA LDYPAGTSGS PILDKCGRVI
JEV VVEPGKAAVN IQTKPGVFRT PFG-EVGAVS LDYPRGTSGS PILDSNGDII
YFV AAAPGKNVVN VQTKPSLFKV RNGGEIGAVA LDYPSGTSGS PIVNRNGEVI
DENV1 AVEPGKNPKN VQTTPGTFKT PEG-EVGAIA LDFKPGTSGS PIVNREGKIV
DENV3 AVEPGKNPKN FQTMPGTFQT TTG-EIGAIA LDFKPGTSGS PIINREGKVV
DENV2 ALEPGKNPRA VQTKPGLFKT NTG-TIGAVS LDFSPGTSGS PIVDKKGKVV
DENV4 AIEPGKNPKH VQTKPGLFKT LTG-EIGAVT LDFKPGTSGS PIINRKGKVI
Consistency 776**86556 7**5*86*88 34*079**96 **854***** **8774*599
160 170 180 190 200
WNV GLYGNGVIMP NGSYISAIVQ GERMEE-PAP AGFE-PEMLR KKQITVLDLH
ZIKV GLYGNGVVIK NGSYVSAITQ GRREEE-TPV ECFE-PSMLK KKQLTVLDLH
JEV GLYGNGVELG DGSYVSAIVQ GDRQEE-PVP EAYT-PNMLR KRQMTVLDLH
YFV GLYGNGILVG DNSFVSAISQ TEVKEE-GKE ELQEIPTMLK KGKTTILDFH
DENV1 GLYGNGVVTT SGTYVSAIAQ AKASQEGPLP EIED--EVFK KRNLTIMDLH
DENV3 GLYGNGVVTK NGGYVSGIAQ TNAEPDGPTP ELEE--EMFK KRNLTIMDLH
DENV2 GLYGNGVVTR SGAYVSAIAQ TEKSIE-DNP EIED--DIFR KKRLTIMDLH
DENV4 GLYGNGVVTK SGDYVSAITQ AERIGE-PDY EVDE--DIFR KKRLTIMDLH
Consistency ******9754 68599*8*5* 555449053 4 8447025768 *657*98*8*
210 220 230 240 250
WNV PGAGKTRKIL PQIIKEAINK RLRTAVLAPT RVVAAEMSEA LRGLPIRYQT
ZIKV PGAGKTRRVL PEIVREAIKT RLRTVILAPT RVVAAEMEEA LRGLPVRYMT
JEV PGSGKTRKIL PQIIKDAIQQ RLRTAVLAPT RVVAAEMAEA LRGLPVRYQT
YFV PGAGKTRRFL PQILAECARR RLRTLVLAPT RVVLSEMKEA FHGLDVKFHT
DENV1 PGSGKTRRYL PAIVREAIKR KLRTLILAPT RVVASEMAEA LKGMPIRYQT
DENV3 PGSGKTRKYL PAIVREAIKR RLRTLILAPT RVVAAEMEEA LKGLPIRYQT
DENV2 PGAGKTKRYL PAIVREAIKR GLRTLILAPT RVVAAEMEEA LRGLPIRYQT
DENV4 PGAGKTKRIL PSIVREALKR RLRTLILAPT RVVAAEMEEA LRGLPIRYQT
Consistency **7***885* *5*879877 6 7***69**** ***88**5** 87*989997*
260 270 280 290 300
WNV SAVHREHSGN EIVDVMCHAT LTHRLMSPHR VPNYNLFIMD EAHFTDPASI
ZIKV TAVNVTHSGT EIVDLMCHAT FTSRLLQPIR VPNYNLYIMD EAHFTDPSSI
JEV SAVQREHQGN EIVDVMCHAT LTHRLMSPNR VPNYNLFVMD EAHFTDPASI
YFV QAFSAHGSGR EVIDVMCHAT LTYRMLEPTR IVNWEVIIMD EAHFLDPASI
DENV1 TAVKSEHTGR EIVDLMCHAT FTMRLLSPVR VPNYNMIIMD EAHFTDPASI
DENV3 TATKSEHTGR EIVDLMCHAT FTMRLLSPVR VPNYNLIIMD EAHFTDPASI
DENV2 PAIRAEHTGR EIVDLMCHAT FTMRLLSPIR VPNYNLIIMD EAHFTDPASI
DENV4 PAVKSEHTGR EIVDLMCHAT FTTRLLSSTR VPNYNLIVMD EAHFTDPSSV
Consistency 5*6556676*6 *99*7***** 7*3*98784* 98*88869** ****8**8*9

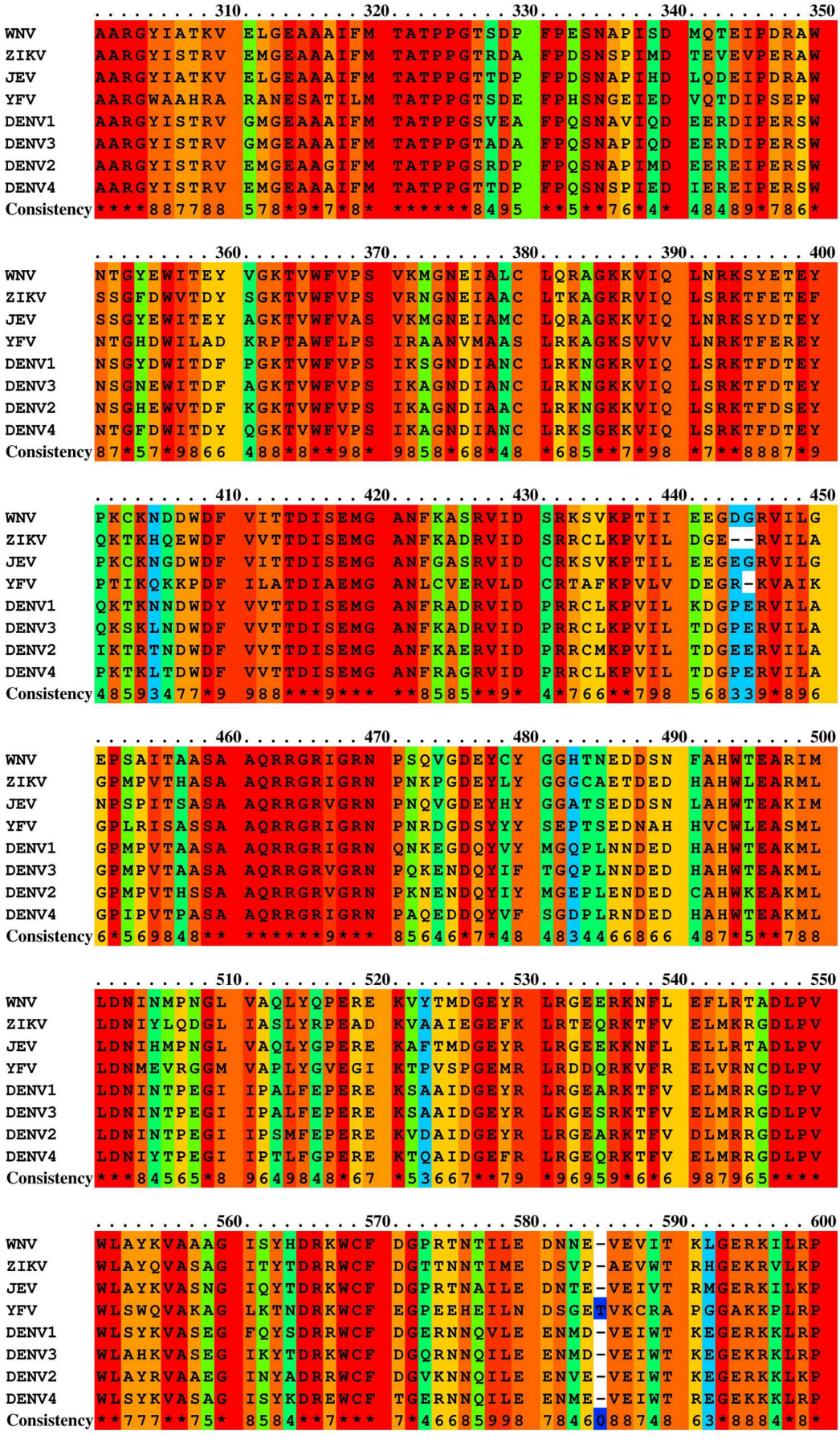
310 320 330 340 350
WNV AARGYIATKV ELGEAAAIFM TATPPGTSDP FPESNAPISD MQTEIPDRAW
ZIKV AARGYISTRV EMGEAAAIFM TATPPGTRDA FPDSNSPIMD TEVEVPERAW
JEV AARGYIATKV ELGEAAAIFM TATPPGTTDP FPDSNAPIHD LQDEIPDRAW
YFV AARGWAAHRA RANESATILM TATPPGTSDE FPHSNGEIED VQTDIPSEPW
DENV1 AARGYISTRV GMGEAAAIFM TATPPGSVEA FPQSNAVIQD EERDIPERSW
DENV3 AARGYISTRV GMGEAAAIFM TATPPGTADA FPQSNAPIQD EERDIPERSW
DENV2 AARGYISTRV EMGEAAGIFM TATPPGSRDP FPQSNAPIMD EEREIPERSW
DENV4 AARGYISTRV EMGEAAAIFM TATPPGTTDP FPQSNSPIED IEREIPERSW
Consistency ****887788 578*9*7*8* ******8495 **5**76*4* 48489*786*
360 370 380 390 400
WNV NTGYEWITEY VGKTVWFVPS VKMGNEIALC LQRAGKKVIQ LNRKSYETEY
ZIKV SSGFDWVTDY SGKTVWFVPS VRNGNEIAAC LTKAGKRVIQ LSRKTFETEF
JEV SSGYEWITEY AGKTVWFVAS VKMGNEIAMC LQRAGKKVIQ LNRKSYDTEY
YFV NTGHDWILAD KRPTAWFLPS IRAANVMAAS LRKAGKSVVV LNRKTFEREY
DENV1 NSGYDWITDF PGKTVWFVPS IKSGNDIANC LRKNGKRVIQ LSRKTFDTEY
DENV3 NSGNEWITDF AGKTVWFVPS IKAGNDIANC LRKNGKKVIQ LSRKTFDTEY
DENV2 NSGHEWVTDF KGKTVWFVPS IKAGNDIAAC LRKNGKKVIQ LSRKTFDSEY
DENV4 NTGFDWITDY QGKTVWFVPS IKAGNDIANC LRKSGKKVIQ LSRKTFDTEY
Consistency 87*57*9866 488*8**98* 9858*68*48 *685**7*98 *7**8887*9
410 420 430 440 450
WNV PKCKNDDWDF VITTDISEMG ANFKASRVID SRKSVKPTII EEGDGRVILG
ZIKV QKTKHQEWDF VVTTDISEMG ANFKADRVID SRRCLKPVIL DGE--RVILA
JEV PKCKNGDWDF VITTDISEMG ANFGASRVID CRKSVKPTIL EEGEGRVILG
YFV PTIKQKKPDF ILATDIAEMG ANLCVERVLD CRTAFKPVLV DEGR-KVAIK
DENV1 QKTKNNDWDY VVTTDISEMG ANFRADRVID PRRCLKPVIL KDGPERVILA
DENV3 QKSKLNDWDF VVTTDISEMG ANFKADRVID PRRCLKPVIL TDGPERVILA
DENV2 IKTRTNDWDF VVTTDISEMG ANFKAERVID PRRCMKPVIL TDGEERVILA
DENV4 PKTKLTDWDF VVTTDISEMG ANFRAGRVID PRRCLKPVIL TDGPERVILA
Consistency 4859347 7*9 988***9*** **8585**9* 4*766**798 5683 39*896
460 470 480 490 500
WNV EPSAITAASA AQRRGRIGRN PSQVGDEYCY GGHTNEDDSN FAHWTEARIM
ZIKV GPMPVTHASA AQRRGRIGRN PNKPGDEYLY GGGCAETDED HAHWLEARML
JEV NPSPITSASA AQRRGRVGRN PNQVGDEYHY GGATSEDDSN LAHWTEAKIM
YFV GPLRISASSA AQRRGRIGRN PNRDGDSYYY SEPTSEDNAH HVCWLEASML
DENV1 GPMPVTAASA AQRRGRIGRN QNKEGDQYVY MGQPLNNDED HAHWTEAKML
DENV3 GPMPVTAASA AQRRGRVGRN PQKENDQYIF TGQPLNNDED HAHWTEAKML
DENV2 GPMPVTHSSA AQRRGRVGRN PKNENDQYIY MGEPLENDED CAHWKEAKML
DENV4 GPIPVTPASA AQRRGRIGRN PAQEDDQYVF SGDPLRNDED HAHWTEAKML
Consistency 6*569848** ******9*** 85646*7*48 48344666866 487*5**788
510 520 530 540 550
WNV LDNINMPNGL VAQLYQPERE KVYTMDGEYR LRGEERKNFL EFLRTADLPV
ZIKV LDNIYLQDGL IASLYRPEAD KVAAIEGEFK LRTEQRKTFV ELMKRGDLPV
JEV LDNIHMPNGL VAQLYGPERE KAFTMDGEYR LRGEEKKNFL ELLRTADLPV
YFV LDNMEVRGGM VAPLYGVEGI KTPVSPGEMR LRDDQRKVFR ELVRNCDLPV
DENV1 LDNINTPEGI IPALFEPERE KSAAIDGEYR LRGEARKTFV ELMRRGDLPV
DENV3 LDNINTPEGI IPALFEPERE KSAAIDGEYR LKGESRKTFV ELMRRGDLPV
DENV2 LDNINTPEGI IPSMFEPERE KVDAIDGEYR LRGEARKTFV DLMRRGDLPV
DENV4 LDNIYTPEGI IPTLFGPERE KTQAIDGEFR LRGEQRKTFV ELMRRGDLPV
Consistency ***845655*8 964984 8*67 *53667**79 *96959*6*6 987965****
560 570 580 590 600
WNV WLAYKVAAAG ISYHDRKWCF DGPRTNTILE DNNE-VEVIT KLGERKILRP
ZIKV WLAYQVASAG ITYTDRRWCF DGTTNNTIME DSVP-AEVWT RHGEKRVLKP
JEV WLAYKVASNG IQYTDRKWCF DGPRTNAILE DNTE-VEIVT RMGERKILKP
YFV WLSWQVAKAG LKTNDRKWCF EGPEEHEILN DSGETVKCRA PGGAKKPLRP
DENV1 WLSYKVASEG FQYSDRRWCF DGERNNQVLE ENMD-VEIWT KEGERKKLRP
DENV3 WLAHKVASEG IKYTDRKWCF DGQRNNQILE ENMD-VEIWT KEGEKRKLRP
DENV2 WLAYRVAAEG INYADRRWCF DGVKNNQILE ENVE-VEIWT KEGERKKLKP
DENV4 WLSYKVASAG ISYKDREWCF TGERNNQILE ENME-VEIWT REGEKKKLRP
Consistency **777**75* 8584**7*** 7*46685998 7846088748 63*8884*8*

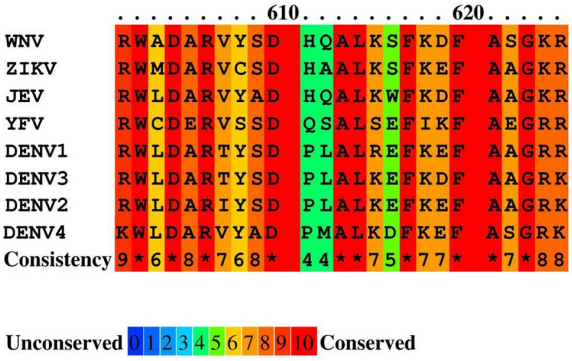

Appendix 1. Alignment of the NS3 proteins from DENV, YFV, WNV, JEV and ZIKV.

Sequences were aligned using PRALINE (Centre for Integrative Bioinformatics Vrije Universiteit Amsterdam, 2017). Each amino acid residue is colored according to its conservation between these virus species, where red is most conserved and blue is least conserved.

PDB code	Virus	Protein	Ligands	Resolution	Authors
2FOM	DENV	NS3 protease	-	1.5Å	(Erbel et al., 2006)
2FP7	WNV	NS3 protease	Substrate-based inhibitor	1.68Å	(Erbel et al., 2006)
2GGV	WNV	NS3 protease	-	1.8Å	(Aleshin et al., 2007)
2IJO	WNV	NS3 protease	Pancreatic trypsin inhibitor	2.3Å	(Aleshin et al., 2007)
2M9P	DENV	NS3 protease	Peptide-like inhibitor	NMR	(Gibbs et al., to be published)
2M9Q	DENV	NS3 protease	Peptide-like inhibitor	NMR	(Gibbs et al., to be published)
2YOL	WNV	NS3 protease	Substrate analog inhibitor	3.2Å	(Hammamy et al., 2013)
3E90	WNV	NS3 protease	Substrate-based inhibitor	2.45Å	(Robin et al., 2009)
3L6P	DENV	NS3 protease	-	2.2Å	(Chandramouli et al., 2010)
3LKW	DENV	NS3 protease	-	2.0Å	(Chandramouli et al., 2010)
3U1I	DENV	NS3 protease	Peptide-based inhibitor	2.3Å	(Noble et al., 2012)
3U1J	DENV	NS3 protease	Pancreatic trypsin inhibitor	1.8Å	(Noble et al., 2012)
4M9F	DENV	NS3 protease	-	2.7Å	(Yildiz et al., 2013)
4M9I	DENV	NS3 protease	-	2.4Å	(Yildiz et al., 2013)
4M9K	DENV	NS3 protease	-	1.46Å	(Yildiz et al., 2013)
4M9M	DENV	NS3 protease	-	1.53Å	(Yildiz et al., 2013)
4M9T	DENV	NS3 protease	-	1.74Å	(Yildiz et al., 2013)
4R8T	JEV	NS3 protease	-	2.13Å	(Weinert et al., 2015)
5GJ4	ZIKV	NS3 protease	-	1.84Å	(Phoo et al., 2016)
5GPI	ZIKV	NS3 protease	-	1.58Å	(Z. Zhang et al., 2016)
5H4I	ZIKV	NS3 protease	Compound fragment	2.0Å	(Z. Zhang et al., 2016)
5IDK	WNV	NS3 protease	Dipeptide boronic acid inhibitor	1.5Å	(Nitsche et al., 2016)
5LC0	ZIKV	NS3 protease	Dipeptide boronic acid inhibitor	2.7Å	(Lei et al., 2016)
5T1V	ZIKV	NS3 protease	-	3.1Å	(Nocadello et al., to be published)
1YKS	YFV	NS3 helicase	-	1.8Å	(Wu et al., 2005)
2BHR	DENV	NS3 helicase	-	2.8Å	(Xu et al., 2005)
2BMF	DENV	NS3 helicase	-	2.41Å	(Xu et al., 2005)
2JLQ	DENV	NS3 helicase	-	1.67Å	(Luo et al., 2008b)
2JLR	DENV	NS3 helicase	AMP-PNP	2.0Å	(Luo et al., 2008b)
2JLS	DENV	NS3 helicase	ADP	2.23Å	(Luo et al., 2008b)
2JLU	DENV	NS3 helicase	ssRNA	2.04Å	(Luo et al., 2008b)
2JLV	DENV	NS3 helicase	AMP-PNP, ssRNA	1.9Å	(Luo et al., 2008b)
2JLW	DENV	NS3 helicase	ssRNA	2.6Å	(Luo et al., 2008b)
2JLX	DENV	NS3 helicase	ADP-vanadate, ssRNA	2.2Å	(Luo et al., 2008b)
2JLY	DENV	NS3 helicase	ADP, ssRNA	2.4Å	(Luo et al., 2008b)
2JLZ	DENV	NS3 helicase	ADP, ssRNA	2.2Å	(Luo et al., 2008b)
2QEQ	KUNV	NS3 helicase	-	3.1Å	(Mastrangelo et al., 2007)

2Z83	JEV	NS3 helicase	-	1.8Å	(Yamashita et al., 2008)
5FFM	YFV	NS3 helicase	-	2.6Å	(Wu et al., 2005)
5GJC	ZIKV	NS3 helicase	ATP	2.2Å	(Tian et al., 2016b)
5JMT	ZIKV	NS3 helicase	-	1.8Å	(Tian et al., 2016a)
5JRZ	ZIKV	NS3 helicase	PPi	1.62Å	(Jain et al., 2016)
5JWH	ZIKV	NS3 helicase	-	1.4Å	(Cao et al., 2016)
5K8I	ZIKV	NS3 helicase	ATP	1.69Å	(Cao et al., 2016)
5K8L	ZIKV	NS3 helicase	GTPγS	1.75Å	(Cao et al., 2016)
5K8T	ZIKV	NS3 helicase	GTPγS	1.85Å	(Cao et al., 2016)
5K8U	ZIKV	NS3 helicase	ADP	1.6Å	(Cao et al., 2016)
5MFX	ZIKV	NS3 helicase	ssRNA	1.6Å	(Jenkins et al., to be published)
5TXG	ZIKV	NS3 helicase	-	2.05Å	(Nocadello et al., to be published)
2VBC	DENV	NS3 full-length	-	3.15Å	(Luo et al., 2008a)
2WHX	DENV	NS3 full-length	ADP	2.2Å	(Luo et al., 2010)
2WZQ	DENV	NS3 full-length	-	2.8Å	(Luo et al., 2010)

Appendix 2. Structures of NS3 protease, NS3 helicase or full-length NS3 of DENV, YFV, WNV, JEV and ZIKV.

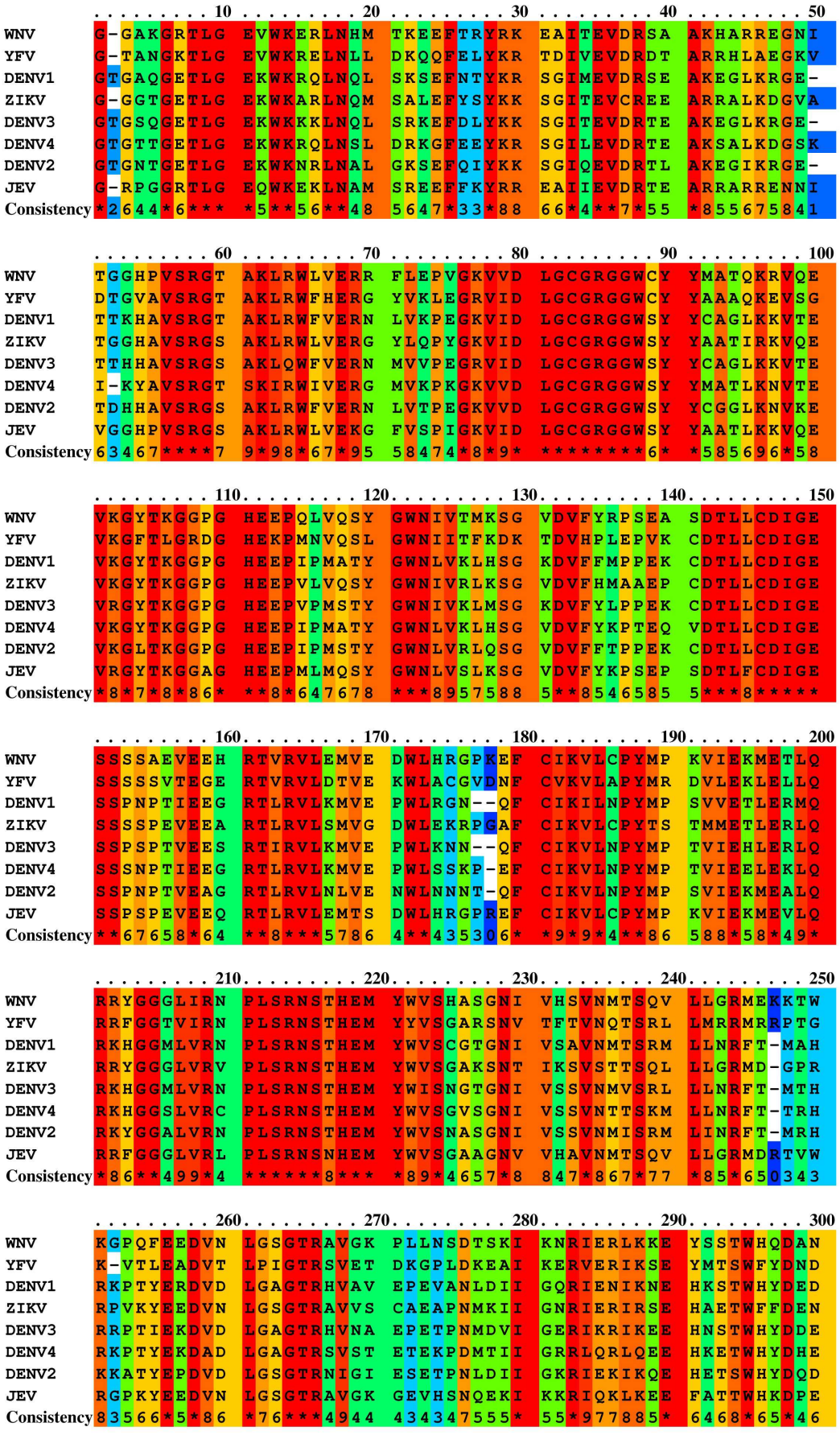
10 20 30 40 50
WNV G-GAKGRTLG EVWKERLNHM TKEEFTRYRK EAITEVDRSA AKHARREGNI
YFV G-TANGKTLG EVWKRELNLL DKQQFELYKR TDIVEVDRDT ARRHLAEGKV
DENV1 GTGAQGETLG EKWKRQLNQL SKSEFNTYKR SGIMEVDRSE AKEGLKRGE-
ZIKV G-GGTGETLG EKWKARLNQM SALEFYSYKK SGITEVCREE ARRALKDGVA
DENV3 GTGSQGETLG EKWKKKLNQL SRKEFDLYKK SGITEVDRTE AKEGLKRGE-
DENV4 GTGTTGETLG EKWKRQLNSL DRKGFEEYKR SGILEVDRTE AKSALKDGSK
DENV2 GTGNTGETLG EKWKNRLNAL GKSEFQIYKK SGIQEVDRTL AKEGIKRGE-
JEV G-RPGGRTLG EQWKEKLNAM SREEFFKYRR EAIIEVDRTE ARRARRENNI
Consistency *2644*6*** *5**56**48 5647*33*88 66*4**7*55 *855675841
60 70 80 90 100
WNV TGGHPVSRGT AKLRWLVERR FLEPVGKVVD LGCGRGGWCY YMATQKRVQE
YFV DTGVAVSRGT AKLRWFHERG YVKLEGRVID LGCGRGGWCY YAAAQKEVSG
DENV1 TTKHAVSRGT AKLRWFVERN LVKPEGKVID LGCGRGGWSY YCAGLKKVTE
ZIKV TGGHAVSRGS AKLRWLVERG YLQPYGKVID LGCGRGGWSY YAATIRKVQE
DENV3 TTHHAVSRGS AKLQWFVERN MVVPEGRVID LGCGRGGWSY YCAGLKKVTE
DENV4 I-KYAVSRGT SKIRWIVERG MVKPKGKVVD LGCGRGGWSY YMATLKNVTE
DENV2 TDHHAVSRGS AKLRWFVERN LVTPEGKVVD LGCGRGGWSY YCGGLKNVKE
JEV VGGHPVSRGS AKLRWLVEKG FVSPIGKVID LGCGRGGWSY YAATLKKVQE
Consistency 63467****7 9*98*67*95 58474*8*9* ********6* *585696*58
110 120 130 140 150
WNV VKGYTKGGPG HEEPQLVQSY GWNIVTMKSG VDVFYRPSEA SDTLLCDIGE
YFV VKGFTLGRDG HEKPMNVQSL GWNIITFKDK TDVHPLEPVK CDTLLCDIGE
DENV1 VKGYTKGGPG HEEPIPMATY GWNLVKLHSG KDVFFMPPEK CDTLLCDIGE
ZIKV VKGYTKGGPG HEEPVLVQSY GWNIVRLKSG VDVFHMAAEP CDTLLCDIGE
DENV3 VRGYTKGGPG HEEPVPMSTY GWNIVKLMSG KDVFYLPPEK CDTLLCDIGE
DENV4 VKGYTKGGPG HEEPIPMATY GWNLVKLHSG VDVFYKPTEQ VDTLLCDIGE
DENV2 VKGLTKGGPG HEEPIPMSTY GWNLVRLQSG VDVFFTPPEK CDTLLCDIGE
JEV VRGYTKGGAG HEEPMLMQSY GWNLVSLKSG VDVFYKPSEP SDTLFCDIGE
Consistency *8*7*8*86* **8*647678 ***895757 88 5**8546585 5***8*****
160 170 180 190 200
WNV SSSSAEVEEH RTVRVLEMVE DWLHRGPKEF CIKVLCPYMP KVIEKMETLQ
YFV SSSSSVTEGE RTVRVLDTVE KWLACGVDNF CVKVLAPYMR DVLEKLELLQ
DENV1 SSPNPTIEEG RTLRVLKMVE PWLRGN--QF CIKILNPYMP SVVETLERMQ
ZIKV SSSSPEVEEA RTLRVLSMVG DWLEKRPGAF CIKVLCPYTS TMMETLERLQ
DENV3 SSPSPTVEES RTIRVLKMVE PWLKNN--QF CIKVLNPYMP TVIEHLERLQ
DENV4 SSSNPTIEEG RTLRVLKMVE PWLSSKP-EF CIKVLNPYMP TVIEELEKLQ
DENV2 SSPNPTVEAG RTLRVLNLVE NWLNNNT-QF CIKVLNPYMP SVIEKMEALQ
JEV SSPSPEVEEQ RTLRVLEMTS DWLHRGPREF CIKVLCPYMP KVIEKMEVLQ
Consistency **67658*64 **8***5786 4**435306* *9*9*4**86 588*58*49*
210 220 230 240 250
WNV RRYGGGLIRN PLSRNSTHEM YWVSHASGNI VHSVNMTSQV LLGRMEKKTW
YFV RRFGGTVIRN PLSRNSTHEM YYVSGARSNV TFTVNQTSRL LMRRMRRPTG
DENV1 RKHGGMLVRN PLSRNSTHEM YWVSCGTGNI VSAVNMTSRM LLNRFT-MAH
ZIKV RRYGGGLVRV PLSRNSTHEM YWVSGAKSNT IKSVSTTSQL LLGRMD-GPR
DENV3 RKHGGMLVRN PLSRNSTHEM YWISNGTGNI VSSVNMVSRL LLNRFT-MTH
DENV4 RKHGGSLVRC PLSRNSTHEM YWVSGVSGNI VSSVNTTSKM LLNRFT-TRH
DENV2 RKYGGALVRN PLSRNSTHEM YWVSNASGNI VSSVNMISRM LINRFT-MRH
JEV RRFGGGLVRL PLSRNSNHEM YWVSGAAGNV VHAVNMTSQV LLGRMDRTVW
Consistency *86**499*4 ******8**** *89*4657*8 847*867*77 *85*650343
260 270 280 290 300
WNV KGPQFEEDVN LGSGTRAVGK PLLNSDTSKI KNRIERLKKE YSSTWHQDAN
YFV K-VTLEADVT LPIGTRSVET DKGPLDKEAI KERVERIKSE YMTSWFYDND
DENV1 RKPTYERDVD LGAGTRHVAV EPEVANLDII GQRIENIKNE HKSTWHYDED
ZIKV RPVKYEEDVN LGSGTRAVVS CAEAPNMKII GNRIERIRSE HAETWFFDEN
DENV3 RRPTIEKDVD LGAGTRHVNA EPETPNMDVI GERIKRIKEE HNSTWHYDDE
DENV4 RKPTYEKDAD LGAGTRSVST ETEKPDMTII GRRLQRLQEE HKETWHYDHE
DENV2 KKATYEPDVD LGSGTRNIGI ESETPNLDII GKRIEKIKQE HETSWHYDQD
JEV RGPKYEEDVN LGSGTRAVGK GEVHSNQEKI KKRIQKLKEE FATTWHKDPE
Consistency 83566*5*86 *76***4944 434347555* 55*977885* 6468*65*46

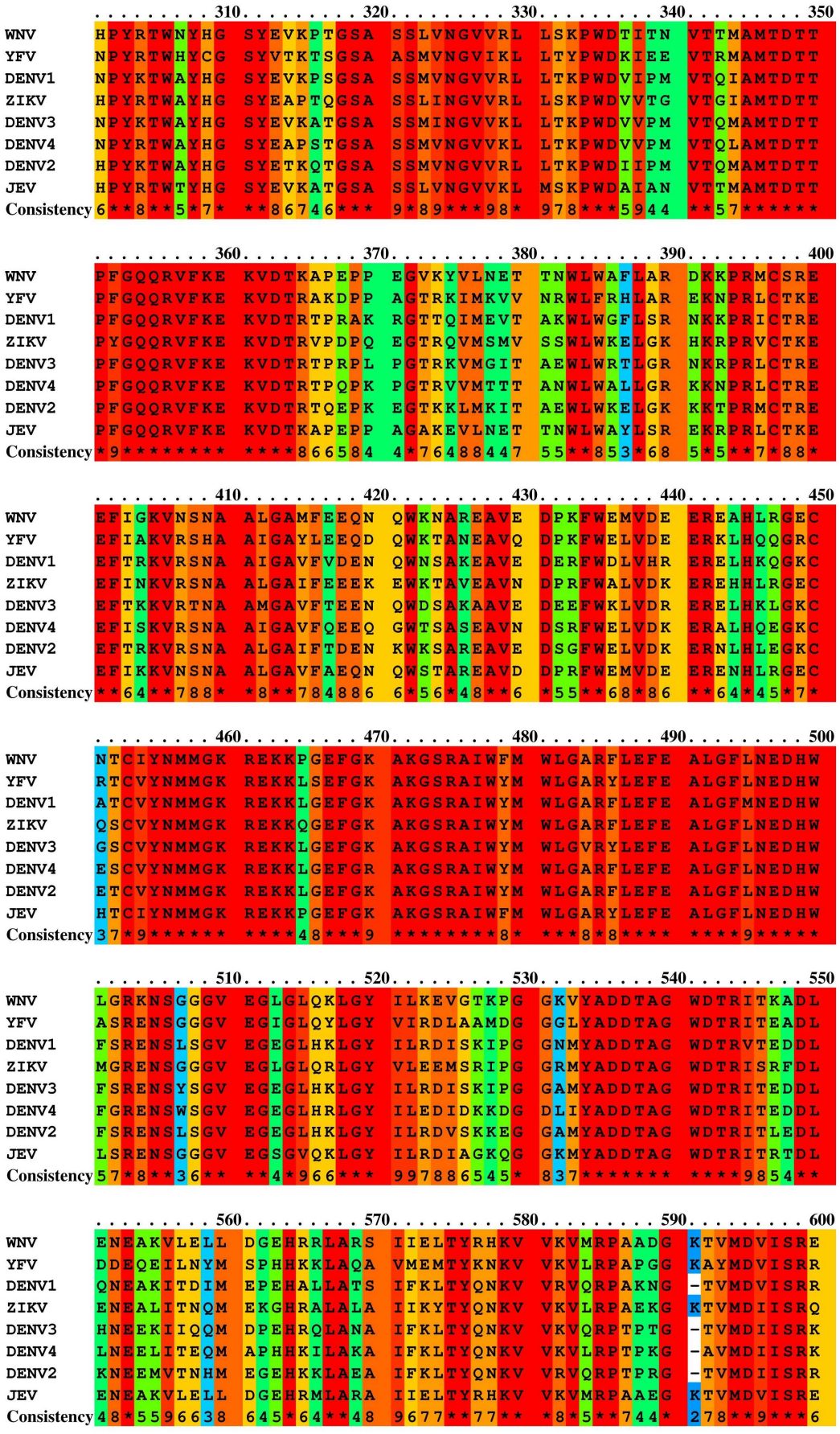
310 320 330 340 350
WNV HPYRTWNYHG SYEVKPTGSA SSLVNGVVRL LSKPWDTITN VTTMAMTDTT
YFV NPYRTWHYCG SYVTKTSGSA ASMVNGVIKL LTYPWDKIEE VTRMAMTDTT
DENV1 NPYKTWAYHG SYEVKPSGSA SSMVNGVVRL LTKPWDVIPM VTQIAMTDTT
ZIKV HPYRTWAYHG SYEAPTQGSA SSLINGVVRL LSKPWDVVTG VTGIAMTDTT
DENV3 NPYKTWAYHG SYEVKATGSA SSMINGVVKL LTKPWDVVPM VTQMAMTDTT
DENV4 NPYRTWAYHG SYEAPSTGSA SSMVNGVVKL LTKPWDVVPM VTQLAMTDTT
DENV2 HPYKTWAYHG SYETKQTGSA SSMVNGVVRL LTKPWDIIPM VTQMAMTDTT
JEV HPYRTWTYHG SYEVKATGSA SSLVNGVVKL MSKPWDAIAN VTTMAMTDTT
Consistency 6**8**5*7* **8674 6*** 9*89***98* 978***5944 **57******
360 370 380 390 400
WNV PFGQQRVFKE KVDTKAPEPP EGVKYVLNET TNWLWAFLAR DKKPRMCSRE
YFV PFGQQRVFKE KVDTRAKDPP AGTRKIMKVV NRWLFRHLAR EKNPRLCTKE
DENV1 PFGQQRVFKE KVDTRTPRAK RGTTQIMEVT AKWLWGFLSR NKKPRICTRE
ZIKV PYGQQRVFKE KVDTRVPDPQ EGTRQVMSMV SSWLWKELGK HKRPRVCTKE
DENV3 PFGQQRVFKE KVDTRTPRPL PGTRKVMGIT AEWLWRTLGR NKRPRLCTRE
DENV4 PFGQQRVFKE KVDTRTPQPK PGTRVVMTTT ANWLWALLGR KKNPRLCTRE
DENV2 PFGQQRVFKE KVDTRTQEPK EGTKKLMKIT AEWLWKELGK KKTPRMCTRE
JEV PFGQQRVFKE KVDTKAPEPP AGAKEVLNET TNWLWAYLSR EKRPRLCTKE
Consistency *9******** ****866584 4*764884 47 55**853*68 5*5**7*88*
410 420 430 440 450
WNV EFIGKVNSNA ALGAMFEEQN QWKNAREAVE DPKFWEMVDE EREAHLRGEC
YFV EFIAKVRSHA AIGAYLEEQD QWKTANEAVQ DPKFWELVDE ERKLHQQGRC
DENV1 EFTRKVRSNA AIGAVFVDEN QWNSAKEAVE DERFWDLVHR ERELHKQGKC
ZIKV EFINKVRSNA ALGAIFEEEK EWKTAVEAVN DPRFWALVDK EREHHLRGEC
DENV3 EFTKKVRTNA AMGAVFTEEN QWDSAKAAVE DEEFWKLVDR ERELHKLGKC
DENV4 EFISKVRSNA AIGAVFQEEQ GWTSASEAVN DSRFWELVDK ERALHQEGKC
DENV2 EFTRKVRSNA ALGAIFTDEN KWKSAREAVE DSGFWELVDK ERNLHLEGKC
JEV EFIKKVNSNA ALGAVFAEQN QWSTAREAVD DPRFWEMVDE ERENHLRGEC
Consistency **64**788* *8**78488 6 6*56*48**6 *55**68*86 **64*45*7*
460 470 480 490 500
WNV NTCIYNMMGK REKKPGEFGK AKGSRAIWFM WLGARFLEFE ALGFLNEDHW
YFV RTCVYNMMGK REKKLSEFGK AKGSRAIWYM WLGARYLEFE ALGFLNEDHW
DENV1 ATCVYNMMGK REKKLGEFGK AKGSRAIWYM WLGARFLEFE ALGFMNEDHW
ZIKV QSCVYNMMGK REKKQGEFGK AKGSRAIWYM WLGARFLEFE ALGFLNEDHW
DENV3 GSCVYNMMGK REKKLGEFGK AKGSRAIWYM WLGVRYLEFE ALGFLNEDHW
DENV4 ESCVYNMMGK REKKLGEFGR AKGSRAIWYM WLGARFLEFE ALGFLNEDHW
DENV2 ETCVYNMMGK REKKLGEFGK AKGSRAIWYM WLGARFLEFE ALGFLNEDHW
JEV HTCIYNMMGK REKKPGEFGK AKGSRAIWFM WLGARYLEFE ALGFLNEDHW
Consistency 37*9****** ****48***9 ********8* ***8*8**** ****9*****
510 520 530 540 550
WNV LGRKNSGGGV EGLGLQKLGY ILKEVGTKPG GKVYADDTAG WDTRITKADL
YFV ASRENSGGGV EGIGLQYLGY VIRDLAAMDG GGLYADDTAG WDTRITEADL
DENV1 FSRENSLSGV EGEGLHKLGY ILRDISKIPG GNMYADDTAG WDTRVTEDDL
ZIKV MGRENSGGGV EGLGLQRLGY VLEEMSRIPG GRMYADDTAG WDTRISRFDL
DENV3 FSRENSYSGV EGEGLHKLGY ILRDISKIPG GAMYADDTAG WDTRITEDDL
DENV4 FGRENSWSGV EGEGLHRLGY ILEDIDKKDG DLIYADDTAG WDTRITEDDL
DENV2 FSRENSLSGV EGEGLHKLGY ILRDVSKKEG GAMYADDTAG WDTRITLEDL
JEV LSRENSGGGV EGSGVQKLGY ILRDIAGKQG GKMYADDTAG WDTRITRTDL
Consistency 57*8**36** **4*966*** 997886545* 837******* ****9854**
560 570 580 590 600
WNV ENEAKVLELL DGEHRRLARS IIELTYRHKV VKVMRPAADG KTVMDVISRE
YFV DDEQEILNYM SPHHKKLAQA VMEMTYKNKV VKVLRPAPGG KAYMDVISRR
DENV1 QNEAKITDIM EPEHALLATS IFKLTYQNKV VRVQRPAKNG -TVMDVISRR
ZIKV ENEALITNQM EKGHRALALA IIKYTYQNKV VKVLRPAEKG KTVMDIISRQ
DENV3 HNEEKIIQQM DPEHRQLANA IFKLTYQNKV VKVQRPTPTG -TVMDIISRK
DENV4 LNEELITEQM APHHKILAKA IFKLTYQNKV VKVLRPTPKG -AVMDIISRK
DENV2 KNEEMVTNHM EGEHKKLAEA IFKLTYQNKV VRVQRPTPRG -TVMDIISRR
JEV ENEAKVLELL DGEHRMLARA IIELTYRHKV VKVMRPAAEG KTVMDVISRE
Consistency 48*559663 8 645*64**48 9677**77** *8*5**744* 278**9***6

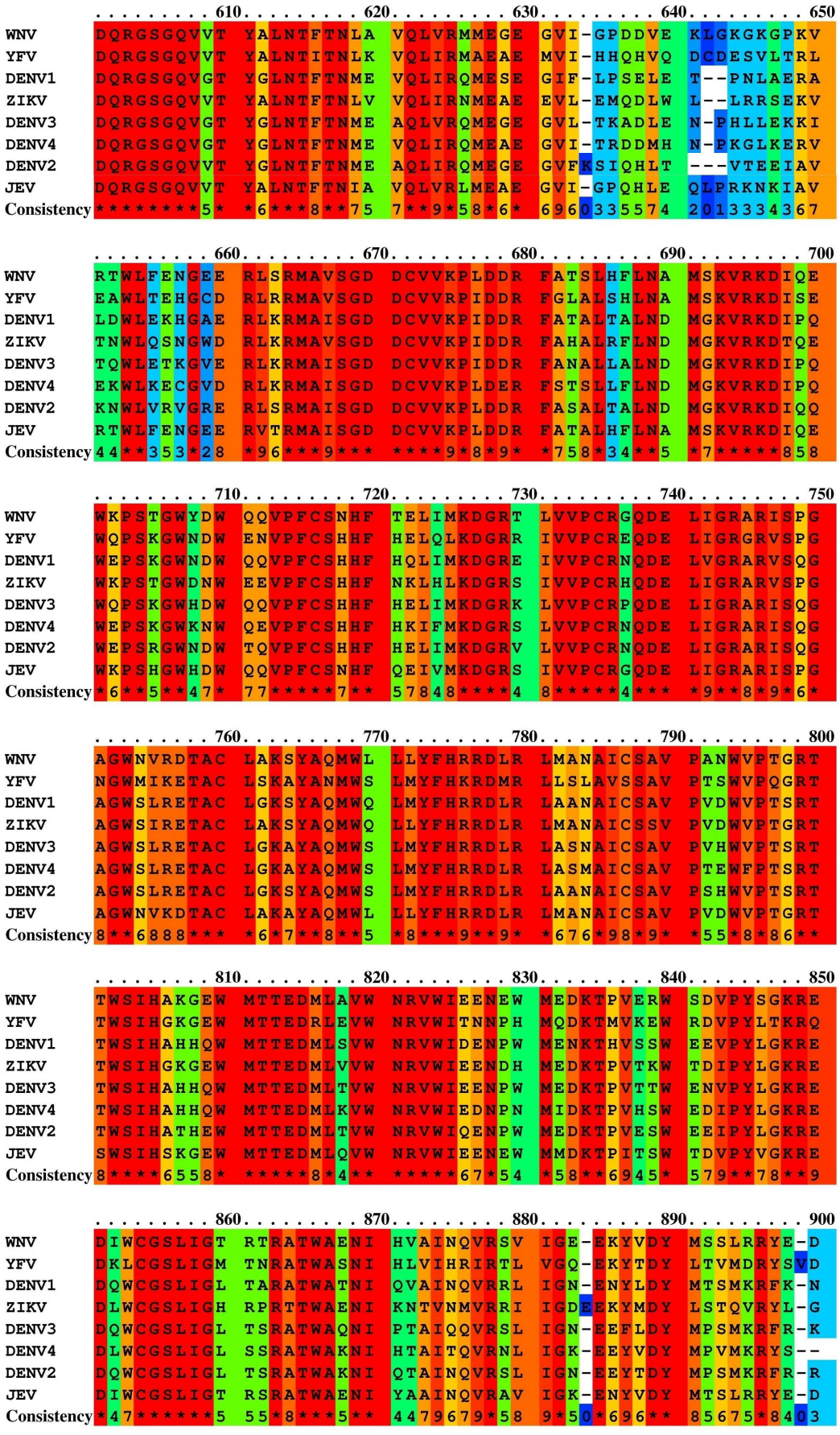
610 620 630 640 650
WNV DQRGSGQVVT YALNTFTNLA VQLVRMMEGE GVI-GPDDVE KLGKGKGPKV
YFV DQRGSGQVVT YALNTITNLK VQLIRMAEAE MVI-HHQHVQ DCDESVLTRL
DENV1 DQRGSGQVGT YGLNTFTNME VQLIRQMESE GIF-LPSELE T--PNLAERA
ZIKV DQRGSGQVVT YALNTFTNLV VQLIRNMEAE EVL-EMQDLW L--LRRSEKV
DENV3 DQRGSGQVGT YGLNTFTNME AQLVRQMEGE GVL-TKADLE N-PHLLEKKI
DENV4 DQRGSGQVGT YGLNTFTNME VQLIRQMEAE GVI-TRDDMH N-PKGLKERV
DENV2 DQRGSGQVVT YGLNTFTNME AQLIRQMEGE GVFKSIQHLT ---VTEEIAV
JEV DQRGSGQVVT YALNTFTNIA VQLVRLMEAE GVI-GPQHLE QLPRKNKIAV
Consistency *******5* *6***8**75 7**9*58*6* 6960335574 2013334367
660 670 680 690 700
WNV RTWLFENGEE RLSRMAVSGD DCVVKPLDDR FATSLHFLNA MSKVRKDIQE
YFV EAWLTEHGCD RLRRMAVSGD DCVVRPIDDR FGLALSHLNA MSKVRKDISE
DENV1 LDWLEKHGAE RLKRMAISGD DCVVKPIDDR FATALTALND MGKVRKDIPQ
ZIKV TNWLQSNGWD RLKRMAVSGD DCVVKPIDDR FAHALRFLND MGKVRKDTQE
DENV3 TQWLETKGVE RLKRMAISGD DCVVKPIDDR FANALLALND MGKVRKDIPQ
DENV4 EKWLKECGVD RLKRMAISGD DCVVKPLDER FSTSLLFLND MGKVRKDIPQ
DENV2 KNWLVRVGRE RLSRMAISGD DCVVKPLDDR FASALTALND MGKVRKDIQQ
JEV RTWLFENGEE RVTRMAISGD DCVVKPLDDR FATALHFLNA MSKVRKDIQE
Consistency 44**353*28 *96***9*** ****9*8*9* *758*34**5 *7*****858
710 720 730 740 750
WNV WKPSTGWYDW QQVPFCSNHF TELIMKDGRT LVVPCRGQDE LIGRARISPG
YFV WQPSKGWNDW ENVPFCSHHF HELQLKDGRR IVVPCREQDE LIGRGRVSPG
DENV1 WEPSKGWNDW QQVPFCSHHF HQLIMKDGRE IVVPCRNQDE LVGRARVSQG
ZIKV WKPSTGWDNW EEVPFCSHHF NKLHLKDGRS IVVPCRHQDE LIGRARVSPG
DENV3 WQPSKGWHDW QQVPFCSHHF HELIMKDGRK LVVPCRPQDE LIGRARISQG
DENV4 WEPSKGWKNW QEVPFCSHHF HKIFMKDGRS LVVPCRNQDE LIGRARISQG
DENV2 WEPSRGWNDW TQVPFCSHHF HELIMKDGRV LVVPCRNQDE LIGRARISQG
JEV WKPSHGWHDW QQVPFCSNHF QEIVMKDGRS IVVPCRGQDE LIGRARISPG
Consistency *6**5**47* 77*****7** 57848****4 8*****4*** *9**8*9*6*
760 770 780 790 800
WNV AGWNVRDTAC LAKSYAQMWL LLYFHRRDLR LMANAICSAV PANWVPTGRT
YFV NGWMIKETAC LSKAYANMWS LMYFHKRDMR LLSLAVSSAV PTSWVPQGRT
DENV1 AGWSLRETAC LGKSYAQMWQ LMYFHRRDLR LAANAICSAV PVDWVPTSRT
ZIKV AGWSIRETAC LAKSYAQMWQ LLYFHRRDLR LMANAICSSV PVDWVPTGRT
DENV3 AGWSLRETAC LGKAYAQMWS LMYFHRRDLR LASNAICSAV PVHWVPTSRT
DENV4 AGWSLRETAC LGKAYAQMWS LMYFHRRDLR LASMAICSAV PTEWFPTSRT
DENV2 AGWSLRETAC LGKSYAQMWS LMYFHRRDLR LAANAICSAV PSHWVPTSRT
JEV AGWNVKDTAC LAKAYAQMWL LLYFHRRDLR LMANAICSAV PVDWVPTGRT
Consistency 8**6888*** *6*7**8**5 *8***9**9* *676*98*9* *55*8*86**
810 820 830 840 850
WNV TWSIHAKGEW MTTEDMLAVW NRVWIEENEW MEDKTPVERW SDVPYSGKRE
YFV TWSIHGKGEW MTTEDRLEVW NRVWITNNPH MQDKTMVKEW RDVPYLTKRQ
DENV1 TWSIHAHHQW MTTEDMLSVW NRVWIDENPW MENKTHVSSW EEVPYLGKRE
ZIKV TWSIHGKGEW MTTEDMLVVW NRVWIEENDH MEDKTPVTKW TDIPYLGKRE
DENV3 TWSIHAHHQW MTTEDMLTVW NRVWIEENPW MEDKTPVTTW ENVPYLGKRE
DENV4 TWSIHAHHQW MTTEDMLKVW NRVWIEDNPN MIDKTPVHSW EDIPYLGKRE
DENV2 TWSIHATHEW MTTEDMLTVW NRVWIQENPW MEDKTPVESW EEIPYLGKRE
JEV SWSIHSKGEW MTTEDMLQVW NRVWIEENEW MMDKTPITSW TDVPYVGKRE
Consistency 8****6558* *****8*4** *****67*54 *58**6945* 579**78**9
860 870 880 890 900
WNV DIWCGSLIGT RTRATWAENI HVAINQVRSV IGE-EKYVDY MSSLRRYE-D
YFV DKLCGSLIGM TNRATWASNI HLVIHRIRTL VGQ-EKYTDY LTVMDRYSVD
DENV1 DQWCGSLIGL TARATWATNI QVAINQVRRL IGN-ENYLDY MTSMKRFK-N
ZIKV DLWCGSLIGH RPRTTWAENI KNTVNMVRRI IGDEEKYMDY LSTQVRYL-G
DENV3 DQWCGSLIGL TSRATWAQNI PTAIQQVRSL IGN-EEFLDY MPSMKRFR-K
DENV4 DLWCGSLIGL SSRATWAKNI HTAITQVRNL IGK-EEYVDY MPVMKRYS--
DENV2 DQWCGSLIGL TSRATWAKNI QTAINQVRSL IGN-EEYTDY MPSMKRFR-R
JEV DIWCGSLIGT RSRATWAENI YAAINQVRAV IGK-ENYVDY MTSLRRYE-D
Consistency *47******5 55*8***5** 447967 9*58 9*50*696** 85675*8403

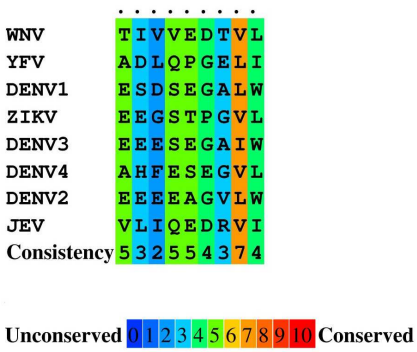

Appendix 3. Alignment of the NS5 proteins from DENV, YFV, WNV, JEV and ZIKV.

Sequences were aligned using PRALINE (Centre for Integrative Bioinformatics Vrije Universiteit Amsterdam, 2017). Each amino acid residue is colored according to its conservation between these virus species, where red is most conserved and blue is least conserved.

PDB code	Virus	Protein	Ligands	Resolution	Authors
1L9K	DENV	NS5 capping enzyme	SAH	2.4Å	(Egloff et al., 2002)
1R6A	DENV	NS5 capping enzyme	SAH, ribavirin	2.6Å	(Benarroch et al., 2004a)
2OY0	WNV	NS5 capping enzyme	SAH	2.8Å	(Zhou et al., 2007)
2P1D	DENV	NS5 capping enzyme	SAH, GMP	2.9Å	(Egloff et al., 2002)
2P3L	DENV	NS5 capping enzyme	SAH, GpppA	2.2Å	(Egloff et al., 2007)
2P3O	DENV	NS5 capping enzyme	SAH, m7GpppA	2.76Å	(Egloff et al., 2007)
2P3Q	DENV	NS5 capping enzyme	SAH, GpppG	2.75Å	(Egloff et al., 2007)
2P40	DENV	NS5 capping enzyme	m7GpppG	2.7Å	(Egloff et al., 2007)
2P41	DENV	NS5 capping enzyme	SAH, m7GpppGm	1.8Å	(Egloff et al., 2007)
2XBM	DENV	NS5 capping enzyme	SAH, GpppA-GAACCUGA	2.9Å	(Yap et al., 2010)
3EVA	YFV	NS5 capping enzyme	SAH	1.5Å	(Geiss et al., 2009)
3EVB	YFV	NS5 capping enzyme	SAH	1.85Å	(Geiss et al., 2009)
3EVC	YFV	NS5 capping enzyme	SAH, GTP	1.6Å	(Geiss et al., 2009)
3EVD	YFV	NS5 capping enzyme	SAH, GTP	1.5Å	(Geiss et al., 2009)
3EVE	YFV	NS5 capping enzyme	SAH, GpppA	1.7Å	(Geiss et al., 2009)
3EVF	YFV	NS5 capping enzyme	SAH, m7GpppA	1.45Å	(Geiss et al., 2009)
3EVG	DENV	NS5 capping enzyme	SAH	2.2Å	(Geiss et al., 2009)
3LKZ	WNV	NS5 capping enzyme	Sinefungin	2.0Å	(Dong et al., 2010)
3P8Z	DENV	NS5 capping enzyme	SAH / inhibitor	1.7Å	(Lim et al., 2011)
3P97	DENV	NS5 capping enzyme	SAM	1.7Å	(Lim et al., 2011)
4CTJ	DENV	NS5 capping enzyme	SAM, inhibitor	1.47Å	(Coutard et al., 2014)
4CTK	DENV	NS5 capping enzyme	SAM, inhibitor	1.53Å	(Coutard et al., 2014)
4R05	DENV	NS5 capping enzyme	-	2.1Å	(M. B. Brecher et al., 2015)
4R8R	DENV	NS5 capping enzyme	-	1.46Å	(Noble et al., 2014)
4R8S	DENV	NS5 capping enzyme	Sinefungin	1.48Å	(Noble et al., 2014)
5CUQ	DENV	NS5 capping enzyme	Compound NSC (inhibitor)	1.7Å	(M. Brecher et al., 2015)
5E9Q	DENV	NS5 capping enzyme	SAM, inhibitor	1.79Å	(Benmansour et al., 2017)
5EC8	DENV	NS5 capping enzyme	SAM, inhibitor	1.71Å	(Benmansour et al., 2017)
5EHG	DENV	NS5 capping enzyme	SAM, inhibitor	2.02Å	(Benmansour et al., 2017)
5EHI	DENV	NS5 capping enzyme	SAM, inhibitor	1.3Å	(Benmansour et al., 2017)
5EIF	DENV	NS5 capping enzyme	SAM, inhibitor	1.5Å	(Benmansour et al., 2017)
5EIW	DENV	NS5 capping enzyme	SAM, inhibitor	1.61Å	(Benmansour et al., 2017)
5EKX	DENV	NS5 capping enzyme	SAM, inhibitor	1.76Å	(Benmansour et al., 2017)
5GOZ	ZIKV	NS5 capping enzyme	SAH, GTP, PPi	2.05Å	(C. Zhang et al., 2016)
5GP1	ZIKV	NS5 capping enzyme	SAH, m7GpppA	2.44Å	(C. Zhang et al., 2016)

5IKM	DENV	NS5 capping enzyme	SAM	1.9Å	(Minasov et al., to be published)
5KQR	ZIKV	NS5 capping enzyme	SAM	1.33Å	(Coloma et al., 2016)
5KQS	ZIKV	NS5 capping enzyme	SAM, m7GDP	1.5Å	(Coloma et al., 2016)
5M5B	ZIKV	NS5 capping enzyme	SAM	2.01Å	(Coutard et al., 2017)
5MRK	ZIKV	NS5 capping enzyme	Sinefungin	1.9Å	(Hercik and Boura, to be published)
2HCN	WNV	NS5 RdRp	-	2.35Å	(Malet et al., 2007)
2HCS	WNV	NS5 RdRp	-	2.5Å	(Malet et al., 2007)
2HFZ	WNV	NS5 RdRp	-	3.0Å	(Malet et al., 2007)
2J7U	DENV	NS5 RdRp	-	1.85Å	(Yap et al., 2007)
2J7W	DENV	NS5 RdRp	GTP	2.6Å	(Yap et al., 2007)
3VWS	DENV	NS5 RdRp	NITD107 (inhibitor)	2.1Å	(Noble et al., 2013)
4C11	DENV	NS5 RdRp	-	2.6Å	(Lim et al., 2013a)
4HDG	JEV	NS5 RdRp	GTP	2.38Å	(Surana et al., 2014)
4HDH	JEV	NS5 RdRp	ATP	2.28Å	(Surana et al., 2014)
4HHJ	DENV	NS5 RdRp	-	1.79Å	(Noble et al., 2013)
4MTP	JEV	NS5 RdRp	-	3.65Å	(Surana et al., 2014)
5F3T	DENV	NS5 RdRp	Inhibitor	2.05Å	(Noble et al., 2016)
5F3Z	DENV	NS5 RdRp	Inhibitor	2.0Å	(Noble et al., 2016)
5F41	DENV	NS5 RdRp	Inhibitor	2.0Å	(Noble et al., 2016)
5HMW	DENV	NS5 RdRp	Inhibitor	2.15Å	(Yokokawa et al., 2016)
5HMX	DENV	NS5 RdRp	Inhibitor	2.4Å	(Yokokawa et al., 2016)
5HMY	DENV	NS5 RdRp	Inhibitor	2.1Å	(Yokokawa et al., 2016)
5HMZ	DENV	NS5 RdRp	Inhibitor	1.99Å	(Yokokawa et al., 2016)
5HN0	DENV	NS5 RdRp	Inhibitor	2.05Å	(Yokokawa et al., 2016)
5I3P	DENV	NS5 RdRp	Inhibitor	2.45Å	(Lim et al., 2016)
5I3Q	DENV	NS5 RdRp	Inhibitor	1.88Å	(Lim et al., 2016)
5IQ6	DENV	NS5 RdRp	HeE1-2Tyr (inhibitor)	3.0Å	(Tarantino et al., 2016)
5K5M	DENV	NS5 RdRp	Inhibitor	2.01Å	(Lim et al., 2016)
4K6M	JEV	NS5 full-length	SAH	2.6Å	(Lu and Gong, 2013)
4V0Q	DENV	NS5 full-length	SAH	2.3Å	(Zhao et al., 2015b)
4V0R	DENV	NS5 full-length	SAH, GTP	2.4Å	(Zhao et al., 2015b)
5CCV	DENV	NS5 full-length	SAH	3.6Å	(Klema et al., 2016)
5DTO	DENV	NS5 full-length	SAH, m7GDP	2.6Å	(Zhao et al., 2015a)
5JJR	DENV	NS5 full-length	SAH, RdRp inhibitor	1.99Å	(Lim et al., 2016)
5JJS	DENV	NS5 full-length	SAH, RdRp inhibitor	1.65Å	(Lim et al., 2016)
5TFR	ZIKV	NS5 full-length	SAH	3.05Å	(Longenecker et al., to be published)
5TMH	ZIKV	NS5 full-length	SAH	3.28Å	(Wang et al., to be published)

Appendix 4. Structures of NS3 protease, NS3 helicase or full-length NS3 of DENV, YFV, WNV, JEV and ZIKV.

Mutant	Sequenced	Expressed	Purified (HisTrap)	Purified (HiLoad)
WT	✓	✓	✓	✓
NS5 D668V	✓	✓	✓	✓
NS3 R185A	✓	✓	✓	✓
NS3 K186A	✓			
NS3 K187A	✓	✓	✓	✓
NS3 R216A	✓	✓	✓	✓
NS3 R218A	✓	✓	✓	
NS3 R250A	✓	✓	✓	✓
NS3 G254A				
NS3 N255A				
NS3 H274A	✓	✓	✓	
NS3 R275A	✓	✓	✓	✓
NS3 V276A	✓	✓	✓	
NS3 V276A N278A	✓			
NS3 V276K	✓	✓	✓	✓
NS3 V276K NS5 K314V				
NS3 V276L	✓	✓	✓	✓
NS3 N278A	✓	✓		
NS3 N278D	✓	✓	✓	✓
NS3 N278K	✓	✓	✓	✓
NS3 N278K NS5 K314N				
NS3 N278Q	✓	✓	✓	✓
NS3 N280A				
NS3 E306A	✓	✓	✓	✓
NS3 L307A	✓			
NS3 E309A	✓	✓		
NS3 P502A				
NS3 N503A	✓	✓	✓	✓
NS3 E523A	✓	✓	✓	✓
NS3 R525A	✓			
NS3 R527A	✓	✓	✓	✓
NS3 E529A	✓	✓	✓	
NS3 E530A				
NS3 K532A	✓	✓	✓	✓
NS3 K532G	✓	✓	✓	✓
NS3 K532G NS5 G750K				
NS3 K532R	✓	✓	✓	
NS5 R45A	✓	✓		
NS5 E46A	✓	✓	✓	
NS5 N48A				

NS5 E289A	✓	✓		
NS5 S291A	✓	✓		
NS5 S292A	✓	✓	✓	
NS5 E312A	✓	✓		
NS5 K314A	✓	✓		
NS5 K314A G750A	✓	✓		
NS5 K314N	✓	✓		
NS5 K314R	✓	✓		
NS5 K314V	✓	✓		
NS5 G317A	✓	✓		
NS5 E416A	✓	✓		
NS5 E417A	✓	✓		
NS5 Q420A	✓	✓		
NS5 K422A				
NS5 E426A	✓	✓		
NS5 D430A	✓	✓		
NS5 G750A	✓	✓		
NS5 G750K	✓	✓	✓	
NS5 G750P	✓	✓		

Appendix 5. Preparation of recombinant proteins for *in vitro* binding assays.

Mutant	Average	Standard deviation	n
WT	100.00%	0.00%	19
NS5 D668V	1.40%	0.92%	19
NS3 R185A	64.82%	4.01%	4
NS3 K186A	1.16%	0.25%	3
NS3 K187A	104.60%	19.77%	3
NS3 R216A	0.24%	0.17%	3
NS3 R218A	2.68%	1.27%	4
NS3 R250A	108.54%	25.03%	4
NS3 G254A	0.32%	0.06%	3
NS3 N255A	52.24%	19.25%	3
NS3 H274A	58.61%	13.80%	4
NS3 R275A	10.65%	6.57%	4
NS3 V276A	5.76%	0.90%	4
NS3 V276A N278A	1.54%	0.71%	3
NS3 V276K	9.47%	0.97%	3
NS3 V276K NS5 K314V	2.21%	0.33%	3
NS3 V276L	62.90%	13.10%	4
NS3 N278A	41.26%	15.31%	3
NS3 N278D	4.38%	3.06%	4
NS3 N278K	2.43%	0.63%	3
NS3 N278K NS5 K314N	1.18%	0.23%	3
NS3 N278Q	51.98%	16.25%	4
NS3 N280A	27.88%	4.55%	3
NS3 E306A	84.63%	14.78%	3
NS3 L307A	12.42%	4.95%	3
NS3 E309A	24.43%	4.09%	3
NS3 P502A	39.54%	7.29%	3
NS3 N503A	41.35%	3.88%	3
NS3 E523A	1.21%	0.85%	3
NS3 R525A	2.31%	0.94%	3
NS3 R527A	0.76%	0.27%	3
NS3 E529A	67.36%	13.33%	4
NS3 E530A	44.18%	10.86%	3
NS3 K532A	41.87%	14.47%	4
NS3 K532G	90.33%	22.23%	3
NS3 K532G NS5 G750K	58.54%	7.35%	3
NS3 K532R	101.26%	26.24%	4
NS5 R45A	128.55%	19.09%	3
NS5 E46A	139.29%	5.49%	3
NS5 N48A	1.26%	0.32%	3

NS5 E289A	73.22%	7.39%	3
NS5 S291A	79.86%	7.63%	3
NS5 S292A	155.69%	33.97%	4
NS5 E312A	130.55%	40.53%	4
NS5 K314A	55.17%	13.58%	4
NS5 K314A G750A	64.85%	26.80%	4
NS5 K314N	86.82%	8.79%	3
NS5 K314R	101.90%	8.03%	4
NS5 K314V	2.63%	0.77%	3
NS5 G317A	0.34%	0.09%	3
NS5 E416A	128.40%	30.03%	4
NS5 E417A	56.21%	3.57%	3
NS5 Q420A	59.16%	14.03%	3
NS5 K422A	36.48%	10.79%	3
NS5 E426A	84.99%	33.64%	3
NS5 D430A	15.97%	5.26%	3
NS5 G750A	87.70%	13.33%	4
NS5 G750K	54.60%	14.85%	3
NS5 G750P	3.49%	1.41%	4

Appendix 6. Luciferase activity of the wild-type replicon and all mutants.